Functional Studies of Type I Inositol Hexakisphosphate Kinase and its Role in Cell Signaling

Dissertation
zur
Erlangung des Doktorgrades
der Naturwissenschaften
(Dr. rer. nat.)

dem
Fachbereich Biologie
der Philipps-Universität Marburg
vorgelegt von

Karen Abel
aus Oldenburg (Oldb)

angefertigt
im
Department of Pharmacology
University of Wisconsin
Madison, USA

Marburg/Lahn 2003

Vom Fachbereich Biologie

der Philipps-Universität Marburg als Dissertation am 27.08.2003 angenommen.

Erstgutachter: Prof. Dr. Michael Bölker

Zweitgutachter: Prof. Dr. Richard A. Anderson

Tag der mündlichen Prüfung am 1.9.2003

Summary

Inositol pentakis- and hexakisphosphates are the most abundant inositolphosphates in cells. Both inositolphosphates can be further phosphorylated by three inositol hexakisphosphate kinase isoforms (IP_6K1, 2 and 3) to form inositol pyrophosphates (IP_7 and $PPIP_4$). Those are the only known high energy molecules that may function as second messengers and may act as phosphate donor. The function of those second messengers remains unknown. However, it has been reported that higher inositolphosphates may play a role in nuclear signaling pathways like transcription, mRNA export and DNA repair.

In this study it was shown, that endogenous IP_6K1 and 2 were localized to different compartments of the cell. IP_6K2 is mainly nuclear whereas IP_6K1 was localized in the nucleus and cytoplasm. Interestingly, when cells were treated with cell cycle blocking agents IP_6K1 localization changed during each phase of the cell cycle. IP_6K1 was cytosolic in synchronized cells blocked at the G1/S border, in S-phase IP_6K1 began to be transported into the nucleus and finally, was mainly nuclear in G2. IP_6K1 also targeted to the kinetochores in prophase and associated with mitotic spindles in mitosis. To further investigate the role of IP_6K1 in the cell cycle siRNA oligos were designed to knock out the protein in HEK293T cells. Knocking out IP_6K1 caused a dramatic increase of cells in G2/M. This phenotype could be rescued by overexpression of IP_6K1 with a silent mutation in the siRNA target region. Further analysis of this phenotype showed, that the majority of the IP_6K1 knock out cells were arrested at the border from G2-phase of the cell cycle to mitosis. This is the first evidence for a specific function of these novel high energy second messengers.

Zusammenfassung

Inositol Pentakisphosphate (IP_5) und Inositol Hexakisphoshate (IP_6) sind die am häufigsten vorkommenden Inositolphosphate in der eucaryotischen Zelle. Drei Inositol Hexakisphospatkinasen Isoformen (IP_6K1, 2 und 3) können IP_5 und IP_6 weiter phoshorylieren. Die entstehenden Produkte, sogenannte Inositol Pyrophosphate, sind die einzigen bis jetzt bekannten energiereichen Moleküle, die das Potential haben sowohl als zweiter Bote (*second messenger*) als auch als Phosphatdonor zu agieren. Die physiologische Function dieser Signalmoleküle ist noch nicht bekannt.

Im Rahmen dieser Arbeit wurde gezeigt, dass IP_6K1 und IP_6K2 unterschiedlich in der Zelle lokalisiert sind. IP_6K2 wurde hauptsächlich im Zellkern vorgefunden, während IP_6K1 im Zellkern von einigen Zellen vorhanden war. In anderen jedoch Zellen wurde IP_6K1 jedoch nur im Cytoplasma lokalisiert. Interessanterweise scheint die intrazellulare Lokalisation von IP_6K1 vom Zellzyklus abzuhängen. Nachdem NIH3T3 Zellen mit unterschiedlichen Zellzyklus blockierenden Reagentien behandelt wurden, konnte gezeigt werden, dass in Zellen, die sich in der G1-Phase des Zellzyklus befanden, IP_6K1 nur im Cytoplasma vorhanden war. Im Gegensatz dazu befand sich IP_6K1 während der G2-phase im Zellkern. In Mitose wurde IP_6K1 ebenfalls an unterschiedlichen Orten vorgefunden. In Prophase befand sich IP_6K1 am Kinetochor und war während der Metaphase mit dem Spindelapparat assoziert. Um eine mögliche Funktion von IP_6K1 im Zellzyklus zu bestimmen, wurde die Kinase mit Hilfe von RNA Interferenz (RNAi) in HEK293T Zellen eliminiert, was in einen dramatischen Anstieg von Zellen in der G2/Mitose-Phase resultierte. In diesen $IP_6K1(-)$-Zellen konnte der Wildtyp durch die Überproduktion einer stillen Mutante von IP_6K1 wiederhergestellt werden. Weitere Analyse der Zellen, in denen IP_6K1 eliminiert war, ergab, dass sich die Zellen wahrscheinlich im Übergang von der G2-phase zur Mitose befanden. Dies ist einer der ersten Hinweise auf eine Funktion dieser neuartigen *second messengers* in humanen Zellen.

Acknowledgements

I would like to express my gratitude to Prof. Richard A. Anderson for this exciting project and his scientific mentorship. I am very thankful to Prof. Michael Bölker, who agreed to supervise my thesis and allowed me to perform my thesis work in the lab of Prof. Anderson, which made it all possible to begin with. I would also like to thank the other members of my thesis committee, Prof. Renate Renkawitz-Pohl and Prof. Klaus Lingelbach for their commitment.

My special thanks definitely have to be dedicated to the members of the Anderson lab. They managed to integrate me quickly into a very friendly and productive atmosphere.

Above all, I would like to thank my family and Veit Bergendahl for their love and support. Especially my parents, who gave me the strength and the patience which guided me through this period. I am also greatly thankful towards my grandparents, who enabled my studies substantially with financial and moral support.

Table of contents

Summary i
Zusammenfassung ii
Acknowledgements iii
1 Introduction 1
1.1 Inositol and inositol phosphates 1
1.1.1 Inositol 1,4,5-trisphosphate 3-kinase 5
1.1.2 Inositol polyphosphate multikinase 8
1.1.3 Inositol 1,3,4,5,6-pentakisphosphate 2-kinase 10
1.1.4 Inositol hexakisphosphate kinase 15
1.2 Nuclear inositol phosphate signaling 21
1.3 Inositol phosphates in cell cycle 23
1.4 Cell signaling in mitosis 24
1.4.1 Entry into mitosis 25
1.4.2 Metaphase-Anaphase transition 26
1.4.3 Exit from mitosis 26
1.5 Specific aim 28
2 Material and Methods 29
2.1 Materials 29
2.1.1 *E. coli* strains 29
2.1.2 Cell lines 29
2.1.3 Chemicals and kits 30
2.1.4 General material 31
2.1.5 Enzymes and proteins 32
2.1.6 Antibodies 33
2.1.7 Nucleic acids 34
2.1.8 Vectors 36
2.1.9 Buffers 37
2.1.10 *E. coli* media 39

2.1.11 Cell culture media 39
2.2 Microbiolocgical and molecular biological methodes 40
2.2.1 Culturing of *E. coli* 40
2.2.2 *E. coli* transformation 40
2.2.3 DNA isolation 40
2.2.4 Polymerase chain reaction (PCR) 41
2.2.5 Colony-PCR to test for positve clones 42
2.2.6 Modification of DNA 43
2.2.7 Preparation of messenger RNA 44
2.2.8 Reverse transcriptase PCR (RT-PCR) 44
2.2.9 Ligation 45
2.2.10 Sequencing of DNA 46
2.2.11 Construction of putative IP_6K kinase dead mutants 47
2.3 Biochemical and immunological methodes 47
2.3.1 Purification of soluble recombinant His_6 tagged IP_6K1 47
2.3.2 SDS-PAGE 48
2.3.3 Immuno blot 48
2.3.4 Immunoprecipitation 49
2.3.5 Determine protein concentrations 49
2.3.6 Kinase assays 50
2.4 Production of polyclonal antibodies 51
2.4.1 Proteinpurification 51
2.4.2 Construction of an mouse IP_6K1 affinity column 51
2.4.3 Production and purification of polyclonal antibodies 52
2.5 Cell biology 53
2.5.1 Cell culture 53
2.5.2 Transfection 53
2.5.3 Immunoflourescence and microscopy 54
2.5.4 Preparation of cell lysates 55
2.5.5 Inducing cell cycle arrest in cell llines 55
2.5.6 Dephosphorylation of proteins in cell lysates 56

2.5.7 Metabolic labeling of HEK29T cells with ^{3}H-inositol 56
2.6 IP_6K1 knock out cells..... 57
2.6.1 RNA interference (RNAi) to knock down endogenous IP_6K1 in HEK293T cells. 57
2.6.2 Rescue of IP_6K1 RNAi phenotype..... 59
2.7 Flow cytometry 60
2.8 HPLC 61
3 Results..... 62
3.1 Cloning of human inositol hexakisphosphate kinase type 1 out of HEK293T cells 62
3.2 Overexpressed IP_6K1 and IP_6K2 localizes to the nucleus 64
3.3 Subcellular localization of endogenous IP_6K1 66
3.3.1 Characterization of polyclonal anti IP_6K1 and IP_6K2 antibodies 66
3.3.2 IP_6K1 is expressed in different cell lines 69
3.4 Cell cyle dependent localization of IP_6K1 71
3.4.1 IP_6K1 transolcates into the nucleus in G2..... 71
3.4.2 IP_6K1 is localized at the kinetochore and mitotic spindles in mitosis 73
3.5 IP_6K1 is posttranslationally modified in cells in G2/M 74
3.6 Characterization of IP_6K1 knock out phenotype 77
3.6.1 Knock out of endogenous IP_6K1 causes G2/M arrest in HEK293T cells..... 77
3.6.2 The IP_6K1 knock out phenotype can be rescued by overexpressing hIP_6K1 81
3.6.3 Depletion of IP6K1 in U2OS cells increased amount of cells in G2M and apoptotic cells 84
3.6.4 Analysis of different mitotic regulting proteins in HEK239T IP_6K1 ko cells..... 86
3.7 Overexpression of hIP_6K1 in HEK293T cells arrests the cells in G1..... 88
3.8 Inositol pyrophosphate levels don't change during cell cycle 89
4 Discussion 92
4.1 Subcellular localization of IP_6K1..... 92
4.1.1 IP_6K1 is localized in the nucleus 92
4.1.2 IP_6K1 is able to shuttle in and out of the nucleus 93
4.2 A role for inositol pyrophosphates in cell cycle regulation 94

4.2.1 Nuclear localization of IP_6K1 is cell cycle dependent 94
4.2.2 IP_6K1 translocates from the kinetochore to the mitotic spindle in mitosis 95
4.2.3 IP_6K1 is postranslational modified in mitosis 97
4.2.4 Characterization of G2/M arrest induced by depletion of IP_6K1 99
4.2.5 Inositol pyrophoshate levels do not change during mitosis 103
5 References 105
Abbreviations 119
Appendix 121

1 Introduction

1.1 Inositol and inositol phosphates

Inositol phosphates have been discovered in biological systems more than eighty years ago, when Posternak discovered that inositol hexakisphoshate is a phosphate store in plant seeds (Posternak, 1919). More than sixty years later the discovery of inositol 1,4,5-trisphosphate as a Ca^{2+} mobilizing second messenger (Streb *et al.*, 1983) led to more interest in inositol phosphate signaling and the existence of different inositol phosphates was discovered. Inositol phosphates contain an inositol ring, which can be phosphorylated on every hydroxyl position of the ring (figure 1).

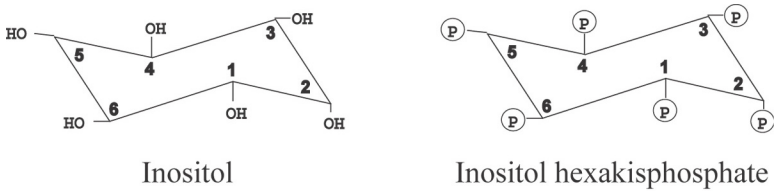

Figure 1: Structure of inositol and inositol hexakisphosphate (IP_6). The numbers on the inositol ring represent the hydroxyl groups on the inositol ring, which can be phosphorylated on every hydroxyl group, resulting in IP_6.

Mathematically, there are more than 60 possible inositol phosphates, but only 21 of them have been confirmed to exist in cells. The function of many of these molecules remains unknown. Not only inositol can be phosphorylated, phosphatidylinositol (PI) also exists in different phosphorylated forms, that increases the diversity of inositol based second messengers (figure 2).

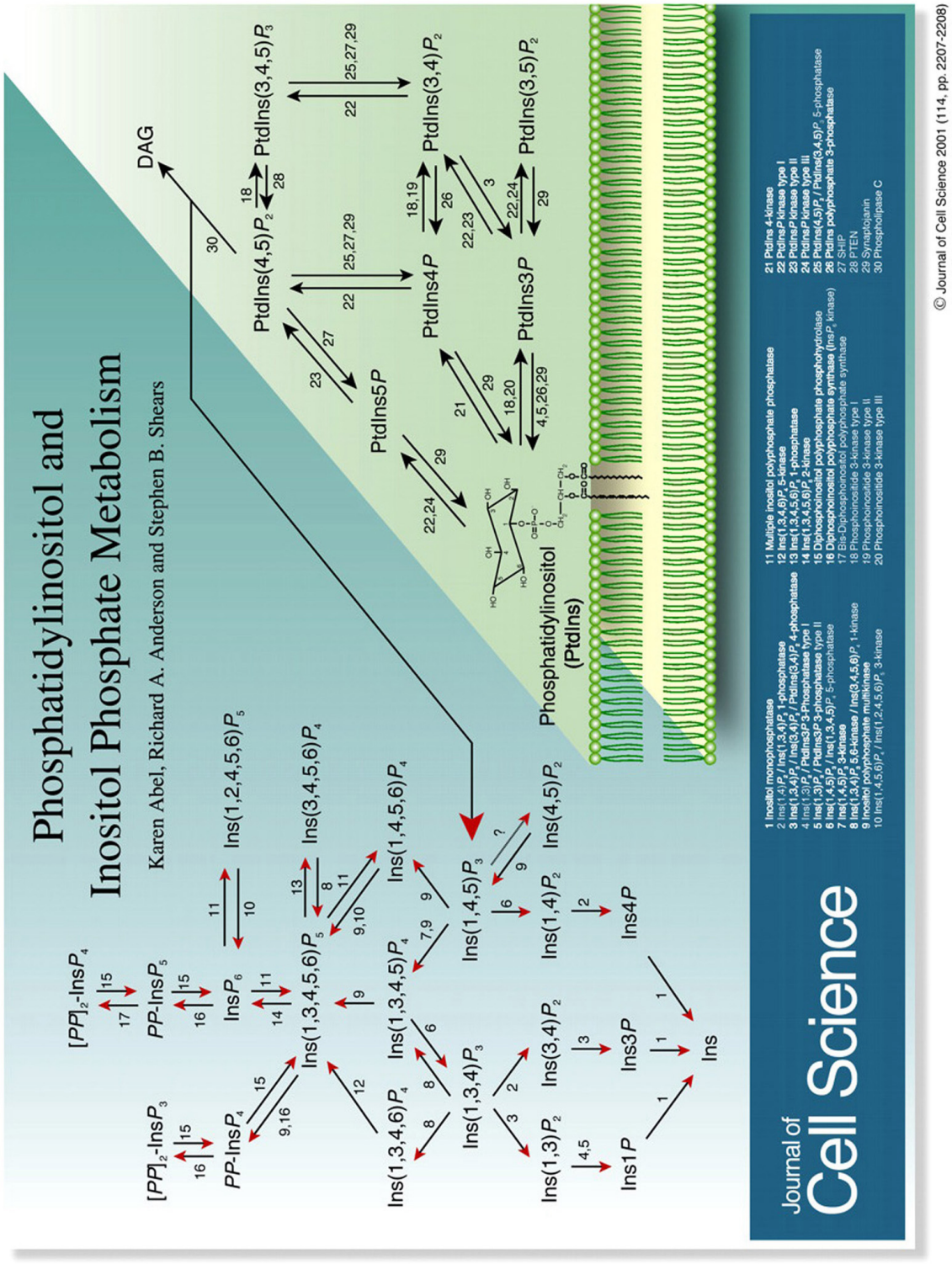

Figure 2: Overview of inositol phosphates and phosphatidyl inositolphosphates (Abel *et al.*, 2001). The variety of inositol phosphates (right site) and phosphatidylinositol phosphates (left site) is achieved by different inositol phosphate kinases and phosphatases.

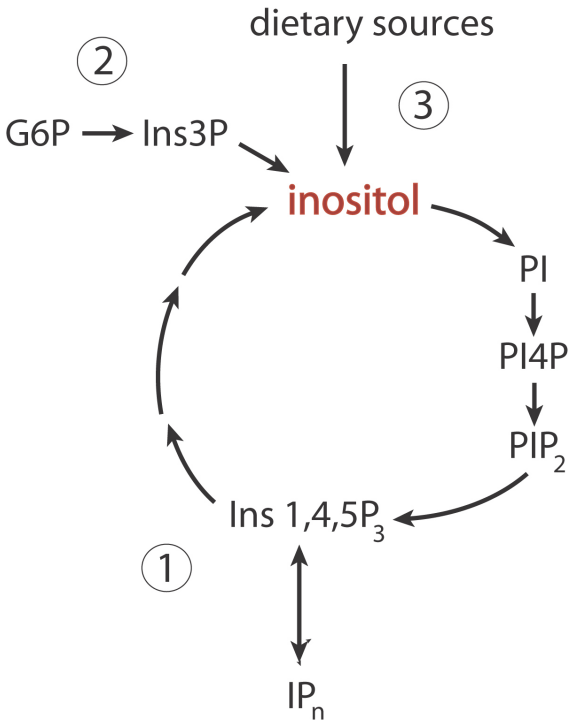

Figure 3: Mechanisms of maintaining constant inositol levels in cells. There are three ways to maintain a constant inositol level in cells. 1: higher phosphorylated inositol phosphates (IP_n) and phosphatidylinositol phosphates are recycled back to inositol. PI: phosphatidylinositol, PI4P: phosphatidylinositol 4-phosphate, PIP_2: phosphatidylinositol 4,5-bisphosphate. 2: Some tissues are able to form inositol from glucose 6-phoshate (G6P) through inositol 3-phopshate (Ins3P). 3: Inositol is part of the daily diet. 1 g inositol in the form of inositol, phytic acid and inositol lipids is consumed daily.

Inositol is required for PI synthesis. In cells, it is produced by recycling of higher phosphorylated inositol phosphates back to inositol. Some tissues, such as brain, testis and especially kidney are able to produce inositol de novo from glucose 6-phosphate (figure 3). Interestingly, the inositol ring can not only be phosphorylated with monophosphates, specific kinases can add a pyrophosphate group onto certain positions of the inositol ring. Pyrophosphate bonds are high energy bonds and therefore have the potential to act as phosphate donors, such as ATP. Thus, inositol pyrophosphates are putative "high energy" second messenger (Menniti *et al.*, 1993; Stephens *et al.*, 1993), but whether they can act as

phosphate donors is still unclear. The metabolic pathway which leads to the syntheses of the inositol pyrophosphates (figure 4) and their possible roles in cell signaling will be discussed in the following paragraphs.

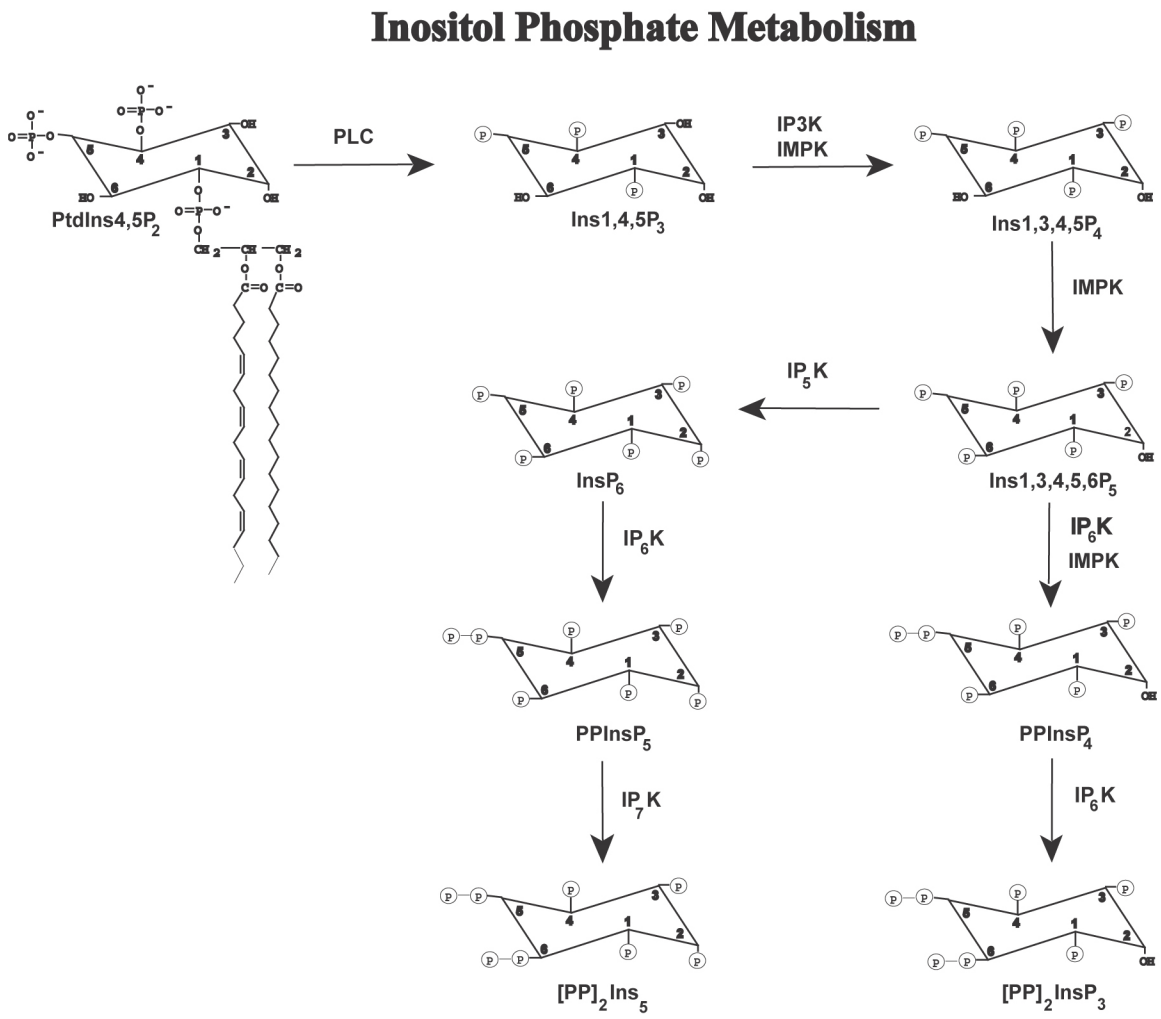

Figure 4: Metabolic pathway of inositol pyrophosphate production. Phosphatidyinositol 4,5-bisphosphate (PIP_2) is the source for inositol phosphates in mammalian cells. Cleavage of PIP_2 by phospholipase C (PLC) results in the production of inositol 1,4,5-trisphosphate (IP_3). IP_3 is further phoshorylated by a variety of kinases to IP_8 and $PPIP_4$. IP3K=inositol 1,4,5-trisphosphate 3-kinase, IPMK=inositolphosphate multikinase, IP_5K=inositol 1,3,4,5,6-pentakisphosphate 2-kinase, IP_6K=inositol hexakisphosphate kinase, IP_7K=inositol heptakisphosphate kinase

1.1.1 Inositol 1,4,5-trisphosphate 3-kinase

The key step in the metabolic pathway of inositol pyrophosphate production is catalized by the inositol 1,4,5-trisphosphate 3-kinase (IP3K). It utilizes inositol 1,4,5-trisphosphate (IP_3) to produce inositol 1,3,4,5-tetrakisphosphate (IP_4). IP_3 is formed by receptor activated hydrolysis of Phosphatidylinositol 4,5-bisphosphate (PIP_2) by Phospholipase C (PLC), which is the source of all inositol phosphates. In response to various extracellular stimuli, such as hormones, growth factors and neurotransmitters, PLC is activated by receptor tyrosine kinases or phosphatidylinositol 3,4,5-trisphoshate (PIP_3) and hydrolyzes PIP_2, producing two second messengers, diacylglycerole (DAG) and IP_3. DAG directly activates protein kinase C, which has been implicated to play a role in many cellular physiological functions, such as secretion, cell proliferation, cell growth and differentiation. IP_3 can bind to IP_3 specific receptors to regulate Ca^{2+} release from intracellular stores into the cytosol (Streb *et al.*, 1983). IP_3 is further phosphorylated on the third position of the inositol ring to form inositol 1,3,4,5-tetrakisphosphate (IP_4) by this specific group of kinases, inositol 1,4,5-trisphosphate 3-kinases (IP3K). IP3K is the most active inositol phosphate kinase detectable in mammals. It leads to a rapid turnover of IP_3 to IP_4, which results in inactivation of the IP_3 signal, potentially one function of IP3Ks. There are three different IP3K isoforms, type A, B and C, all of which are regulated by calmodulin. IP3K A and B are also phosphorylated by Ca2+/calmodulin dependent kinase (Takazawa *et al.*, 1988; Choi *et al.*, 1990; Lee *et al.*, 1990; Takazawa *et al.*, 1990; Takazawa *et al.*, 1990; Thomas *et al.*, 1994; Communi *et al.*, 1997; Woodring *et al.*, 1997; Communi *et al.*, 1999; Dewaste *et al.*, 2000).

Figure 5: Family of inositol phosphate kinases. The family of inositol phosphate kinases shares a conserved carboxyl-terminus (blue), containing a highly conserved inositol phosphate binding domain (pink). The amino-terminus of this family is diverse and contains regulatory and targeting regions, such as calmodulin binding domain (green) and F-actin binding domain (yellow).

All IP3Ks share a conserved carboxyl terminus, which contains the catalytic domain. It is also conserved between members of the inositolphosphate kinase family (figure 5). The amino-terminus is more diverse and plays a role in targeting and regulating. (Soriano *et al.*, 1997; Togashi *et al.*, 1997; Dewaste *et al.*, 2003). For example, the N-terminal end of rat IP3KA targets the enzyme to filamentous actin rich dendritic spines in neurons (Schell *et al.*, 2001). Truncated rat IP3KB was shown to localize at the endoplasmatic reticulum and the cytosol (Soriano *et al.*, 1997). Recently it has been reported that rat IP3KC is able to shuttle actively between the nucleus and cytoplasm. A putative nuclear localization site (NES) is located in the N-terminus of IP3KC. (Nalaskowski *et al.*, 2003).

Besides inactivating the IP_3 signal IP_4 has been implicated to act as a second messenger itself. It has been suggested that IP_4 plays a role in Ca^{2+} signaling itself, specifically in Ca^{2+} homeostasis, transferring calcium between intracellular stores and regulating calcium entry across the plasma membrane (Irvine, 1991). Irvine and colleges showed that IP_4 can bind and activate a GTPase activating protein (GAP) of the GAP1 family (GAP^{IP4BP}) *in vitro* which has GAP activity against Ras, suggesting a role in a variety of signaling pathways (Cullen *et al.*, 1995). Whether GAP^{IP4BP} is the IP_4 effector in Ca^{2+} signaling still remains unclear. In mouse L-1210 lymphoma cells, addition of GAP^{IP4BP} enhanced the ability of IP_4 to potentiate IP_3 stimulated Ca^{2+} release. (Cullen *et al.*, 1990; Loomis-Husselbee *et al.*, 1996) However, changes in GAP^{IP4BP} levels in other cell lines failed to have any effect on Ca^{2+} release (Walker *et al.*, 2002). Despite the studies mentioned above there is still some debate over whether IP_4 has a biological significant function at all.

Independent of the possibility of IP_4 to act as a second messenger, it is a substrate for other inositol phosphate kinases to produce higher phosphorylated inositol phosphates. Thus, the activity of IP3Ks is responsible for regulating the levels of a large number of inositol phosphates that might be important in cellular signaling.

1.1.2 Inositol polyphosphate multikinase

Inositol polyphosphate multikinase (IPMK) has the ability to utilize a variety of inositol phosphates as substrates. IPMK was first discovered in yeast as the only known inositol phosphate kinase that is able to phosphorylate IP_3. IPMK from yeast is also known as Ipk2, or Arg82. Ipk2 was discovered in a genetic screen to find proteins that are involved in mRNA export. (York *et al.*, 1999). Later it was reported that Ipk2 is a multi specific IP_3/IP_4 kinase (Ipk2) which contains the same conserved elements in the catalytic domain than IP3K and belongs to the same family of inositol phosphate kinases (figure 5). It is encoded by the same gene Arg82 is (Odom *et al.*, 2000; Saiardi *et al.*, 2000). Arg82 was only known to be an transcription factor in the ArgR-Mcm1 complex. This complex compromises four proteins, Arg80, Arg81, Arg82 and Mcm1. Arg80 and Arg81 function as argenine specific transcription factors, whereas Arg82 and Mcm1 are pleiotropic transcription factors. (Bechet *et al.*, 1970; Messenguy *et al.*, 1993). Later it was discovered that Ipk2 is able to utilize IP_3 to produce inositol 1,3,4,5-tetrakisphosphate, but in contrast to IP3Ks in mammals Ipk2 predominantly phosphorylates IP_3 on the sixth position of the ring to produce inositol 1,4,5,6-tetrakisphosphate, which is the predominant isoform in yeast. This IP_4 isomer can then be further phosphorylated to inositol 1,3,4,5,6-pentakisphosphate (IP_5). (Odom *et al.*, 2000; Saiardi *et al.*, 2000). Interestingly, Ipk2 has the ability to produce one inositol pyrophosphate *in vitro*. Another phosphate group can be added by Ipk2 on the fifth position of the inositol ring of IP_5 to produce PP-IP_4 (figure 7) (Zhang *et al.*, 2001).

In yeast the pathway described above seems to be the only pathway to produce inositol hexakisphosphate (IP_6) since a yeast Ipk2 deletion mutant failed to produce any IP_6. Instead, this mutant accumulated high amounts of IP_3 suggesting that there is no other inositol phosphate kinase, that is able to phosphorylate IP_3 (Saiardi *et al.*, 2000). Functional studies of this deletion mutant showed that Ipk2 protein but not kinase activity is required to form the ArgR-Mcm1 transcriptional complex on DNA promotor elements. Nevertheless, inositol kinase activity and thereby production of inositol phosphates was necessary for this complex to be active, implicating a role for inositol phosphates in transcriptional regulation. (Odom *et al.*, 2000).

In mammals IPMK seems to have a different substrate specificity than the yeast enzyme. Saiardi *et al.* reported that rat IPMK (rIPMK) is capable of phosphorylating inositol 4,5-bisphosphate to IP_3, which would be a novel pathway to produce IP_3. Further rIPMK can utilize IP_3 to produce IP_4, the same way than IP3Ks. IP_4 can then be further phosphorylated to IP_5 (Saiardi *et al.*, 2001). Recently it has been reported that human IPMK (hIPMK) has a different substrate specificity than the rat isoform. It has been proposed that hIPMK prefers inositol 1,3,4,6-tetrakisphosphate as a substrate to generate IP_5. Additionally, hPMK was not able to rescue the Ipk2 deletion mutant, suggesting that the human and yeast kinase have different preferences for substrates or protein binding (Chang *et al.*, 2002). The question why the rat and the human isoforms of IPMK have different substrate specificities remains unanswered. Thus, the *in vivo* substrate usage of IPMK in rat and human is still to be investigated. However, both postulated pathways lead to the production of IP_5 and until now there has not been another inositol phosphate kinase discovered that is able to produce IP_5.

inositol 1,3,4,5,6-pentakisphosphate

Inositol 1,3,4,5,6-pentakisphosphate is the predominant IP_5 isoform in mammalian cells. It serves as metabolic precursor for higher phosphorylated inositol phosphates, but whether it has any other physiological function in mammalian cells remains unknown. In several animal species with nucleated erythrocytes, IP_5 can bind to haemoglobin and thereby impair the normal regulation of its affinity for O_2 by 2,3-bisphosphateglycerate (Arnone *et al.*, 1974). The significance of the haemoglobin-IP_5 interaction still remains to be investigated. It has also been reported that IP_5 plays a role in chromatin remodeling (Shen *et al.*, 2003; Steger *et al.*, 2003), that will be discussed in paragraph 1.2.

1.1.3 Inositol 1,3,4,5,6-pentakisphosphate 2-kinase

Yeast inositol 1,3,4,5,6-pentakisphosphate 2-kinase (Ipk1) was found in the same genetic screen than Ipk2, as a protein important for m-RNA export (York *et al.*, 1999). Ipk1 does not share sequence homology with any inositol phosphate kinase and does not belong to this specific family of inositol phosphate kinases (Ives *et al.*, 2000). Studies with protein A-tagged Ipk1 in yeast showed that Ipk1 was localized in the nucleus and at the nuclear pore complex, implicating a role in nuclear signaling events and/or nuclear transport. The localization of Ipk1 was confirmed by subcellular fractionation of the cells. The majority of protein A tagged Ipk1 was purified with the nuclei. Overexpression of protein A tagged Ipk1 in Ipk1 deletion mutants rescued the mRNA deficient phenotype (York *et al.*, 1999). This data suggests that the production of IP_6 is required for mRNA export from the nucleus. Recently the human homologue, inositol 1,3,4,5,6-pentakisphosphate 2-kinase (IP_5K), was cloned (Verbsky *et al.*, 2002)

inositol hexakisphosphate

Inositol hexakisphosphate, also known as phytic acid, was the first inositol phosphate discovered. It was found to serve as phosphate store for seeds in plants. About 50-80 % of the total phosphorous in plants is IP_6. But the concentration of IP_6 is not only high in plants, it is the most abundant inositol phosphate in mammalian cells. In general, the intracellular concentration is between 10 and 60 μM in animals and can be up to 700 μM in slime moulds (Martin *et al.*, 1987; Szwergold *et al.*, 1987; Pittet *et al.*, 1989). However, it is doubted that all cellular IP_6 is free in the cytosol, because it has the tendency to form insoluble complexes with divalent cations (Irvine *et al.*, 1988). Since there is no evidence for precipitates of IP_6 in animals, it is still unclear, how precipitation of IP_6 is prevented. There is evidence from *in vitro* studies that IP_6 is bound to the plasma membrane. The polyphosphate is proposed to be held in place by the formation of an electrostatically bonded IP_6-cation-phospholipid sandwich (Poyner *et al.*, 1993). A significant amount of IP_6 is also believed to be bound to proteins. In recent years, IP_6 has been shown to interact *in vitro* with several intracellular proteins which will be explained in the following paragraphs.

IP_6 in vesicular trafficking

Studies showed that IP_6 has the ability to bind with high affinity to AP2. AP2 is an adaptor protein that promotes the formation of clathrin coated vesicles in receptor mediated endocytosis (Beck *et al.*, 1991; Chang *et al.*, 1993). IP_6 was able to inhibit AP2 mediated clathrin assembly (Theibert *et al.*, 1991; Chadwick *et al.*, 1992; Timerman *et al.*, 1992; Voglmaier *et al.*, 1992). Additionally IP_6 was found to bind to AP3 which is an adaptor protein similar to AP2, but it is only expressed in neuronal cells, suggesting a role in synaptic vesicle biogenesis and recycling (Kohtz *et al.*, 1988; Sousa *et al.*, 1992; Morris *et al.*, 1993; Zhou *et al.*, 1993). IP_6 also inhibits AP3 mediated clathrin assembly reaching a maximum of inhibition at a physiological relevant concentration of 25 – 50 μM (Norris *et al.*, 1995). IP_5 and inositol hexasulfate (IS_6), which is used as a high charge control, failed to inhibit endocytosis by binding to AP2 and AP3, implicating that the six phosphate groups are necessary for the inhibitory function of IP_6 and that the interaction is not due to high charge of the molecule.

Recently, Hilton *et al*. discovered a IP_6 regulated protein kinase that phosphorylates pacsin/syndapin I. Pacsin/syndapin I is a synaptic vesicle-associated protein that couples the endocytotic machinery to the cytoskeleton and is highly expressed in brain. Phosphorylation of the protein leads to an increase in interaction of pacsin/syndapin I with dynamin I, which is one of the proteins of a multiprotein complex involved in clathrin-mediated synaptic vesicle recycling at nerve terminals. IP_6 was able to stimulate the protein kinase activity in a dose dependent manner with maximal effect at a concentration of 50 μM (Hilton *et al.*, 2001) and thus, regulates the assembly of a protein involved in the endocytotic machinery. These data suggest that IP_6 might play a role in vesicle trafficking *in vivo*. The concentrations of IP_6 used in these studies were all in the physiological range of IP_6 in mammalian cells . Additionally, IP_4, IP_5 and IS_6 did not show an effect, suggesting a specific role for IP_6.

IP_6 in mRNA export

The yeast data described in chapter 1.1.3 leads to the hypothesis that IP_6 is involved in regulating m-RNA export. Deletion mutants in the pathway of IP_6 production, including Plc, Ipk2 and Ipk1, showed an defect in m-RNA export out of the nucleus (York *et al.*, 1999; Saiardi *et al.*, 2000). Interestingly, a similar phenomenon was observed in mammalian cells. Overexpression of a bacterial inositol phosphate phosphatase (SopB) in the nucleus diminished nuclear inositol phosphate levels, including IP_5 and IP_6, and inhibited nuclear export of polyadenylated mRNA (Feng *et al.*, 2001), suggesting a role for inositol phosphates, specifically IP_6, in mRNA export.

IP_6 in DNA repair

It has been shown that IP_6 might be involved in DNA double strand break repair, specifically in non homologous endjoining (NHEJ). NHEJ is a DNA ligase dependent DNA repair mechanism, independent of homologous recombination. One of the enzymes involved in NHEJ is DNA-PK. DNA-PK consists of the catalytic subunit and the Ku70 and Ku80 DNA binding subunits. The DNA-PK complex binds to the free DNA ends and protects them from nucleases, while the NHEJ complex ligates the free DNA ends together (figure 6). Inositol hexakisphosphate was found to act as a cofactor for the DNA-PK complex in non-homologous endjoining *in vitro* and stimulated NHEJ activity at a concentration of 100 nM, indicating that intracellular concentration of IP_6 would be more than sufficient to stimulate NHEJ activity. Lower phosphorylated inositol phosphates showed less or no effect on NHEJ activity, and IS_6 was not able to stimulate NHEJ activity either, suggesting that the effect is IP_6 specific. (Hanakahi *et al.*, 2000; Hanakahi *et al.*, 2002; Ma *et al.*, 2002)

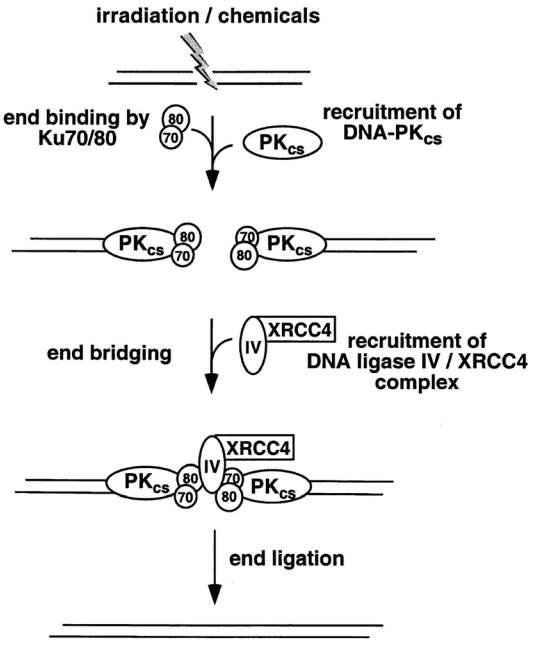

Figure 6: Mechanism of non homologous endjoining. After DNA damage by irradiation or chemicals the DNA-PK-Ku70/80 protein complex binds to free DNA ends. The DNA ligase complex is recruited to the site of the DNA damage and ligates the free DNA ends together.

IP_6 as anti-cancer agent

A striking anti cancer action of IP_6 has been demonstrated *in vitro* and *in vivo*, which is based on the hypothesis that exogenously added IP_6 may be internalized, dephosphorylated, and inhibits cells growth. The molecular mechanism by which IP_6 functions as an anti cancer agent has not yet been defined. Some studies showed that IP_6 arrested carcinoma cells in G1-phase of the cycle (El-Sherbiny *et al.*, 2001; Singh *et al.*, 2003), which might be a reason for the effect of IP_6 as an anti cancer agent. One hypothesis for how IP_6 blocks cells in G1-phase is by inhibiting cyclin dependent kinases (CDK), which modulate cell cycle progression. Their activation and inactivation are important steps to progress from one phase of the cell cycle to another. CDK inhibitors (CDKI) negatively regulate cell cycle progression from one stage to the other (Grana *et al.*, 1995). Exogenous IP_6 strongly increased expression of two CDKI, Cip17p21 and Kip1/p27, that led to an inactivation of cyclin dependent kinase 2, 4 and 6 (CDK2, 4 and 6) and cyclin D1 and E associated kinases. Further studies showed that

IP_6 also increased hyperphosphorylated levels of the retinoblastoma related proteins, pRb/p107 and pRb2/p120. These molecular effects of IP_6 could be one of the possible mechanisms that result in G1 arrest (Singh *et al.*, 2003)

Other studies suggest that IP_6 can act through the Akt-NFκB pathway. Treatment of Hela cells with 1 mM IP_6 induced apoptosis by inhibiting the Akt-NFκB pathway (Ferry *et al.*, 2002). Phosphatidylinositol 3-phosphate kinase (PI3K) is a key regulator upstream of Akt (protein kinase B). PI3K phosphorylates phosphatidylinositol ,4,5-bisphosphate (PIP_2) to phosphatidylinositol 3,4,5-trisphosphate (PIP_3). Translocation of Akt to the plasma membrane by binding to PIP_3 activates Akt and transforms it in its phosphorylated active form, which then leads to nuclear localization of the transcription factor NFκB. This pathway is known to be a strong cell survival pathway (Ozes *et al.*, 1999). It has been shown that IP_6 inhibits Akt activation, but not PI3K activity. By binding to Akt IP_6 probably inhibits Akt binding to PIP_3 and therefore inhibits translocation of Akt to the plasmamembrane (Ferry *et al.*, 2002). The hypothesis is, that Akt then remains in its inactive form, NFκB does not translocate to the nucleus and the cells undergo apoptosis.

These are two examples how IP_6 might act as anti-cancer agent. In both cases it was shown that after adding IP_6 to the cells the level of lower inositol phosphates, specifically IP_4 and IP_5 increased. Treatment of HeLa cells with IP_4 and IP_5 had the same antiproliferating and apoptotic effect than IP_6. It remains to be investigated which inositol phosphate has the best potential to act as anti cancer drug. There is no report about inositol pyrophosphate levels after IP_6 treatment and it might be interesting to determine if these potential second messengers might play a role in IP_6 induced cell cycle arrest.

The concentration used in these assays was between 1 and 5 mM. This is above the physiological range (10-70 μM) of IP_6. Whether the anti cancer effect is due to a high concentration of IP_6 or whether IP_6 plays a biological significant role in cell cycle events remains to be investigated.

1.1.4 Inositol hexakisphosphate kinase

As mentioned earlier IP_6 was the first inositolphosphate discovered. For a long time it was believed that IP_6 is the highest phosphorylated form of inositol phosphates in cells. Using ^3H-inositol to label cells, it was shown by HPLC analysis that higher phosphorylated forms of inositol phosphate exist (Glennon *et al.*, 1993; Menniti *et al.*, 1993). These so called inositol pyrophosphates contain a pyrophosphate group on the fifth and sixth position on the completely phosphorylated inositol ring (figure 7) (Albert *et al.*, 1997). This pyrophosphate bond is a high energy bond and it has been proposed that inositol pyrophosphates may be high energy second messengers and may serve as phosphate donors for protein phosphorylation. Until now there is no proof that inositol pyrophosphates can serve as phosphate donors.

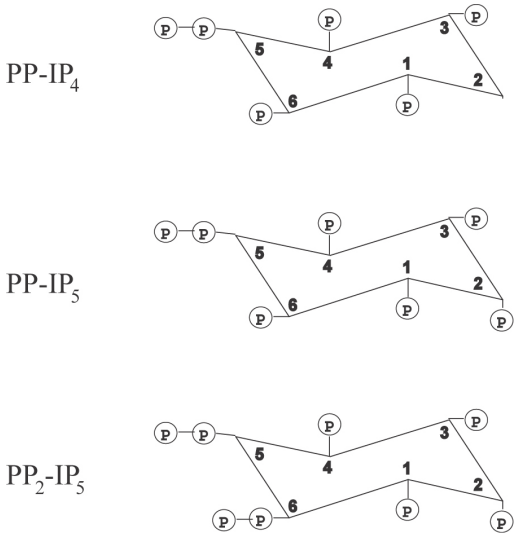

Figure 7: Inositol pyrophosphates in mammalian cells. Inositol pentakisphosphate and inositol hexakisphosphate are precursor for inositol pyrophosphate production. The inositol ring can contain a pyrophosphate group on the fifth position. The most common position for the second pyrophosphate group is the sixth position, though the first and second position have also been discussed as putative sites for pyrophosphate groups.

The phosphorylation of IP_6 to inositol heptakisphosphate (IP_7) is catalyzed by inositol hexakisphosphate kinase (IP_6K), the phosphorylation of IP_7 to IP_8 by inositol heptakisphosphate kinase (IP_7K). IP_7K has not yet been cloned, but active IP_7 kinase has been purified from different cell types (Huang *et al.*, 1998). Putative functions of IP_6Ks and inositol pyrophosphates will be discussed in this chapter.

1.1.4.1 Inositol hexakisphosphate kinase in mammals

Irvine and colleagues discovered inositol IP_6Ks by looking at a protein called PiUS (P_i-update stimulator). Injection of PiUS cRNA into xenopus oocytes led to an Na^{2+} dependent P_i uptake (Norbis, 1997). Sequence analysis of PiUS showed similarities to the family of inositol phosphate kinases. Examination of different inositol phosphates as substrates for PiUS showed that PiUS contains kinase activity towards IP_6 (Schell *et al.*, 1999). Thus, it was named inositol hexakisphosphate kinase. In earlier studies, fractions with IP_6K activity were purified from rat brain (Voglmaier *et al.*, 1996). Later, analysis of this protein by peptide mass fingerprinting and DNA data base screening resulted in the sequence of two different IP_6K isoforms, IP_6K1 and IP_6K2 (Saiardi *et al.*, 1999). IP_6K2 is the same protein than PiUS. Recently, a third isoform of IP_6K, IP_6K3, was identified (Saiardi *et al.*, 2001). The kinases contain a highly conserved carboxyl-terminus and a more diverse amino-terminus with homology domains unknown function (figure 8).

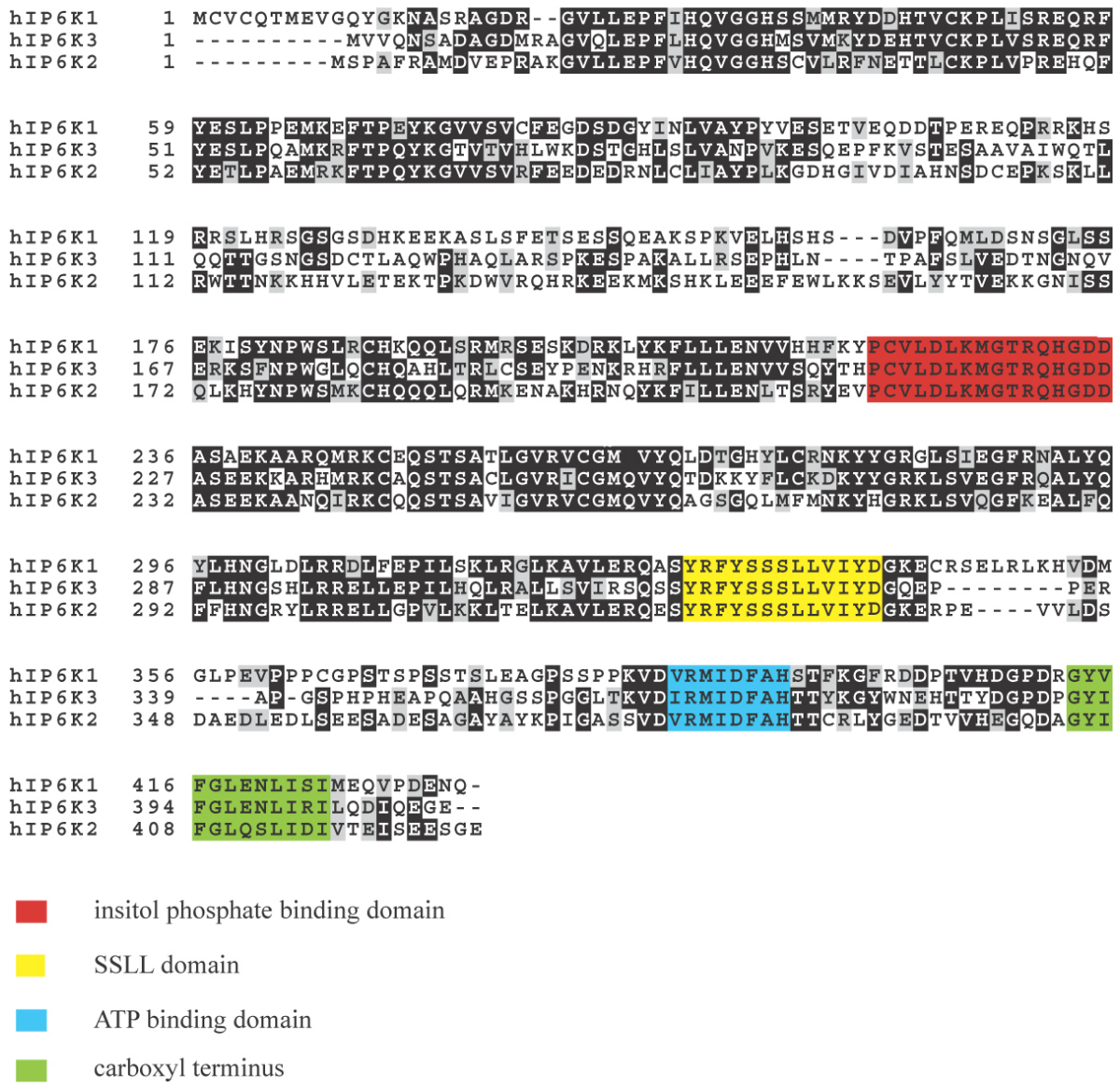

Figure 8: Alignment of human inositol hexakisphosphate kinase isoforms. Insitol hexakisphoshate kinases contain conserved carboxyl-terminus with four distinct domains. The first one is the insitol phosphate binding domain (red), which is the catalytic center, the second one is the SSLL (yellow), which is important for kinase activity, the third one is the ATP binding domain (blue) and the fourth one is a domain at the end of the carboxyl-terminus and its function is still unclear. These four domains are conserved between members of the family of inositol phosphate kinases described in figure 5.

All of the three IP_6K isoforms are not only able to phosphorylate IP_6 to IP_7, they can also utilize I 1,3,4,5,6 P_5 to produce a different inositol pyrophosphate, diphosphoinositol tetrakisphosphate (PP-IP_4). PP-IP_4 also contains a pyrophosphate group on the fifth position of the insitol ring, but does not have a phosphate group on the second position (Saiardi *et al.*, 1999; Saiardi *et al.*, 2000; Saiardi *et al.*, 2001). Though all three isoforms are able to phosphorylate IP_5 and IP_6 *in vitro*, they have different activities towards the substrates and show different subcellular localizations (Saiardi *et al.*, 2000; Saiardi *et al.*, 2001), suggesting a specific *in vivo* function for the different isoforms depending on their substrate preference and localization. Interestingly, it was shown that IP_6K also contained ATP synthase activity. It was able to transfer a phosphate group from IP_7 to ADP to produce ATP (Voglmaier *et al.*, 1996), which implicates that IP_7 is able to serve as phosphate donor. It remains to be investigated if the phosphate group can also be transferred onto proteins.

The function of IP_6K and inositol pyrophosphates is still unclear. There is some evidence that IP_6Ks are involved in vesicle trafficking and cell proliferation. In a yeast two hybrid screen IP_6K1 was found to bind a guanine nucleotide exchange factor (GEF) for Rab3A, named GRAB. Rab3A is a member of the Rab family of small G-proteins that are involved in vesicle trafficking in many different cell types. Rab3A is specifically expressed in neuronal cells and is localized at synaptic vesicles. GRAB functions as a GEF and exchanges GDP, bound to Rab3A, to GTP and thereby activates Rab3A. IP_6K1 can compete with Rab3A for GRAB binding and hence, compete in regulating the GTP loading of Rab3A. The effect was independent of kinase activity, since a IP_6K1 kinase dead mutant was also able to compete with Rab3A, suggesting that the protein but not the inositol pyrophosphates influences the interaction of GRAB to Rab3A (Luo *et al.*, 2001). Interestingly, IP_7 and IP_8 bind with the same affinity to proteins involved in vesicle trafficking than IP_6 (see chapter 1.1.3), supporting the hypothesis that inositol pyrophosphates might also play a role in vesicle trafficking (Voglmaier *et al.*, 1992; Ye *et al.*, 1995).

There is no evidence that IP_6K2 is involved in vesicle trafficking events. Instead, IP_6K2 was shown to be involved in cell proliferation and apoptotic events. In ovarian carcinoma cells IP_6K2 mediated interferon β (INFβ) induced apoptosis. (Morrison *et al.*, 2001). In general the family of interferons (INF) stimulate antiviral, antitumor, antiproliferative and immunoregulatory activities. INFβ supressed the growth of ovarian tumor xenografts in nude

mice through apoptosis. One gene involved in INFβ induced cell death is IP_6K2. Antisense DNA that knocked out IP_6K2 levels in ovarian cancer cells resulted in a resistant to INFβ induced apoptosis. In contrast, overexpression of IP_6K2 enhanced the apoptotic effects of INFβ. An IP_6K2 dominant negative mutant, was resistant to the antiproliferative and apoptotic functions of INFβ (Morrison *et al.*, 2001). Thus, kinase activity and therefore inositol pyrphosphates were necessary to enhance the apoptotic effect of INFβ. This data suggests a role for IP_6K2 in INFβ induced apoptosis in ovarian carcinoma cells.

More evidence that IP_6K2 might be involved in cell proliferating events came from a different direction. IP_6K2 was found in a screen for target genes of β-catenin induced transcription. In the cytoplasm β-catenin plays a role in cell adhesion. After receptor activated hyperphosphorylation of β-catenin, it is translocated to the nucleus and binds to the lymphoide-enhancer binding factor (LEF) to form a transcriptional complex that activates specific target genes (Eastman *et al.*, 1999; Mann *et al.*, 1999). One of the genes discovered to be upregulated after nuclear translocation of β-catenin was IP_6K2 (Aoki *et al.*, 2002).

In summary, IP_6K1 has been suggested to play a role in vesicle trafficking, specifically in brain, whereas IP_6K2 might be involved cell proliferating events.

1.1.4.2 Inositol hexakisphoshate kinase in yeast

There is a single known IP_6K in yeast (KCS1). KCS1 was found in a genetic screen with mutated protein kinase C (PKC) (Huang *et al.*, 1995). The PKC mutant showed abnormalities in recombination which could be rescued by deletion of KCS1. These studies suggested that inositol pyrophosphates are required for DNA hyperrecombination in Pkc mutants in yeast (Huang *et al.*, 1995; Luo *et al.*, 2002). Later it was reported that KCS1 is an inositol hexakisphosphate kinase (Saiardi *et al.*, 1999). A deletion mutant of IP_6K resulted in endocytotic defective phenotype. The cells showed abnormal vacuole morphology and endocytosis was inhibited (Dubois *et al.*, 2002; Saiardi *et al.*, 2002), supporting the hypothesis that IP_6Ks are involved in vesicle trafficking. The same phenotype was observed in Ipk2, but not in Ipk1 deletion mutants. Ipk1 mutants do not produce IP_6 but contain high

concentration of IP_5, which can be utilized by IP_6K to produce $PPIP_4$, suggesting that inositol pyrophosphates in general and not only IP_7 and IP_8 might be important for vacuole morphology in yeast.

1.1.4.3 Diphosphoinositol phosphate phosphohydrolase

Inositol pyrophosphates are turned over rapidly. Inhibiting phosphatases in cell lysates with 10-50 mM NaF resulted in an dramatic increase of IP_7 and IP_8, which are generally difficult to detect in mammalian systems (Glennon *et al.*, 1993). The phosphatases catalyzing the dephosphorylation of IP_7 and IP_8 are diphosphoinositol-polyphosphate phosphohydrolases (DIPP). There are five different isoforms of DIPP cloned, DIPP1 (Safrany *et al.*, 1998), DIPP2α and β (Caffrey *et al.*, 2000) and DIPP3α and β (Hidaka *et al.*, 2002). The active site of this enzyme contains the Nudix type (NudT or MutT) motif (Safrany *et al.*, 1998). NudT motifs are also present in the active site of a family of enzymes that hydrolyze nucleoside phosphates. They have also been identified in a transcriptional regulator (Gaudon *et al.*, 1999) and in a protein regulating mRNA decay (Dunckley *et al.*, 1999). The family of enzymes containing a NudT motif have been proposed to act as "surveillance enzymes" (Xu *et al.*, 2001), that function to eliminate potentially toxic metabolites from the cell and to regulate concentrations and availability of substrate, cofactors and signaling molecules (Bessman *et al.*, 1996). DIPP are the only enzymes in this family that utilize inositol pyrophosphates and not nucleosides. The specific function of DIPP remains to be determined. It has bee speculated that inositol pyrophosphates could influence proteins the same way GDP and GTP regulate G-protein function. In this case the rapid turnover of IP_7 and IP_8 by phosphatases would be as important as the production of inositol pyrophosphates (figure 9).

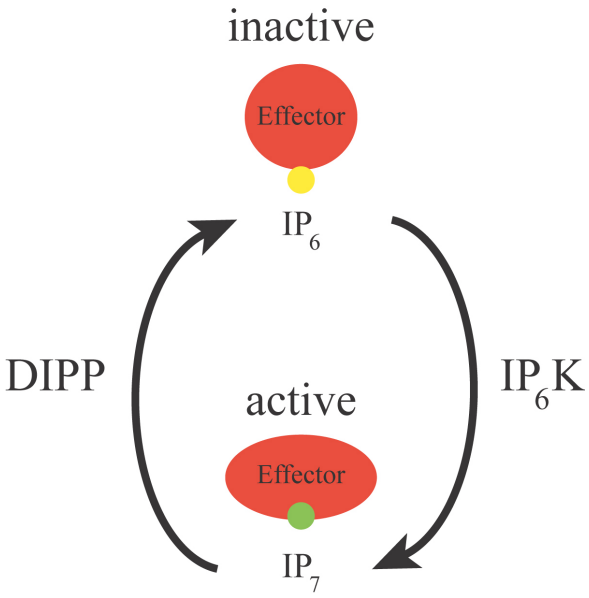

Figure 9: Model for how inositol pyrophosphates might act as molecular switches. IP_6 (yellow) bound to an effector (red) might keep it in an inactive state. After phosphorylation of IP_6 by inositol hexakisphosphate kinases (IP_6K), IP_7 (green) might still remain bound to the effector, but might induce a conformational change, which results in an activation. Dephosphorylation of IP_7 by diphosphoinositol phosphate phosphohydrolases (DIPP) results in regeneration of the IP_6 bound inactive form.

1.2 Nuclear inositol phosphate signaling

In yeast two putative functions for inositol phosphates in the nucleus have been reported in the past. First, the transcription factor ARG82 is an inositolphosphate multi kinase (Ipk2) and inositolphosphate kinase activity seems to be important for the transcriptional complex to be active (see 1.1.2). Second, production of IP_6 has been implicated in mRNA export in yeast. In mammals there is no evidence that inositol phosphates are involved in transcription, but it has been postulated that they play a role in mRNA export (see 1.1.3).

Recently, a new nuclear function for inositol phosphates in yeast and higher eukaryotes has been suggested. Different inositol phosphates influence ATP-dependent chromatin remodeling in different ways. IP_6 inhibits nucleosome mobilization by inhibiting nucleosome-dependent ATPase activity in drosophila and yeast, but IS_6 and IP_5 do not.

Instead, inositol 1,4,5,6-tetrakisphosphate, which is the major IP_4 isomer in yeast, and IP_5 stimulated nucleosome mobilization (Shen *et al.*, 2003). This data was confirmed by the fact, that in yeast Plc and Ipk2 deletion mutants failed to modulate the ability of chromatin remodeling complexes to induce transcription (Steger *et al.*, 2003). Inositol pyrophosphates did not seem to play a role in chromatin remodeling events.

Currently available data about localization and function of inositol phosphates is summarized in figure 10.

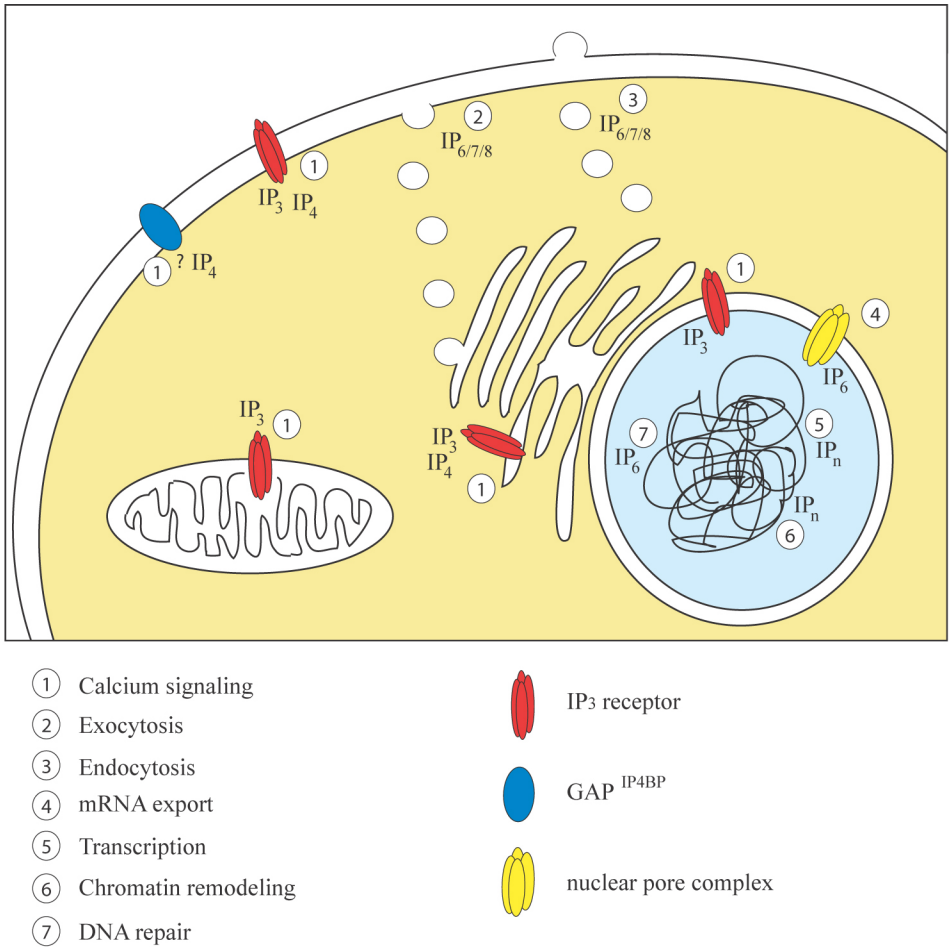

Figure 10: Localization and putative function of inositol phosphates. Inositol phosphates have been implicated to play a role in a variety of signaling events in different compartments of the cell. IP_3 and IP_4 have been reported to be involved in Ca 2+ signaling (1) at the plasma membrane, endoplasmatic reticulum and mitochondria. IP_6, IP_7 and IP_8 might play a role in vesicle trafficking events (2 and 3). A variety of inositol phosphates have been suggested to be involved in nuclear signaling events, such as mRNA export (4), transcription (5), chromatin remodeling (6) and DNA repair (7).

1.3 Inositol phosphates in cell cycle

There is some evidence that inositol pyrophosphate might play a role during the cell cycle of the single cell slime mold *Dictyostelium discoideum*. During the life cycle of *D. discoideum* IP_6 and IP_8 levels changed whereas IP_7 concentration remained constant. In the first two hours of starvation the amount of IP_6 increased more than two-fold and then decreased transiently during the next three hours. At the same time the concentration of IP_8 increased (figure 11), suggesting a role for IP_8 in the life cycle of *D. discoideum* (Laussmann *et al.*, 2000).

Early studies showed, that levels of highly phosphorylated inositol phosphates can change after receptor activation or during cell cycle progression in mammalian cells. For example, in the myolide cell line HL-60 stimulation with the chemotactic peptide formyl- methiony-leucyl-phenylalanine (fMLP) led to distinct alteration in at least seven different inositol phosphates. Four different IP_4 isoforms showed a four fold increase in intracellular concentration after peptide stimulation, whereas IP_5 concentration was only 1,5 fold higher and IP_6 did not change at all (Pittet *et al.*, 1989). In proliferating rat thymocytes it was demonstrated that IP_5 and IP_6 levels underwent changes during cell cycle progression. At the beginning of the cell cycle IP_5 and IP_6 levels were decreased and stayed constant in S-phase. The intracellular concentration of both inositolphosphates was high during cell division (Guse *et al.*, 1993). Intracellular levels of inositol pyrophosphates were not investigated in the experiments. The only molecular mechanism of IP_5 and IP_6 involved in cell cycle events has been reported in studies with IP_6 as anti cancer agent (see chapter 1.1.3). In these studies IP_6 was added to cells in very high concentrations, above the physiological range, and it is not known if these mechanisms as discussed for IP_6 play a role in biological systems.

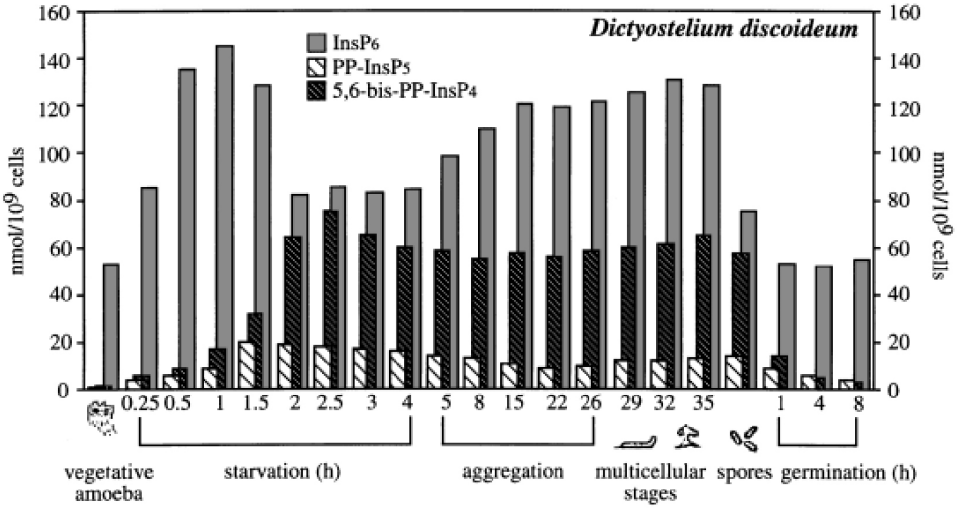

Figure 11: Amounts of highly phosphorylated inositol phosphate during the life cycle of *D. discoideum* (Laussmann *et al.*, 2000).

1.4 Cell signaling in mitosis

In this study it is proposed that inositol hexakisphosphate kinases are involved in cell cycle regulating events, specifically in mitosis. To understand some of the experiments carried out in this thesis, a short introduction in mitotic signaling events is presented in this chapter.

Mitosis can be divided into different phases. In prophase the chromosomes start to condense and the centromeres are localized at the opposite sites of the nucleus. Once the cells enter metaphase the chromosome align at the metaphase plate, the spindles form and attach at the chromosome to separate the sister chromatides in anaphase. In telophase the separation is finished and the cytokinese takes place to create two identical daughter cells. These phases have to be highly regulated to ensure that the chromatides are separated correctly, resulting in two identical daughter cells. The key steps in cell signaling in mitosis (figure 12) will be discussed in the following chapters.

1.4.1 Entry into mitosis

Progression of the cell cycle is controlled by cyclin dependent kinases (Cdk) and their regulatory subunits, the cyclins. Different Cdk-cyclin associations control the transition between different phases of the cell cycle. The Cdk1-cyclin B1 complex is necessary for the transition from G2 phase to mitosis (Lew *et al.*, 1996; Morgan, 1997; Ohi *et al.*, 1999). During interphase Cdk1-cyclin B1 is found entirely in the cytoplasm (Pines *et al.*, 1991). Cdk1 activity is highly regulated to prevent to early entry into mitosis. Cdk1 is phosphorylated by two protein kinases, Wee1 and Myt1, on position Thr14 and Tyr15, which inactivates Cdk1 kinase activity (Gould *et al.*, 1989; Lee *et al.*, 1992; Parker *et al.*, 1992; Parker *et al.*, 1992; Atherton-Fessler *et al.*, 1994; Mueller *et al.*, 1995). At the onset of mitosis Wee1 and Myt1 are inactivated and the phosphatase Cdc25C is activated. Activated Cdc25C dephosphorylates Cdk1 on position Thr14 and Tyr15, which results in an active form of Cdk1 (Russell *et al.*, 1986; Gautier *et al.*, 1991; Borgne *et al.*, 1996; Qian *et al.*, 1998). In late prophase the active Cdk1-cyclin B1 complex is rapidly transported into the nucleus. Cdk1 phosphorylates a variety of proteins and thereby triggers directly or indirectly the early events of mitosis such as chromosome condensation, nuclear envelope breakdown and spindle formation.

During chromosome condensation in prophase the kinetochore formed on each chromosome. The kinetochore is a protein complex at the centromere, where the mitotic spindles attach to separate the two chromatides.

1.4.2 Metaphase-Anaphase transition

At prometaphase the mitotic chromosomes align at the metaphase plate, reaching metaphase, once they are all aligned. The mitotic spindle attaches to the kinetochore to separate the two chromatides. This step is critical for the cell because it has to be sure that all kinetochores are attached to the spindles to guaranty correct separation. The metaphase to anaphase (M-A) checkpoint senses the existence of unattached kinetochores (Rieder *et al.*, 1995). The major player in this checkpoint is the checkpoint protein Mad2. Mad2 is localized at the kinetochore. As long as the spindles are not attached to the kinetochore, it diffuses through the nucleus and thereby inhibits the anaphase promoting complex/cyclosome (APC/C) by binding to its activator Cdc20 (Fang *et al.*, 1998; Howell *et al.*, 2000; Sudakin *et al.*, 2001). Once all chromosomes are attached to the mitotic spindles, Mad2 translocates along the spindles to the spindles poles and does not bind to Cdc20 anymore. Thus, Cdc20 can activate APC/C and the cells can progress into anaphase (figure 12).
APC/C is a large ubiquitin ligase , which ubiquitinates the anaphase inhibitors, securins. The following degradation of securin leads to the activation of the protease separase. Separase cleaves a subunit of the cohesion complex, that connects the two sister chromatides, thereby destroys the cohesion between chromatides and triggers the onset of anaphase (Holloway *et al.*, 1993; Cohen-Fix *et al.*, 1996; Uhlmann *et al.*, 1999; Zou *et al.*, 1999; Uhlmann *et al.*, 2000; Waizenegger *et al.*, 2000; Hagting *et al.*, 2002; Nasmyth, 2002). The spindles then pull the two sister chromatides towards the opposite poles of the cell.

1.4.3 Exit from mitosis

APC/C is not only responsible for securin degradation it also ubiquitinates cyclin B1 (Irniger *et al.*, 1995; King *et al.*, 1995; Sudakin *et al.*, 1995; Morgan, 1999). Degradation of cyclin B1 leads to inactivation of Cdk1 and the cells exit from mitosis. The spindles are being disassembled and the cells undergo cytokinesis.

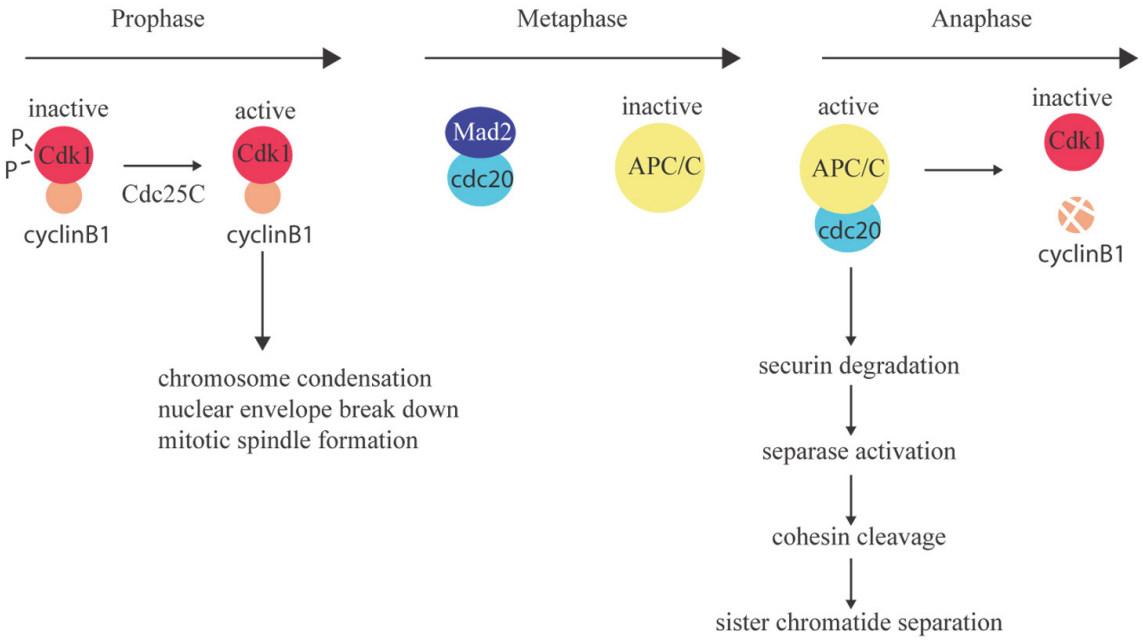

Figure 12: Key steps of signaling events in mitosis. At the onset of mitosis the inactive phosphorylated form of cyclin dependent kinase 1(Cdk1)-cyclin B1 is dephosphorylated by Cdc25C, which leads to an activation of Cdk1 kinase activity and the beginning of mitotic events. During metaphase the checkpoint protein Mad2 binds to the anaphase promoting complex/cyclosome (APC/C) activator Cdc20 and thereby keeps APC/C in an inactive state. After the spindles are attached to the kinetochore Mad2 does not bind Cdc20 anymore and APC/C is activated leading to chromosome separation, cyclin B1 degradation and exit out of mitosis.

1.5 Specific aim

Inositol pyrophosphates have been known for 10 years, but the biological function and significance is still unclear. Deletion of the single yeast IP_6K implicated an involvement of the kinase in vesicle trafficking. In contrast to yeast, there are three different IP_6K isoforms in humans, suggesting that IP_6Ks are involved in more than one signaling pathway and might be regulated in a spatial and temporal manner. In this thesis the subcellular localization of IP_6Ks was investigated to gain more insight into the characteristics of the kinases. Because of its interesting different localizations within the cell, it was focused on IP_6K1 isoform. The goal was to characterize this kinase further and collect evidence for a biological function of this enzyme and its products, the inositol pyrophosphates.

2 Material and Methods

2.1 Materials

2.1.1 *E. coli* strains

To clone different constructs the *E. coli* strain novablue (Novagen) was used. The strain has the following genotype: *endA, hsdR17 (r_{K12}^- m_{K12}^+) supE44 thi-1 recA1 gyrA96 relA1 lac*[F' *proA*$^+$*B*$^+$ *lac*^{q}*Z*Δ*M15*:: Tn*10* (Tc^R)]

Overexpression of recombinant IP_6K1 and IP_6K2 was performed using the *E. coli* strain BL21 (Novagen) with the genotype: F^- *ompT hsdS*$_B$ ($r_B^-m_B^-$) *gal dcm*

2.1.2 Cell lines

All cell lines used were purchased from ATCC:

NIH3T3 cells are mouse embryonal fibroblasts. They are highly contact inhibited cells established from NIH swiss mouse embryo cultures.
HEK293T cells are human embryonal kidney cells, which have a epithelial morphology. The cell line is transformed with the SV40 T-antigen. The advantage of this transformation is, that the cells can replicate the plasmid, they are transfected with, which results in a higher transfection efficiency. The disadvantage is, that this cell line is difficult to fix on coverslips and therefore, was not used for the majority of the immunofluorescence experiments.
U2OS cells are human osteosarcoma cells with a epithelial morphology.

Cos-7 cells are a monkey kidney cell line, transfected with the SV40 T-antigen, resulting in a high transfection efficiency. Cos-7 cells have a fibroblast morphology.
NIH3T3, U2OS and COS-7 cells are easy to fix on coverslips and therefore good cell lines to perform immunofluorescence experiments. The majority of immunofluorescence experiments was performed with NIH3T3 and U2OS cells.

2.1.3 Chemicals and kits

Table 1: Chemicals

chemical	supplier	chemical	supplier
Acidic acid	Fisher brand	Hydrochloric acid	Fisher brand
Acrylamide	BioRad	Hydroxyurea	Calbiochem
Agarose	GeneMate	Imidazole	Sigma
Ampicilin	Sigma	^{3}H-inositol	Perkin Elmer
Ammonium persulfate	Sigma	Inositol hexakisphosphate	Sigma
Anorganic salts	Fisher brand	^{3}H-inositol polyphosphate	Perkin Elmer
Aphidicolin	Calbiochem	IPTG	Sigma
aprotinin	Sigma	isopropanol	Fisher brand
Bacto-Agar	Becton Dickinson Microbiolody	kanamycin	Sigma
Bacto-Pepton	Becton Dickinson Microbiology Systems	leupeptin	Sigma
Beta-mercaptoethanol	Sigma	methanol	Fisher brand
Big Dye	Amersham Pharmacia	nocodazol	Calbiochem
Bromphenolblue	Sigma	Penicillin/Streptomycin	Cellgro
Coomassie brilliant blue	Fisher brand	Perchloric acid	Fisher brand
desoxyribonulceotides	Promega	Phosphoric acid	Fisher brand
Dithiothreitol (DTT)	Sigma	PMSF	Sigma
DMSO	Sigma	SDS	Fisher brand
DOC	Sigma	TEMED	BioRad
Ethanol (200 and 190 proof)	Aaper alcohol and chemical company	Tris	Fisher brand
Ethidium bromide		Triton X-100	Sigma
Etoposide (VP16)	Calbiochem	Trypsin	Cellgro
Glycerol	Sigma	Trypton	Becton Dickinson Microbiology Systems
Glycine	Fisher brand	Tween 20	BioRad
Hepes	Sigma	Yeast extract	Becton Dickinson Microbiology Systems

Table 2: Kits

kit	supplier
blunt end ligation kit	Novagen
His bind purification kit	Novagen
Ligation kit	Takara
One step RT-PCR kit	Qiagen
QIAquick gel extraction kit	Qiagen
QIAprep spin miniprep kit	Qiagen
QIAfilter plasmid maxi kit	Qiagen
Quick change mutagenesis kit	Stratagen
RNeasy Mini kit	Qiagen

2.1.4 General material

Table 3: General materials

material	supplier
CleanSEQ magnetic beads	Agencourt
Coverslips	Fisher brand
Cyanobromide activated sepharose 4B	Sigma
Dialysis filter 0.25 μm	Millipore
Gel code	Pierce
FLO-AP scintillation fluid	Perkin Elmer
FuGENE transfection reagent	Roche
Immobilon-P	Millipore
Mounting media	Vectra
Non fat dry milk	Nestle
Snake skin 10.000 MWCO dialysis tubing	Pierce
Supersignal West Pico chemoluminescent substrate	Pierce
Tissue culture dishes	Sarstedt
X-Omat AR film	Kodak
Whatman paper	fisher

2.1.5 Enzymes and proteins

Restriction enzymes were purchased from Promega unless otherwise noted.

Table 4: Enzymes and proteins

Enzyme	supplier
Calf alkaline phosphatase (CIP)	New England Biolabs
Bovine serum albumin (BSA)	Jackson ImmunoResearch laboratories
Fetal bovine serum (FBS)	Cellgro
Lysozyme	Sigma
Pfu Ultra	Stratagen
Phospho creatine kinase	Sigma
Prestained protein molecular weight marker	Invitrogen
RNase A	Sigma
Taq polymerase	promega

2.1.6 Antibodies

Table 5: Antibodies

Antibody	Supplier	used for	Dilution
Actin, mouse mAb	ICN	Western blot	1:10000
Cdk1, mouse mAb	BD Transduction Laboratories	Western blot	1:2500
Cdk1 pY15, Mouse mAb	Bd Transduction labs	Western Blot	1:250
CENP-F, goat pAb	Santa Cruz	IF	1:100
Cyclin B1, mouse mAb	Santa Cruz	Western Blot	1:200
Histone 3, pS10, mouse mAb	Upstate	Flow cytometry	
myc, mouse mAb	Covance	IF Western blot flow cytometry	1:1000 1:1000 1 µg/sample
β-tubulin, mouse mAB	Upstate	IF western blot	1:1000 1:2000

All secondary antibodies were obtained from Jackson ImmunoResearch laboratories and used at a concentration of 1:200 for IF and 1:10000 for western blots. Secondary antibodies for immunofluorescence were either conjugated to FITC or texas red, secondary antibodies for western blots were conjugated to horseradish peroxidase (HRP).

2.1.7 Nucleic acids

Table 6: Primers

name	Sequence (5'-3')	Used for
T3pro	AAT TAA CCC TCA CTA AAG GG	sequencing colony PCR
T7pro	GTA ATA CGA CTC ACT ATA GGG	Sequencing colony PCR
T7ter	GCT AGT TAT TGC TCA GCG G	sequencing colony PCR
SP6	TCA GAT TTA GGT GAC ACT ATA	sequencing colony PCR
5'G3PDH	GGT CTT ACT CCT TGG AGG CCA TGT	RT-PCR control forward primer
3'G3PDH	GAC CCC TTC ATT GAC CTC AAC TAC A	RT PCR control reverse primer
Talin 52-75	GCG CAG GTA TAG CCA GGC TGG AGA	RT-PCR control forward primer
Talin 1503-1530	CGA GCG GGA GGA GGC CCA GTA CGA CCT G	RT PCR control reverse primer
IP6K1hfwRT	ATG TGT GTT TGT CAA ACC ATG GAA GTG GGG	RT PCR forward primer
IP6K1hrevRT	CTA CTG GTT CTC GTC CCG CAT CTG TTC CAT	RT-PCR reverse primer
IP6K1fwRNAi-1	GTG ACC ACA AGG AAG AAA AGG CCA GCC TGT CC	PCR (quickchange mutagenesis) forward primer
IP6K1revRNAi-1	GGA CAG GCT GGC CTT TTC TTC CTT GTG GTC AC	PCR (quickchange mutagenesis) reverse primer
IP6K1hDLKAAAfw	CCC TGC GTG TTG GCC GCG GCG ATG GGC ACG CGG	PCR (quickchange mutagenesis) forward primer
IP6K1hDLKAAArev	CCG CGT GCC CAT CGC CGC GGC CAA CAC CAC GCA GGG	PCR (quickchange mutagenesis) reverse primer
IP6K2DLK-AAA fw	GTC CTT GCC GCC GCG ATG GGC ACA CGA CAA CAT	PCR (quickchange mutagenesis) forward primer

All primer were purchased from MWG-Biotech.

All siRNA oligos were purchased from Dharmacon

Table 7: SiRNA oligos

name	Sequence (5'-3')	comment
IP_6K1 siRNA	AAG GAG GAG AAA GCC AGC CTG	
IP_6K1 siRNA 2	AAG TTC CTC CTG CTT GAG AAC	
Control siRNA	AAG ACG CGG TGG CAG CCA GTA	rat IPMK sequence, different than human IPMK

As DNA standard 1 kb PLUS DNA ladder from Invitrogen was used.

2.1.8 Vectors

Table 8: Vectors and vector constructs

Name	description
pSTBlue1 blunt	EcoRV treated pSTBlue1 vector from Novagen
pET28b	His and T7 tag *E. Coli* expression vector from Novagen
pCMV3A	Myc tag mammalian expression vector from Stratagen
pTrcHisB-mIP6K1	Mouse IP_6K1 cloned into *E. coli* expression vector pTrcHisB was a gift from A. Saiardi
pTrcHisB-hIP6K2	Human IP_6K2 cloned into pTrcHisB was a gift from S. Shears
pSTBlue1-hIP6K1	ORF of human IP_6K1 (RT-PCR) was cloned into pSTBlue1-blunt
pET28b-mIP6K1	Mouse IP_6K1 cloned out of pTrcHisB-mIP6K1 into pET28b using BamHI and HindIII restriction enzymes
pET28B-hIP6K2	Human IP_6K2 was cloned out of pTrcHisB-hIP_6K2 into pET28b using BamHI and HindIII restriction enzymes
pCMV3A-mIP6K1	Mouse IP_6K1 was cloned into pCMV3A the same way than into pET28B
pCMV3A-hIP6K2	Human IP_6K2 was clone into pCMV3A the same way than into pET28b
pCMV3A-hIP6K2DLK-AAA	pCMV3A-hIP_6K2 mutated at D220 to A, L221 to A and K222 to A, to obtain a kinase dead mutant
pCMV3A-hIP6K1	Human IP_6K1 was cloned out of pSTBlue1-hIP_6K1 using BamHI and HindIII restriction enzymes
pCMV3A-hIP6K1rescue	pCMV3A-hIP_6K1 with three silent mutation at bp position
pCMV3A-hIP6K1rescueDLK-AAA	pCMV3A-hIP_6K1rescue mutated at D224 to A, L225 to A and K226 to A, to obtain a kinase dead mutant
pCMV3A-hIP6K2DLK-AAA	pCMV3A-hIP_6K2 mutated at D220 to A, L221 to A and K222 to A, to obtain a kinase dead mutant

2.1.9 Buffers

Acetate buffer:
100 mM acetic acid, glacial
500 mM NaCl
pH 4.0

Ampicilin solution:
100 mg/ml in ddH_2O, sterile filtered

1.3 M ammonium phosphate (HPLC buffer B):
1.3 M ammonium
inddH2O
pH 3.85 adjusted with perchloric acid

Azide solution
10 % sodium azide in ddH_2O

Binding buffer (his bind purification):
5 mM imidazol
500 mM NaCl
20 mM Tris-HCl pH 7.9

Coomassie staining solution:
30 % methanol
1 % acidic acid, glacial
0.01 % coomassie blue
in ddH_2O

Coomassie destaining solution:
30 % methanol
1 % acidic acid, glacial
in ddH_2O

Dialyse buffer for antibodies:
0.02 % sodium azide
1 mM DTT
in PBS

NP-40 lysis buffer:
50 mM Tris/HCl pH 7.4
150 mM NaCl
10 % glycerol
1 % NP40
1 mM Na_2EDTA

PBS (10x):
200 mM sodium phosphate
1.5 M NaCl
pH 7.4

PMSF solution:
100mM PMSF in 100 % ethanol

Propidium iodide staining solution:
33 µg/ml propidium iodide
1 mg/ml RNase A
in PBS

RIPA buffer:
1 % NP40
1 % DOC
0.1 % SDS
150 mM NaCl
10 mM sodium phosphate
2 mM Na_2EDTA

RNase A solution:
10 mg/ml RNase A
in 10 mM NaAc pH 5,4, boil 15 min.
add 0.1 vol 1 M Tris/HCL pH 7.5

Running buffer for SDS PAGE:
25 mM Tris/HCl pH 8.8
200 mM Glycine
0.1 % (w/v) SDS

SDS sample buffer (5X)
665 mM Tris/HCl pH 6.8
10 % SDS
50 mM DTT
60 % (w/v) glycerol
0.01 % bromphenolblue

DNA loading buffer (6X):
50 % glycerol
0.25 % bromphenolblue
in TE buffer

Elution buffer (His bind purification):
1 M imidazol
500 mM NaCl
20 mM Tris-HCl pH 7.9

Glycerol dialyze buffer for proteins:
50 mM Tris-base
1 mM EGTA
150 mM NaCl
20 % glycerol
0.01 % sodium azide
in ddH2O, adjust pH 7.5

Kanamycin solution:
50 mg/ml kanaycin
in ddH_2O
sterile filtered

Kinase buffer:
20 mM Hepes, pH 7.0
12 mM MgSO4
1 mM DTT
10 mM ATP
20 mM phosphocreatine
1 mM Na2EDTA
0.02 mg/ml phospho creatine kinase
0.5 mg/ml BSA

Lysozyme solution:
10 mg/ml Lysozyme
in 10 mM Tris/HCl pH 8.0

TAE (50x):
2 M Tris-acetate
100 mM Na_2EDTA
in ddH_2O

TE:
1 mM Na_2EDTA
In 10 mM tris/HCl pH 8.0

Transferbuffer for western blots:
25 mM Trisbase
192 mM glycine
20 % methanol
in ddH_2O

Tris-HCl (1M)
1 M trisbase
adjusted to pH 7.5, 8.0 and 8.8 with HCl
in ddH_2O

Wash buffer (His bind purification):
60 mM imidazol
500 mM NaCl
20 mM Tris-HCl pH 7.9

2.1.10 *E. coli* media

E. coli suspension cultures were grown in LB medium, and *E. coli* colonies were grown on LB agar plates.

LB media (Sambrook, 1989):
10 g trypton
5 g yeast extract
10 g NaCl
add ddH_2O to 1 l
for plate 1.5 % agar was added.

2.1.11 Cell culture media

All cell lines were grown in DMEM (Cellgro), supplemented with 10 % FBS and penicilin/streptomycin. The FBS was heat inactivated at 60 °C for 30 min before adding to the media.

2.2 Microbiological and molecular biological methods

2.2.1 Culturing of *E. coli*

E. coli suspension cultures were grown in LB media under aerobe conditions at 37 °C. Depending on the experiment the following antibiotics were added to the media.
Kanamycin: 50 μg/ml
Ampicilin: 100 μg/ml
To grow *E. coli* colonies on plates LB with 1.5 % agar was used under the same conditions and antibiotic concentrations than in suspension cultures.

2.2.2 *E. coli* transformation

50 μl heat shock competent *E. coli* cells were combined with 10 ng plasmid or 1-10 μl ligation. The cells were incubated for 5 min on ice, 40 seconds in 42 °C waterbath. After additional 2 min incubation on ice 900 or 100 μl LB respectively were added to the cells and incubated for 30 min at 37°C. 100 μl were plated an LB agar plate with the necessary antibiotics.

2.2.3 DNA isolation

Analytical DNA isolation
Plasmide DNA isolated from 2 ml *E. coli* over night culture using QIAprep spinMiniprep kit (Qiagen) as described by supplier. Briefly, 2ml *E. coli* cells were centrifuged and the pellet lysed under alkaline conditions. The lysate was neutralized and adjusted to high-salt binding

conditions. The plasmid DNA was bound to a silica gel membrane and eluted with 10 mM Tris-HCl ph 8.0.

Preparative DNA isolation

The analytical way of DNA isolation does not result in a high amount of DNA and can be contaminated with proteins. Protein contamination can inhibit the transfection efficiency of mammalian cell lines. Thus, to get more and higher quality DNA the QIAfilter Maxi kit (Qiagen) was used to isolate plasmid DNA for transfection of mammalian cells. The plasmide DNA was also isolated using the alkaline lysis method, but the plasmid DNA containing solution was additionally purified by filtration.

2.2.4 Polymerase chain reaction (PCR)

To amplify a specific DNA fragment the method of polymerase chain reaction (PCR) was used (Saiki *et al.*, 1988). The reaction was done under the following conditions. 50 ng DNA, 25 pmole each primer, 1 mM dNTPs and 2.5 U Pfu Ultra DNA polymerase was mixed in 50 µl Pfu Ultra buffer (total volume). To amplify IP_6K1 the reaction was cycled in a Triblock Thermocycler (Biometra) with the following program.

1. Denaturing:	95 °C	1 min
2. Denaturing:	95 °C	1 min
3. Hybridization:	55 °C	1 min
4. Polymerization:	68 °C	2 min
5. Polymerization:	68 °C	7 min

Step 2 to 4 was cycled 24 times.

2.2.5 Colony-PCR to test for positive clones

To test for positives clones after ligation and transformation colonies were analyzed by colony-PCR. Therefore a small amount of a colony was resuspended in 10 µl ddH_2O and streaked out on a plate to grow for 8 hours at 37 °C. The resuspended colony was analyzed by PCR with vector specific primers to amplify the possible insert under the following conditions.

10 µl colony suspension
20 pmole each primer
20 mM dNTP mix
5 µl taq 10 x buffer
0.25 U taq DNA polymerase
in 50 µl

The reaction was performed using the following program.

1. Lyses of *E. coli* cells:	5 min	95 °C
2. Denaturing:	1 min	95 °C
3. Annaeling:	1 min	55 °C
4. Polymerization:	2 min	72 °C
5. Polymerization:	7 min	72 °C

Step 2 to 4 were cycled 24 times. The PCR was analyzed on a 1 % agarose gel. Positive colonies were inoculated from the plate into 3 ml over night cultures for DNA preparation.

2.2.6 Modification of DNA

2.2.6.1 Restrictionendonucleases

Treatment of DNA with restriction endonucleases (Promega) was performed as described by supplier. The resulting DNA fragments were separated by agarose gel electrophoresis and purified using a QIAquick gel extraction kit (Qiagen).

2.2.6.2 Quick change^{TM} mutagenesis

To mutate IP_6K1 and IP_6K2 the Quick change^{M} site directed mutagenesis kit (Stratagen) was used. Therefore, about 30 bp long primers were designed (see 2.1.7), which contained the desired mutation and annealed at the same sequence on the opposite strands of the plasmid. The reactions were prepared as followed.

5 µl 10 x Pfu Ultra reaction buffer
50 ng template DNA
10 pmole each primer
1 µl dNTP mix (25 mM each dNTP)
2.5 U Pfu Ultra
ddH2O to final volume of 50 µl

The reaction was cycled using the following parameters.

1.Denaturing:	95 °C	30 sec
2.Denaturing:	95 °C	30 sec
3.Annealing:	55 °C	1min
4.Polymerization:	68 °C	1 min per kb of plasmid length

Step 2 to 4 was cycled 15 times. The PCR was treated with 10 U Dpn I restriction enzyme for

1 hour at 37 °C to remove the methylated template DNA. The PCR product is not methylated and thus, remained in the reaction tube. 1 µl reaction was transformed into 50 µl novablues.

2.2.7 Preparation of messenger RNA

To determine mRNA levels in cells mRNA was prepared and analyzed by reverse transcriptase PCR. Therefore, cell were grown on a 6 cm tissue culture dish to 70 % confluence. The cells were treated with trypsine, combined with the cells floating in the media and spin down for 5 min at 300 x g. The mRNA was prepared with RNeasy kit (Qiagen) as described by supplier. The concentration of the mRNA was measured using a biophotometer (Eppendorf) with a wavelength of 260 nm.
The same method was used to clone hIP_6K1 out of HEK293T cells.

2.2.8 Reverse transcriptase PCR (RT-PCR)

To determine the concentration of a specific mRNA in the cell, 1 µg mRNA was used as template in a RT-PCR kit as described by manufactor. HIP_6K1 specific primers and G3DPH or talin primers as control primer were used to amplify hIP_6K1 and a 900 bp fragment of G3DPH or 1500 bp talin fragment. The cycle reaction was performed under the following conditions.

1.	reverse transcription:	50 °C	30 min
2.	denaturing of reverse transcriptase:	95 °C	15 min
3.	denaturing:	95 °C	1 min
4.	annealing:	55 °C	1 min
5.	polymerization:	72 °C	2 min

Step 3 to 5 were repeated 25 times. The resulting DNA was analyzed on a 1 % agarose gel.
This method was also used to clone hIP_6K1 out of HEK293T cells

2.2.9 Ligation

2.2.9.1 Bluntend ligation

PCR products were ligated into pSTBlue1 using the blunt end ligation kit (Novagen). Briefly, 5 µl PCR product was treated with an end conversion mix to cleave of the 3' adenoside overhang. This 3' adenoside overhang can occur during a PCR using taq DNA polymerase. After denaturing the end conversion mix for 15 min at 75 °C, T4 ligase was added to the reaction and incubated over night at 16 °C. 1 µl of the ligation was transformed into 50 µl novablues.

2.2.9.2 "Sticky end" ligation

DNA fragments resulting from a restriction enzyme reaction were ligated using a ligation kit (Takara). Vector and insert DNA were mixed at a molar ratio of 1:3 in 5 µl total volume. 40 µl buffer A and 5 µl buffer B was added. The ligation reaction was incubated over night at 16 °C and 8 µl were transfected into 50 µl novablues.

2.2.10 Sequencing of DNA

DNA sequences were determined using the big dye kit (Amersham pharmacia). The reaction was set up as follows.

100-400 ng DNA
20 pmole primer
2 µl Big Dye
2 µl 2.5 X buffer
add ddH_2O to 10 µl

The reaction was cycled using the following program.

1. denaturing:	94 °C	30 min
2. denaturing:	96 °C	10 sec
3. annealing and polymerization:	58 °C	4 min
4. polymerization:	72 °C	7 min

Step 2 to 3 were cycled 50 times.
The sequence reaction was purified using magnetic beads (CleanSEQ, Agencourt) as described by supplier. Briefly, 10 µl sequencing reaction was mixed with 10 µl magnetic particle solution. 42 µl 85 % ethanol was added, mixed and incubated for 3 min on a SPRIplate96^{TM}-R to separate the beads from solution. The beads were washed two times on the plate with 100 µl 85 % ethanol, air dried and resuspended in 40 µl ddH_2O. The purified sequencing reaction was run by the University of Wisconsin Biotech center sequencing facility. The sequences were returned in a Edit view format and analyzed using Biology Workbench 3.2 and DNA strider 1.1.

2.2.11 Construction of putative IP_6K kinase dead mutants

The carboxyl terminus of inositol phosphate kinase consists of four conserved domains. To design mutants, which do not contain kinase activity anymore, amino acids were mutated, that are conserved in the family of inositol phosphate kinases and between species. The inositol phosphate binding domain (figure 8) contains a DLK motif. The glutamate (D) and the lysine (K) are conserved amino acids. To create a putative kinase dead mutant the entire motif was mutated to alanines.

2.3 Biochemical and immunological methods

2.3.1 Purification of soluble recombinant His_6 tagged IP_6K1

The *E. Coli* strain BL21 was transformed with pET28b-mIP_6K1. 5 ml LB containing kanamycin were inoculated with a single colony and grown over night at 37 °C. 500 ml Lb containing kanamycin was inoculated 1:100 with the over night culture. Then the cells were grown at room temperature, because recombinant mIP_6K1 is highly insoluble and by growing the cells at room temperature an higher amount of soluble protein was achieved. At OD_{600} between 0.5 and 0.6 the protein expression was induced with 0.5 mM IPTG. After 2.5 hours the cells were harvest by centrifugation at 6000 rpm at 4 °C for 10 min. The pellet was resuspended in 20 ml bindingbuffer, containing 100 µg/ml lysozyme and incubated for 15 min at roomtemperature. After three times sonication for 30 sec, the soluble protein was separated from the insoluble by centrifugation at 39.000 x g for 20 min at 4 °C. The soluble protein was purified using the his bind purification kit (Novagen) as described by manufactor. The purified protein was dialyzed into glycerol dialyze buffer, the protein concentration was determined, the protein was frozen in liquid nitrogen and stored at –80 °C.

2.3.2 SDS-PAGE

Proteins were separated by molecular weight using SDS-PAGE. 10 % and 7.5 % acrylamide gels were used as running gels. The acrylamide concentration in the stacking gel was 5 %. The gels were prepared as follows.

5 %	7.5 %	10 %
5 % acrylamide : bisacrylamide 29:1	7.5 % acrylamide : bisacrylamide 29:1	10 % acrylamide : bisacrylamide 29:1
125 mM Tis-HCl pH 6.8	375 mM Tis-HCl pH 8.8	375 mM Tis-HCl pH 8.8
0.1 % (w/v) SDS	0.1 % (w/v) SDS	0.1 % (w/v) SDS
0.1 % (w/v) APS	0.1 % (w/v) APS	0.1 % (w/v) APS
0.025 % (w/v) Temed	0.025 % (w/v) Temed	0.025 % (w/v) Temed

The electrophoretic separation of protein was performed for 45 min at 200 V. The gels were either stained with Gelcode staining solution (Pierce) as described by manufacture or prepared for immunoblotting (see 2.4.2).
Prestained Benchmark molecular weight marker (Invitrogen) was used as a standard.

2.3.3 Immuno blot

Proteins separated by SDS-PAGE were transferred to PVDF membranes using the wet transfer system (BioRad). Pads, Whatman filter paper, gels and PVDF membrane, in 100 % methanol, were soaked in transferbuffer and set up as described by supplier. The transfer was performed for 2 hours at 100 volt at 4 °C. The prestained marker demonstrated the efficiency of the transfer and no additional staining of the membrane was necessary. The membrane was blocked in 5 % (w/v) skim milk, 0.1 % Tween-20 in PBS (PBS-T) for 30 min at room temperature. The proteins of interest were detected using a specific primary antibody and the membranes were incubated for 1 hour at roomtemperature or over night at 4 °C with the antibody diluted in 5 % skim milk in PBS-T. After washing the membrane with PBS-T a

horseradish peroxidase coupled secondary antibody, diluted 1:10.000 in 5 % skim milk in PBS-T, was used. Peroxidase catalyzes the oxidation of The Super signal West Pico substrate (Pierce), that leads to a light emission at a wavelength of 420 nm which can be detected on a X-omat AR film (Kodak).

2.3.4 Immunoprecipitation

HIP_6K1 amino-terminal fused to the myc tag (myc-hIP_6K1), was transfected into HEK293T cells. The cells were lysed as described in chapter 2.5.4. 1 µg anti myc antibody was added to 500 µl lysed cells and incubated rotating end over end over night at 4 °C. To prepare 50 µl of a 50 % solution of protein A resin (Roche), the resin was washed three times in lysis buffer and added to the cells and incubated for 1 hour at 4 °C. The protein A resin binds the antibody which is bound to myc-hIP_6K1. This immune complex was pelleted at 12000 x g for 20 seconds and the pellet was washed three times in lysis buffer and one time in 10 mM Tris-HCl pH 8.0. The final pellet was resuspended in 30 µl sample buffer, boiled 5 min at 95 °C and analyzed by SDS-PAGE and immunoblotting. To detect hIP_6K1 on the membrane, mouse monoclonal anti myc antibody was used. Additionally, polyclonal anti mIP_6K1 antibody was also used to detect immunoprecipitated myc tagged hIP_6K1.
Endogenous IP_6K1 was immunoprecipitated with polyclonal anti IP_6K1 antibody from non transfected cells using the same protocol. In the following western blot polyclonal anti IP_6K1 was used as primary antibody. Endogenous IP_6K1 and IgG heavy chain are almost the same size. To avoid detection of heavy chain on the membrane horseradish peroxidase coupled to protein A (Pierce) was used instead of a secondary antibody. Protein A only detects not denatured IgGs. Thus, only the primary antibody was detected, and not the in the SDS-PAGE denatured antibody used to immunoprecipitate.

2.3.5 Determine protein concentrations

Total protein concentrations in cell lysates or concentration of purified antibodies were

determined using the BCA protein assay (Pierce) as described by supplier. In this assay Cu^{2+} is reduced by protein to Cu1+ (the biuret reaction). Cu1+ can then be detected by two molecules bicichoninic acid (BCA) in a purple colored reaction. This water soluble complex exhibits a strong absorbance at 562 nm, that is linear with increasing protein concentration. The following dilutions of BSA in the same buffer than the protein of interest were used to make a standard curve: 0.125, 0.25, 0.5, 0.75, 1.0, 1.5 mg/ml. The protein samples were analyzed using a biophotometer (Eppendorf) with a built in computer program to calculate protein concentrations using the BCA assay.

2.3.6 Kinase assays

Immunoprecipitated hIP_6K1 and hIP_6K1 kinase dead (see chapter 2.2.11) or 100 ng of recombinant protein were incubated with 1 µCi ^3H-IP_6 in 20 µl kinase buffer for 30, 60 and 120 min. The reaction was quenched with 4 µl 2 M perchloric acid, 0.2 mg/ml IP_6 and neutralized with 8 µl 1 M K_2CO_3, 5 mM Na_2EDTA. The final pH had to be between 6.5 and 7.5. After 15 min incubation on ice, the reaction was centrifuged and the supernatant was mixed with ddH_2O to final volume of 200 µl. 100µl were loaded on a SAX-HPLC column (Agilent) (Shears, 1997; Saiardi *et al.*, 2000).

2.4 Production of polyclonal antibodies

2.4.1 Proteinpurification

500 ml BL21 *E. coli* cultures transformed with pET28B-IP_6K1 and –IP_6K2 were grown to an OD_{600} between 0.5 and 0.6 and then induced with 0.5 mM IPTG. The cells were harvested by centrifugation at 8000 x g for 10 min 2.5 hours after induction and resuspended in 20 ml lysisbuffer with 100 µg/ml lysozyme. After incubation for 30 min on ice the cells were sonicated three times for 30 seconds on ice. The recombinant protein in form of inclusion bodies was separated from the soluble lysate by centrifugation at 27000 x g for 20min. The inclusion body pellet was washed once in 20 ml lysis buffer + 0.5 % Triton X-100, and twice in 20 ml deionized water. The pellet was resuspended in 10 ml Laemmli sample buffer and 2.5 ml were loaded on a preparative gel. The gel was stained in Coomassie staining solution for 15 min at room temperature and washed three times for 15 min in destain solution. The band corresponding to the size of IP_6K1 or 2 was cut out of the gel, washed twice in 30 % methanol and once in water. The protein was electroeluted out of the gel and dialyzed in PBS + 0.01 % SDS. The concentration of the protein was determined using SDS-PAGE with known BSA standards. This method was chosen, because the proteins were already stained with coomassie, that made it impossible to use exacter methods such as BCA or Bradford.

2.4.2 Construction of an mouse IP_6K1 affinity column

0.5 g cyanogen bromide activated Sepharose 4B (Sigma) was washed four times in 1 mM HCl and one time in PBS. The resulting gel was added to 10 mg IP_6K1 in 0.01 % SDS in PBS, and mixed over night at 4 °C. Unreacted groups were blocked in 0.2 M glycine, pH 8.0 over night at 4 °C. The resin was washed in PBS following acetate buffer three times. The column was packed and stored in PBS at 4 °C.

2.4.3 Production and purification of polyclonal antibodies

Recombinant mouse IP_6K1 and human IP_6K2 were purified as described in chapter 2.3.1. Polyclonal antibodies were manufactured by Covance using purified protein and standard protocols. Therefore, 250 µg protein was injected 6 times in 3 week intervals. The resulting six bleeds were analyzed by immunoblotting for cross reactivity and detection of the protein in cell lysates. The bleeds were pooled and purified over an IP_6K1 or IP_6K2 specific affinity column. Therefore, the sera was loaded on the affinity column over night at room temperature. The column was washed with PBS and 500 mM NaCl in PBS till the UV detector measuring the protein concentration reached baseline. The antibody was eluted with 100 mM glycine pH 2.5 and washed with 10 mM Tris-HCl pH 8.8 till the elution reached pH 8.8. A second antibody elution was performed with 100 mM triethylamine to collect the base-sensitive antibodies. The column was washed with 10 mM Tris-HCl pH 8.0 and stored in PBS. The resulting antibodies were dialyzed in antibody dialysis buffer and the protein concentration was determined as described in chapter 2.3.5. The purified antibodies were again analyzed by immunoblotting. The acidic elution was always better than the base. Thus only the acidic eluted antibodies were used.

2.5 Cell biology

2.5.1 Cell culture

All cell lines used were maintained in DMEM supplemented with 10 % (v/v) fetal bovine serum (FBS) at 37 °C in a 5 % CO_2/95 % air atmosphare. Cells were split when they reached 75-90 % confluence.

2.5.2 Transfection

Different cell lines were transfected with mammalian expression vector constructs using the following transfection methods.

2.5.2.1 FuGene6 transfection

70 % confluent cells in a 6 well plate were transfected with 1 µg Maxi preped DNA and 3 µl FuGene6 transfection reagent (Roche) as described by supplier.

2.5.2.2 Calcium phosphate transfection

6 µg DNA was mixed with 250 µl buffer B for calcium phosphate transfection. 250 µl buffer A was added, mixed and immediately added to 70 % confluent cells in a 60 mm tissue culture dish. After incubation for 8 hours under cell culture conditions the media was changed. Depending on the experiment the cells were analyzed 24, 48 or 72 hours after transfection by immunoblotting, immunoprecipitation, immunofluorescence or flow cytometry. Cells grown in 6 well plates were transfected with half of the amount of DNA and buffer.

2.5.3 Immunofluorescence and microscopy

2.5.3.1 Methanol fixation

Cells grown on a coverslip were washed twice in 37 °C PBS and fixed with 100 % -70 °C methanol on dry ice for 20 min. The coverslips were rinsed twice in PBS and the cells were blocked in 3 % BSA in PBS for 30 min at room temperature or over night at 4 °C.

2.5.3.2 Paraformaldehyde fixation

Cells grown on a coverslip were washed twice in 37 °C PBS and fixed with 4 % paraformaldehyde in PBS for 20 min at room temperature. After rinsing the coverslip once in PBS the cells were permeabilized in 0.2 % Triton X-100 in PBS for 5 min at room temperature. The coverslips were again rinsed twice in PBS and then incubated in PBS for 5 min. The cells were blocked in 3 % BSA in PBS for 30 min or over night at 4 °C.

2.5.3.3 Staining and microscopy

Fixed cells were stained with a primary antibody, diluted in 3 % BSA in PBS for 1 hour at 37 °C, unless otherwise noted. The coverslips were washed three times for 5 min in 0.1 % Triton X-100 in PBS and stained with a secondary antibody conjugated to texas red or FITC in a 1:200 dilution in 3 %BSA in PBS for 30 min at 37 °C. To stain DNA 1 µg DAPI was added to the antibody solution. After 1 min incubation the coverslips were again washed three times in 0.1 % Triton X-100 PBS and mounted on a slide using mounting media (Vectra). The coverslips were sealed with nail polish and the cells were analyzed using a Axiovert 135 microscope (Zeiss) with 40X Achrostigmat objective (Zeiss) with a numeric aperture of 1.3. The pictures were taken with a CCD-camera (Coolsnap) and saved with metaview software. Further preparation of the pictures was performed with Adobe Photoshop. Alternatively, cells were analyzed using a MRC laser scanning confocal (Bio Rad) with 60X objective and numeric aperture of 1.4 (Nikon). The pictures were saved using Bio Rad lasersharp software and further processed with Adobe photoshop.

2.5.4 Preparation of cell lysates

Cells were grown in 6 well plate format to 70-80 % confluence. Cells floating in the media were colleted by spinning them down at 300 X g for 5 min. Cells were resuspended in 250 µl RIPA buffer (+ 1 mM PMSF, 50 mM NaF) and combined with cells on plate. After 15 min incubation on ice the cells were scraped of the plate and sonicated for 5 sec to destroy DNA. The total protein concentration was determined using the BCA kit (Pierce) (see chapter 2.3.5).
Additionally, cells were lysed directly in sample buffer. In this case the protein concentration was not determined.

2.5.5 Inducing cell cycle arrest in cell lines

Different chemicals block cells in specific phases of the cell cycle, which was used to analyze cells in different phase of the cell cycle. Aphidicolin inhibits DNA polymerase α and δ in eucaryotic cells, which blocks the cell at the G1 border or early S-phase. Hydroxyurea also blocks cell in S-phase, but it inhibits ribonucleotide reductase which is involved in dNTP production. VP16 also known as etoposide is a topoisomerase II inhibitor and has the potential to block cells in G2 phase of the cell cycle. Nocadozol inhibits mitosis because of his antimicrotubular activity. Paclitaxel (taxol) is known for its antitumor potency and his used in cancer therapy. It also blocks cells in mitosis, but it promotes microtubule assembly. To arrest cells in different phases of the cell cycle, 50% confluent NIH3T3 und U2OS cells were treated with 10 µg/ml aphidicolin, 1mM hydroxyurea, 0.5 µM VP16, 100 ng nocodazol and 10 µg/ml taxol in DMEM +10 % FBS over night or for 24 hours respectively. Cell were analyzed by immunoblotting, flow cytomtetry or immunofluorescence.

2.5.6 Dephosphorylation of proteins in cell lysates

To determine whether a mobility shift on a SDS-PAGE was due to phosphorylation, the cell lysates were treated with calf alkaline phosphatase (CIP). This phosphatase has the ability to dephosphorylate phosphorylated serine, threonine and tyrosine. 30 µl cell lysates were incubated with 4 U CIP in CIP buffer in 80 µl total volume for 1 hour at 37 °C. The reaction was stopped by adding 20 µl 5x protein sample buffer and incubating the samples for 5 min at 95 °C. In parallel 30 µl lysate was boiled in 1x sample buffer in 100µl total volume to analyze the proteins without phosphatase treatment. The samples were analyzed by SDS-PAGE, followed by immunoblotting.

2.5.7 Metabolic labeling of HEK29T cells with ^{3}H-inositol

HEK293T cells were grown in a 6 well plate format. Cells at a plating density that allowed the cells to grow through five to seven divisions before becoming confluent were treated with 25 µCi/ml ^{3}H-inositol. After six days the media was aspirated and the cells were quenched with 250 µl 0.6 M perchloric acid + 0.1 mg/ml IP_6. After 15 min incubation on ice the cells were centrifuged for 5 min, 60 µl 1 M K_2CO_3 was added to the supernatant and centrifuged again for 2 min. The supernatant was transferred to HPLC vial and 100 µl was loaded on the HPLC column (see chapter 2.8)

2.6 IP_6K1 knock out cells

2.6.1 RNA interference (RNAi) to knock down endogenous IP_6K1 in HEK293T cells

A knock out of a protein of interests in mammalian cell lines can be achieved using the RNAi technique. RNAi was first discovered in the nematode worm *Caenorhabditis elegans* as a response to double stranded RNA (dsRNA), which resulted in sequence specific gene silencing (Fire *et al.*, 1998). The phenomenon of RNAi occurs in *C. elegans*, plants and *Drosophila melanogaster*. Injection of dsRNA in Drosophila embryos induced sequence specific silencing at the postranscriptional level (Kennerdell *et al.*, 1998). RNAi is initiated by the dicer enzyme, which processes double-stranded RNA into 22 nucleotide small interfering RNAs (siRNAs) (Bernstein *et al.*, 2001). The siRNAs are incorporated into a multicomponent nuclease, RNA induced silencing complex (RISC) and are used as template for substrate recognition. ATP dependent unwinding of the dsRNA activates RISC and it binds to the mRNA which then is being degraded (figure 13) (Wu-Scharf *et al.*, 2000; Zamore *et al.*, 2000; Tijsterman *et al.*, 2002). A homologue of the dicer enzyme in mammalian cell has not yet been found, but it has been shown that it is possible to knock out specific genes in mammalian cell using 21 bp double stranded RNA nucleotides. The optimal siRNA is a 19 bp duplex with 3'TT overhangs on both sides (Elbashir *et al.*, 2001).

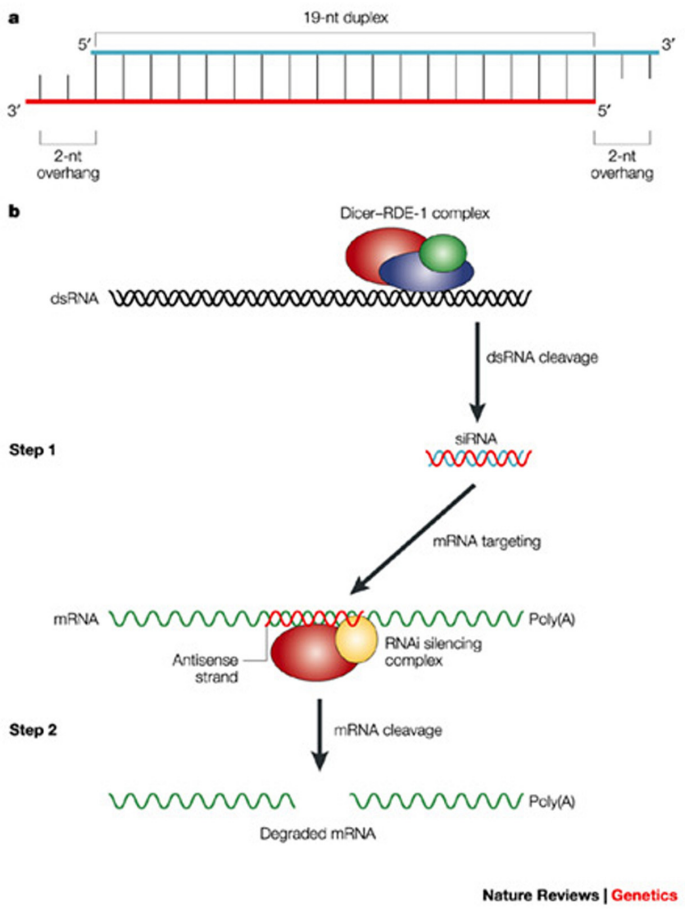

Figure 13: Mechanism of RNA interference in vertebrats . a) 21 bp small interfering RNA (siRNA) with 3' 2 nucleotide (nt) overhang. b) The dicer complex recognizes double strand DNA (dsDNA) and cleaves it into siRNA as shown in a). The RNAi silencing complex binds the siRNA, which is used as a template to recognize the target mRNA. The mRNA is been degraded resulting in a knock out of this specific protein.

To knock out IP_6K1 in mammalian cell, an IP_6K1 specific oligo was designed. As mentioned above the method requires a 21 bp fragment 100 % homologous to IP_6K1, which contained two adenoside at the amino terminus, resulting in the 3'TT overhang (Figure 14). The carboxyl-terminal 3'TT overhang was not necessary to be in the IP_6K1 sequence. The sequence was analyzed using the Blast webpage searching for sequence homologies between the siRNA oligo and the human EST and genome data base to confirm that there is no sequence homology in this specific region to other genes.

HEK293T cells were grown in 6 well plates or 6 cm dishes. When the cells reached about 30 % confluence they were transfected with 20 or 40 mM (final concentration) IP_6K1 specific siRNA, respectively, using calcium phosphate (see 2.6.2). For cotransfection with vector DNA 3 or 6 μg DNA were added to the siRNA buffer B solutions. Cells were grown for 50-72 hours and then analyzed by immunoblotting, immunofluorescence or flow cytometry.

Figure 14: SiRNA oligo design. The siRNAi oligo was designed that it was 100 % homologous to mouse and human IP_6K1, and contained only low homology to IP_6K2.

2.6.2 Rescue of IP_6K1 RNAi phenotype

To rescue the IP_6K1 knockout phenotype in HEK293T cells, the following experiment was performed. RNAi knock out of a protein can only be achieved if there is 100 % homology between the siRNA oligo and the wildtyp mRNA. Thus, a hIP_6K1 mutant was designed which contained three silent mutation in the siRNA targeting region (figure 15) using Quick change™ mutagenisis (Stratagene) with pCMV3A-hIP_6K1 as template. The resulting IP_6K1 rescue construct (pCMV3A-hIP_6K1rescue) was cotransfected with IP_6K1 siRNA using calcium phosphate (see chapter 2.5.2). After 72 hours the cells were analyzed by western blot and flow cytometry.

Figure 15: Design of silent mutation in the siRNA oligo targeting region of IP_6K1. The third base in three codons was mutated (red), resulting in the same protein sequence (blue), but different DNA and thereby mRNA sequence.

2.7 Flow cytometry

One method to determine the phase of the cell cycle of a single cell, is flow cytometry. The advantage of this method is, that it is possible to analyze transfected cell separately from untransfected cells in the same experiment. Cells were collected from a tissue culture dish by treatment with trypsine. The trypsine treated cells and the cells floating in the media, mostly detached mitotic, apoptotic and dead cell, were pooled by centrifugation for 5 min at 300 x g at room temperature. Cells were resuspended in ice-cold 5 ml PBS (+ 1 mM EDTA) and the cell number was determine using a hemacytometer. After centrifugation at 4 °C the cells were resuspended in ice-cold PBS EDTA to a cell density of $5x10^6$ cell/ml. 1 ml of the cell suspension was transferred to a new 1.5 ml tube and centrifuged again. The cells were resuspended in 100 µl ice-cold PBS EDTA and 900 µl –20 °C 80% ethanol was added to the cell suspension and incubated over night at 4 °C to fix the cells. Cells were washed in cold PBS and stained over night with 1 µg anti myc antibody in 500 µl PBS + 1% BSA (PBS BSA) in a end over end rotator. After washing the cells with PBS BSA, 200 µl secondary anti mouse IgG antibody conjugated to FITC (50 µg antibody/ml in PBS BSA) was added and incubated for 30 min at room temperature. Cells were again washed in PBS BSA and incubated in 500 µl propidium iodide staining solution (500 µg/m RNase A, 33 µg/ml propidium iodide in PBS) to stain for DNA for 20 min at room temperature or 4 °C over

night. The cells were analyzed by flow cytometry using a 488 nm laser excitation, collecting in FL3 set to linear scale, with doublet-discriminator module (DDM) turned on. The cell cycle profile of transfected and untransfected cell was determine using ModFit LT software. If only the DNA content was determined, the cells were only incubated in propidium iodide staining solution after fixation.

2.8 HPLC

100 µl of kinases assays were loaded on a SAX HPLC column (Agilent). Inositol phosphates were eluted using a gradient mixing ddH_2O (buffer A) with 1.3 M ammonium phosphate (buffer B) as follows (Saiardi *et al.*, 2000).

0-5 min	buffer B: 0 %
5-10 min	buffer B: 0-45 %
10-60 min	buffer B: 45-100 %
60-70 min	buffer B: 100 %
70-85 min	buffer B: 0%

100 µl of cell extracts (chapter 2.5.7) were loaded on the same column, but eluted with a different program:

0-20 min	buffer B: 0 %
20-100 min	buffer B: 0-82%
100-110 min	buffer B: 82-100%
110-125 min	buffer B: 0 %

The samples were analyzed with a Radiomatic flow scintillation analyzer (Packard), by mixing the HPLC eluates at a 1:3 ration with Ultima FLO-AP scintillation fluid (Perkin Elmer) and measuring the radioactivity with a 500 µl LQ flow cell (Packard). The samples were then analyzed with FLO software (Packard).

3 Results

3.1 Cloning of human inositol hexakisphosphate kinase type 1 out of HEK293T cells

The only IP_6K1 cDNA available and used in different laboratories encodes the mouse isoform (Saiardi *et al.*, 1999; Saiardi *et al.*, 2000). The sequence of the human IP_6K1 is published in the human genome data base but the full length cDNA has not yet been cloned. Mouse and human IP_6K1 are 96 % identical, except for an 8 amino acid insert in the carboxyl-terminus of hIP_6K1 (figure 16). This insert and some different amino acids in the carboxyl-terminus may lead to a structural changes or at least can effect the binding of regulatory proteins.

```
mIP6K1     1 MCVCQTMEVGQYGKNASRAGDRGVLLEPFIHQVGGHSSMMRYDDHTVCKPLISREQRFYE
hIP6K1     1 MCVCQTMEVGQYGKNASRAGDRGVLLEPFIHQVGGHSSMMRYDDHTVCKPLISREQRFYE

mIP6K1    61 SLPPEMKEFTPEYKGVVSVCFEGDSDGYINLVAYPYVESETVEQDDTPEREQPRRKHSRR
hIP6K1    61 SLPPEMKEFTPEYKGVVSVCFEGDSDGYINLVAYPYVESETVEQDDTTEREQPRRKHSRR

mIP6K1   121 SLHRSGSGSDHKEEKASLSFETSESSQEAKSPKVELHSHSDVPFQMLDSNSGLSSEKISY
hIP6K1   121 SLHRSGSGSDHKEEKASLSLETSESSQEAKSPKVELHSHSEVPFQMLDGNSGLSSEKISH

mIP6K1   181 NPWSLRCHKQQLSRMRSESKDRKLYKFLLLENVVHHFKYPCVLDLKMGTRQHGDDASAEK
hIP6K1   181 NPWSLRCHKQQLSRMRSESKDRKLYKFLLLENVVHHFKYPCVLDLKMGTRQHGDDASAEK

mIP6K1   241 AARQMRKCEQSTSATLGVRVCGMQVYQLDTGHYLCRNKYYGRGLSIEGFRNALYQYLHNG
hIP6K1   241 AARQMRKCEQSTSATLGVRVCGMQVYQLDTGHYLCRNKYYGRGLSIEGFRNALYQYLHNG

mIP6K1   301 LDLRRDLFEPILSKLRGLKAVLERQASYRFYSSSLLVIYDGK--------ECRSELRLKH
hIP6K1   301 LDLRRDLFEPILSKLRGLKAVLERQASYRFYSSSLLVIYDGKECRAESCLDRRSEMRLKH

mIP6K1   353 VDMGLPEVPPPCGPSTSPSSTSLEAGPSSPPKVDVRMIDFAHSTFKGFRDDPTVHDGPDR
hIP6K1   361 LDMVLPEVASSCGPSTSPSNTSPEAGPSSQPKVDVRMIDFAHSTFKGFRDDPTVHDGPDR

mIP6K1   413 GYVFGLENLISIMEQVPDENQ
hIP6K1   421 GYVFGLENLISIMEQMRDENQ
```

Figure 16: Alignment of mouse and human inositol hexakisphosphate kinase. HIP_6K1 and mIP_6K1 are 96 % homologous. HIP_6K1 contains a 8 amino acid insert in the carboxyl terminus.

To be sure that an active form of the enzyme was expressed in different human cell lines, the human IP_6K1 isoform was cloned out of HEK293T cell using reverse transcriptase-PCR (RT-PCR) with specific primers for the amino- and carboxyl-terminus of hIP_6K1. The resulting single PCR fragment had a mobility of about 1.3 kb in a 1 % agarose gel (figure 17), which corresponded to the size of hIP_6K1 (1326 bp) and was cloned into the mammalian expression vector pCMV3A. The fact that there was only one PCR product suggests that there is not another splice variant of IP_6K1 in HEK293T cells. The sequence of hIP_6K1 from HEK293T cells was confirmed by sequencing to be 100 % identical to the hIP_6K1 sequence published in the data base (data not shown), confirming that HEK293T cells contain and express an wildtype IP_6K1 cDNA.

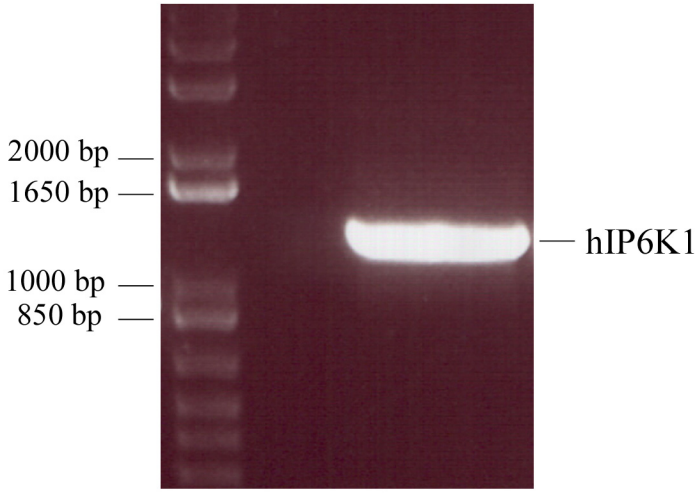

Figure 17: Cloning of hIP_6K1 out of HEK293T cells. HIP_6K1 specific primers were used to amplify full length hIP_6K1 from 1 µg RNA from HEK293T cells. The size of hIP_6K1 is 1326 bp.

3.2 Overexpressed IP_6K1 and IP_6K2 localizes to the nucleus

Previously, unique localization of overexpressed mouse IP_6K1, human IP_6K2 and 3 fused to GFP have been reported in HEK293T cells. GFP-IP_6K1 was shown to localize to the nucleus and cytoplasm, IP_6K2 to the nucleus and IP_6K3 mostly to the cytoplasm (Saiardi *et al.*, 2001). To confirm the intracellular localization of overexpressed $IP_6K1$and IP_6K2 in NIH3T3, MG63 and COS-7 cells, IP_6K1 and IP_6K2 fused to the myc tag were transiently transfected into these cell lines, using FuGENE6. A myc tagged version of the proteins was used instead of GFP-fusions in order to avoid undesired effects of these constructs, such as toxicity, non specific interactions and size. Additionally, hIP_6K1 was transfected into U2OS cells. As shown in figure 18 both enzymes were localized in the nucleus in every cell line tested. From previous studies there is no evidence that IP_6Ks are involved in nuclear signaling events, but the fact that two overexpressed isoforms are localized in the nucleus point to the conclusion, that inositol hexakisphoshate kinases and inositol pyrophosphates also play a role in nuclear signaling events.

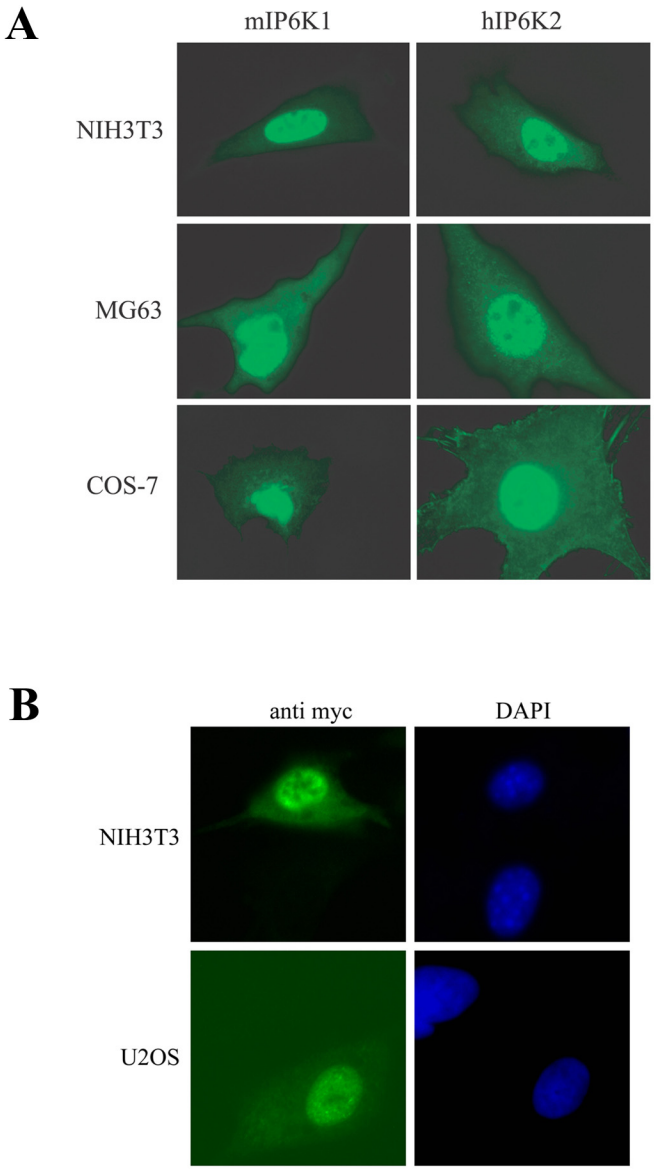

Figure 18: Overexpression of IP_6K1 and IP_6K2 in different cell lines. Myc-mouse IP_6K1 and myc-human IP_6K2 were transiently transfected into NIH3T3, MG63 and COS-7 cells (A). Additionally, myc-human IP_6K1 was transiently transfected into NIH3T3 and U2OS cells (B). In both cell lines hIP_6K1 is localized in the nucleus as shown by visualized of the DNA with DAPI.

3.3 Subcellular localization of endogenous IP_6K1

3.3.1 Characterization of polyclonal anti IP_6K1 and IP_6K2 antibodies

To examine the subcellular localization of endogenous IP_6Ks, polyclonal antibodies were raised against mIP_6K1 and hIP_6K2. The antibodies were characterized using immunofluorescence and immunoblot. The affinity purified antibodies against IP_6K1 did not react with IP_6K2 under denaturing conditions as shown in western blot (figure 19). To characterize the antibody under native conditions NIH3T3 cells were transfected with myc tagged mIP_6K1 and hIP_6K2 constructs and stained with polyclonal anti IP_6K1 antibody. Polyclonal anti IP_6K1 antibody seemed to recognized overexpressed IP_6K2 to some extent under native conditions as shown by immnunofluorescence (figure 20). IP_6K2 expressing cells showed a slight increase in fluorescence compared to the background fluorescence araising from endogenous IP_6K1, which differed from cell to cell in intensity in general. However fluorescence araising from overexpressed IP_6K1 increased dramatically from its endogenous background. IP_6K2 affinity purified antibody, probing for IP_6K1 protein, did not show any crossreactivity towards the other isoform (figure 20 and appendix). Both antibodies did not crossreact with the other isoform *in vitro* and *in vivo* and thus, are isoform specific. Interestingly, both IP_6K isoforms were localized in the nucleus when stained with isoform specific polyclonal antibodies (figure 20). IP_6K2 was localized in the nucleus in every cell (appendix), whereas IP_6K1 was found to be also localized in the cytoplasm (see chapter 1.3.2).

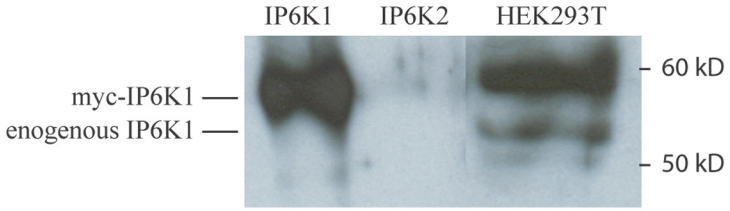

Figure 19: Characterization of anti IP_6K1 pAb by immuno blotting. 5ng of recombinant mIP_6K1 and hIP_6K2, and 10 µg of HEK293T lysates were separated on a SDS-PAGE. In the following immunoblot it was probed with anti IP_6K1 pAB. The IP_6K1 specific antibody did not recognize IP_6K2, but a second band was detected in the lysates.

The IP_6K1 specific antibody detected two protein bands different size in HEK293T lysates. The lower band corresponded to the size of IP_6K1 (54 kD). The upper band does not represent IP_6K2 since the molecular size is the same and the antibody did not show any cross reactivity. Furthermore, the molecular size of IP_6K3 is smaller than IP_6K1 and IP_6K2. It is unlikely that this band presents a splice variant of IP_6K1, because RT-PCR analysis of IP_6K1 resulted in a single band (figure 17). The protein corresponding to the upper band only seems to interact with anti IP_6K1 antibody under denaturing conditions because the protein could not be immunoprecipitated using the IP_6K1 antibody. There was only one band visible in the immunoprecipitate, implicating that the IP_6K1 antibody is specific *in vivo* (immunofluorescence).

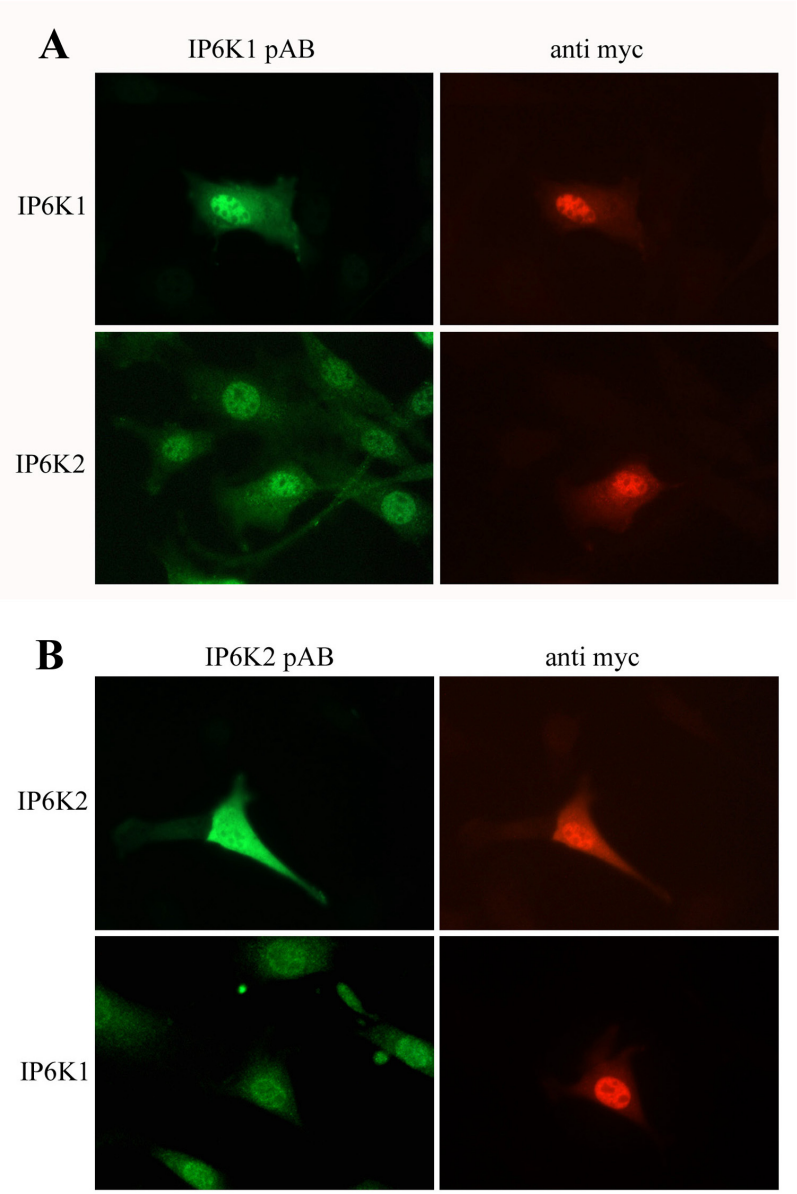

Figure 20: Characterization of anti IP_6K1 and IP_6K2 pAB by immunofluorescence. NIH3T3 cells were transiently transfected with either mIP_6K1 or hIP_6K2. The cells were fixed with methanol and costained with anti-myc mAb and anti mIP_6K1 pAb (A) or anti hIP_6K2 pAb (B). The pictures showing IP_6K1 overexpressing NIH3T3, stained with anti IP_6K1 pAb were taken with shorter exposure time than IP_6K2 expressing cells. In this case the exposure time was too short to see endogenous IP_6K1 in surrounding cells. This was the same case in IP_6K2 overexpressing cells, stained with anti IP_6K2 pAb

3.3.2 IP_6K1 is expressed in different cell lines

It has been shown by northern blot that IP_6K1 is ubiquitiously expressed at high levels in brain, (Saiardi *et al.*, 1999). To determine a cell line with high expression levels of IP_6K1, different lysates were probed with anti IP_6K1 antibody. As shown in figure 21 IP_6K1 is expressed in HEK293T, NIH3T3, HeLa, U2OS cells and at the highest level in brain lysates as shown by both western blot and RT-PCR. To examine the intracellular localization of endogenous IP_6K1, NIH3T3 cells were plated on coverslips and stained with anti IP_6K1 antibody. Interestingly, some cells showed bright nuclear staining, whereas some did not contain IP_6K1 in the nucleus at all (figure 22), suggesting that IP_6K1 might be able to shuttle between the cytosol and the nucleus.

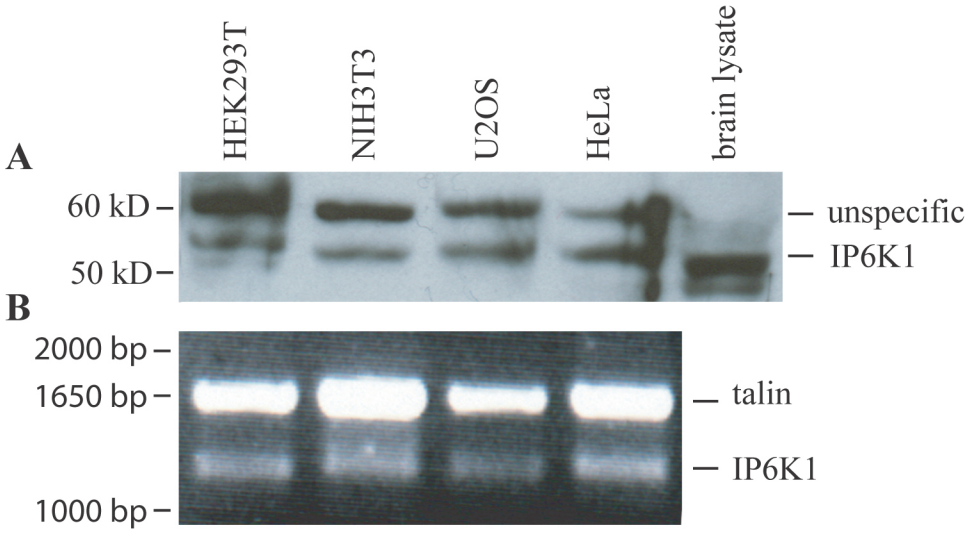

Figure 21: Characterization of IP_6K1 expression in different cell lines. 10 µg cell lysates were separated by SDS-PAGE and probed with anti IP_6K1 pAB (A). Additionally, 1 µg of mRNA was analyzed by RT-PCR with hIP_6K1 and mIP_6K1 (NIH3T3) specific primers, resulting in the full length PCR product, talin specific primers were used as control (B).

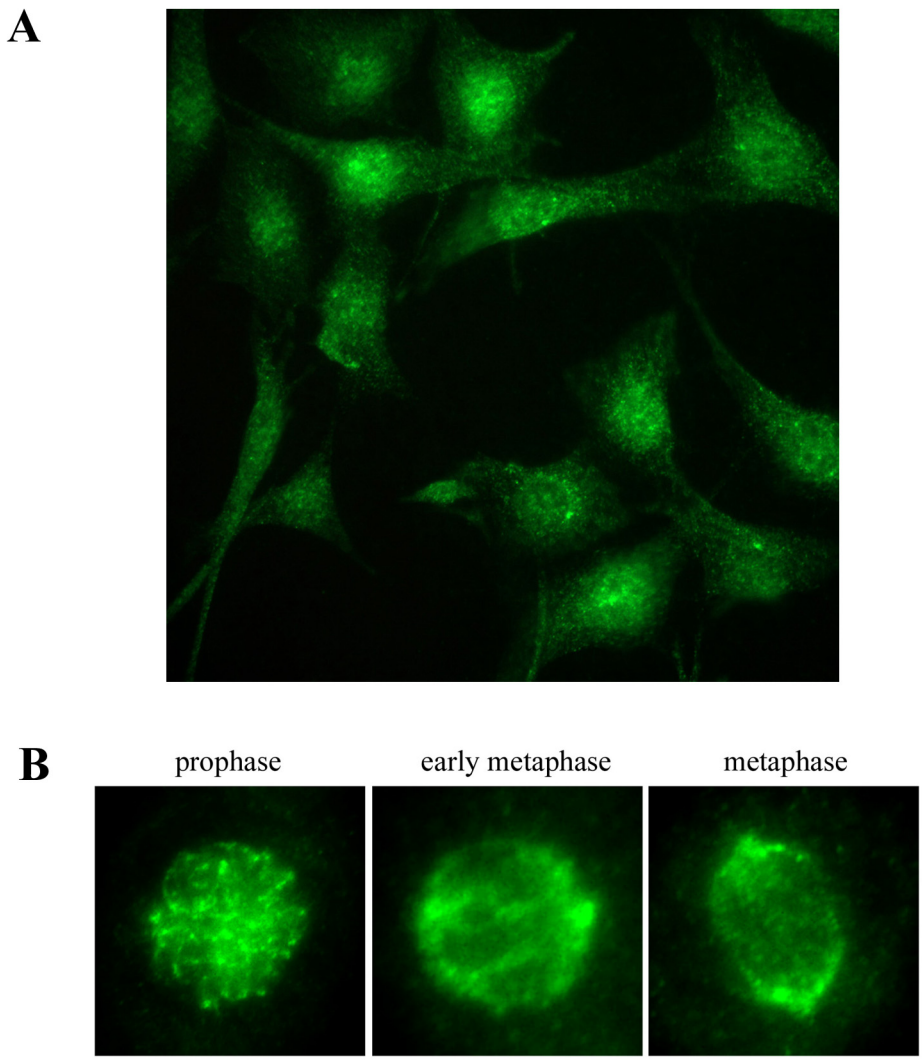

Figure 22: Localization of endogenous IP_6K1 in NIH3T3 cells. NIH3T3 cells, plated on coverslips, were stained with anti IP_6K1 pAb. A: In some cells IP_6K1 is strongly localized to the nucleus, whereas in other cells IP_6K1 seemed to be excluded from the nucleus. B: During mitosis IP_6K1 is localized at different positions. In prophase it is localized at the DNA and translocates to the mitotic spindles and the **spindlepoles in metaphase.**

3.4 Cell cycle dependent localization of IP_6K1

3.4.1 IP_6K1 translocates into the nucleus in G2

The observation that IP_6K1 seems to shuttle in and out of the nucleus (figure 22) led to the question what caused the nuclear import or export of IP_6K1. One possibility is, that the intracellular localization of IP_6K1 is cell cycle dependent. To examine whether the nuclear localization of IP_6K1 is dependent on the cell cycle, NIH3T3 cells were treated with different cell cycle arresting agents. The effect on the agent of the cell cycle profile was confirmed by propidium iodide staining and analysis by flow cytometry. As shown in figure 23, in cells treated with aphidicolin, which blocks the cells at the G1/S border, IP_6K1 was excluded from the nucleus. In contrast, cells arrested in G2 phase of the cycle with VP16, showed almost exclusively nuclear staining of the kinase. 75 % of the cells were in G2/M phase of the cell cycle (table 9). The number correlates with the number of cell showing nuclear staining of IP_6K1. This data suggests that IP_6K1 might be transported into the nucleus during late S-phase and is localized in the nucleus in G2 phase. This hypothesis is supported by the fact that cells treated with hydroxyurea and thereby blocked in S-phase, showed an increasing amount of IP_6K1 in the nucleus compared to aphidicolin treated cells (data not shown). The observation was confirmed in U2OS cells.

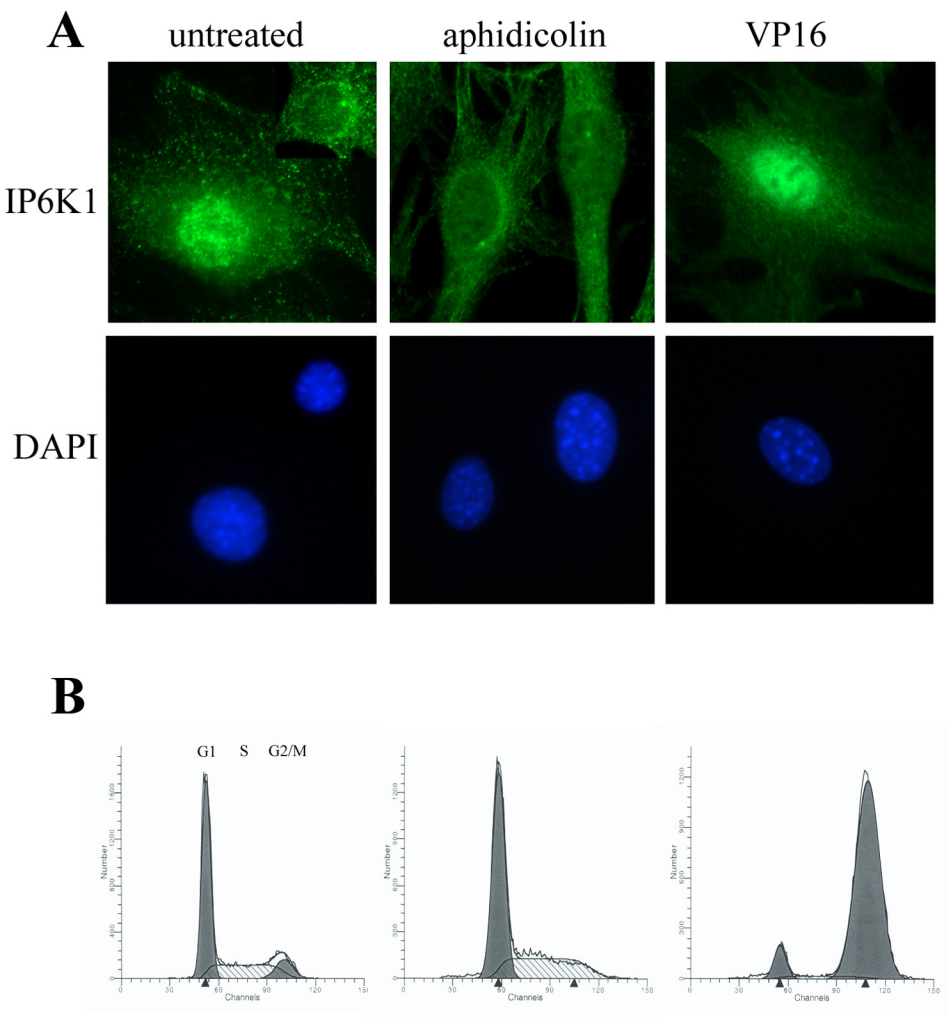

Figure 23: IP_6K1 translocates into the nucleus in G2 phase of the cell cycle. NIH3T3 cells were treated with aphidicolin and VP16 to block the cells at the G1 border and in G2 phase, respectively. The cells were stained with anti mIP_6K1 pAb and anti rabbit IgG FITC conjugated secondary antibody, and the DNA was stained with DAPI (A) and the cell cycle arrest was confirmed DNA analysis using flow cytometry (B).

Table 9: Quantification of % cells in cell cycle phases after treatment with cell cycle arresting agents

treatment	G1	S	G2/M
untreated	57.8	32.3	9.9
aphidicolin	63.2	36.9	nd
nocodazol	11.7	13.3	75

3.4.2 IP_6K1 is localized at the kinetochore and mitotic spindles in mitosis

Another striking observation in cells stained with ant IP_6K1 pAb was, that the kinase seemed to be localized at mitotic spindles. To further examine the subcellular localization of IP_6K1 different marker for mitotic proteins were used. U2OS cells were costained with anti IP_6K1 and anti centromere protein-F (CENP-F) pAb. CENP-F is a nuclear matrix kinetochore protein, that plays a role in mitotic events (Liao *et al.*, 1995; Zhu *et al.*, 1995).A replicated chromosome includes two kinetochores that control chromosome segregation during mitosis. The kinetochore is a DNA-protein complex at the centromere that faces the spindle poles. The mitotic spindles attach to the kinetochore to separate the two chromatides. (Rieder *et al.*, 1998; Choo, 2000). In HeLa cells CENP-F is preferentially expressed in mitosis where it mediates the G2 to M-phase transition. Upon completion of mitosis it is rapidly degraded (Ashar *et al.*, 2000).

In cells stained for IP_6K1 and CENP-F the mitotic phase of the cell cycle was demonstrated by staining the DNA with DAPI. In early prophase the DNA starts to be condensed but has not yet built the metaphase plate. During mitosis the DNA is organized in the metaphase plate and the mitotic spindles can attach at the kinetochore to separate the chromatides. Costaining of IP_6K1 and CENP-F in U2OS cells showed colocalization of both proteins at the kinetochore in early prophase (figure 24A). As the cells progress through mitosis IP_6K1 translocates to the mitotic spindle in metaphase which is demonstrated by costaining with anti IP_6K1 pAb and β-tubulin in figure 24B. The mitotic spindle is a highly dynamic molecular machine composed of tubulin, motors and other molecules. β-tubulin is one of the tubulin isoforms part of the mitotic spindle and is commonly used as marker for mitotic spindles.

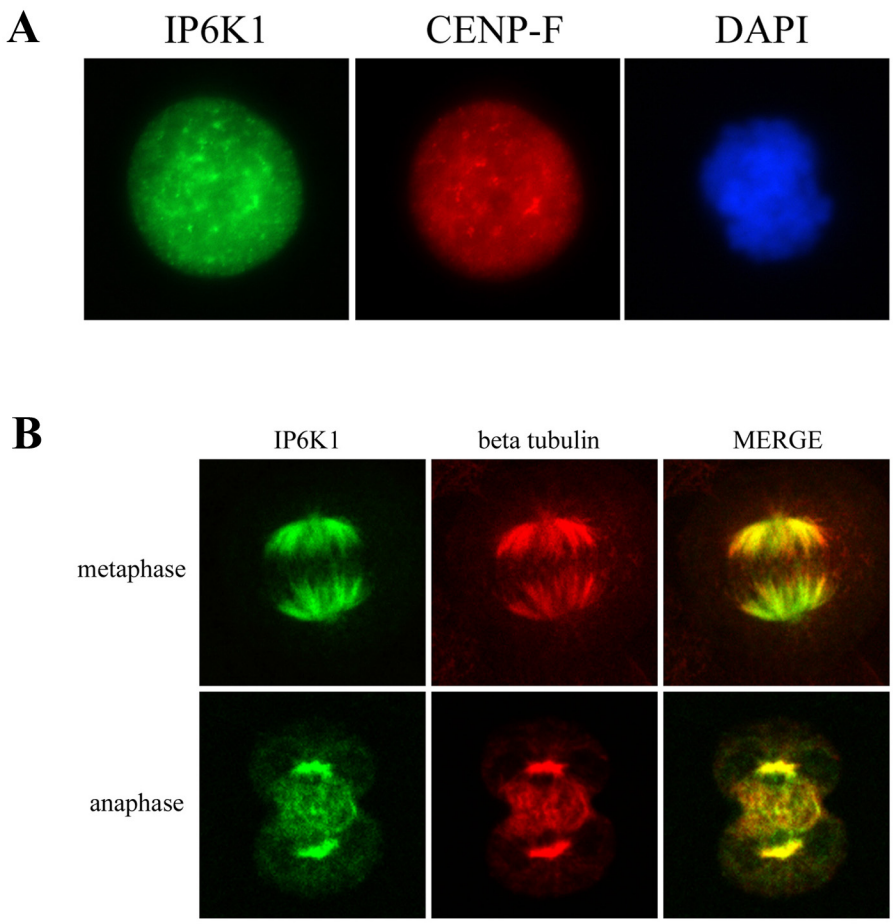

Figure 24: IP_6K1 localized at the kinetochore in prophase and translocates to the mitotic spindle. U2OS cells were costained with anti mIP_6K1 pAb and anti centromere protein F (CENP-F) pAb (A) or anti β-tubulin mAb (B).

3.5 IP_6K1 is posttranslationally modified in cells in G2/M

The observation above suggests a possible strict regulation of IP_6K1. Whether this might be by posttranscriptional modification or expression, was determined in the following experiment. HEK293T cells were blocked in different phases of the cell cycle as described in chapter 2.5.5. As shown in figure 25 there is no significant difference in expression levels of IP_6K1 through out the cell cycle. Interestingly, cells blocked in mitosis by nocodazol and

paclitaxel showed a mobility shift. In mitotic cell lysates IP_6K1 migrated slower by SDS-PAGE which might be due to posttranslational modification. This mobility shift was also visible in HeLa and U2OS cells, but not in NIH3T3 and MG63 cells (data not shown). NIH3T3 and MG63 have a fibroblast morphology, compared to a epithelial like morphology of HEK293T, HeLa and U2OS cells, suggesting that the mobility shift might depend on the morphology of the cell line. One possible posttranslational modification is phosphorylation, which often results in a visible mobility shift and is a common regulatory modification in mitosis. To determine if IP_6K1 is phosphorylated in nocodazol treated cells, the untreated and mitotic cell lysates were incubated with and without calf intestinal phosphatase (CIP), which dephosphorylates phosphorylated serine, threonine and tyrosine residues. As shown in figure 26 the nocodazol induced mobility shift of IP_6K1 was abolished by CIP treatment, implicating that IP_6K1 is phosphorylated in nocodazol induced mitotic cell.

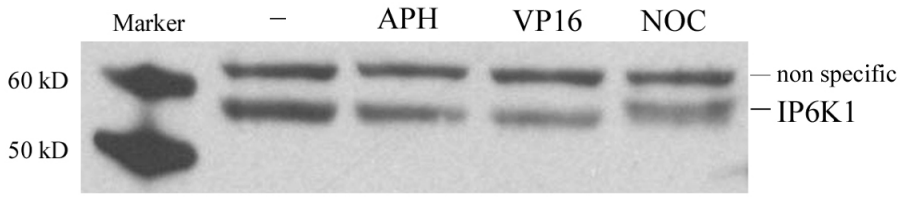

Figure 25: Nocodazol treatment of HEK293T cells resulted in an mobility shift of IP_6K1. HEK293T cells were either treated with aphidicolin (APH), VP16 or nocodazol (NOC) over night or were untreated (-). The cell lysates were separated by SDS-PAGE and it was probed with anti IP_6K1 pAb. In nocodazol treated cells IP_6K1 migrated slower in SDS-PAGE compared to untreated, aphidicolin and VP16 treated cells.

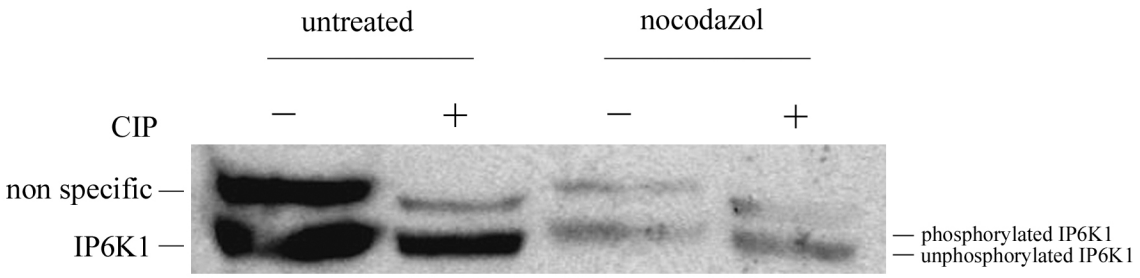

Figure 26: IP_6K1 is phosphorylated in nocadazol treated HEK293T cells. HEK293T cells were treated with or without nocodazol (NOC) over night. The lysates were treated with or without calf alkaline phosphatase (CIP) and analyzed by immuno blotting using anti IP_6K1 pAb.

3.6 Characterization of IP_6K1 knock out phenotype

3.6.1 Knock out of endogenous IP_6K1 causes G2/M arrest in HEK293T cells

To further investigate the role of IP_6K1 in mitosis, small interfering (si) RNA oligos were designed to knock out endogenous levels of IP_6K1. As shown by RT-PCR and western blot, IP_6K1 is almost completely depleted in HEK293T cells incubated with siRNA targeting IP_6K1 for 72 hours (figure 27).

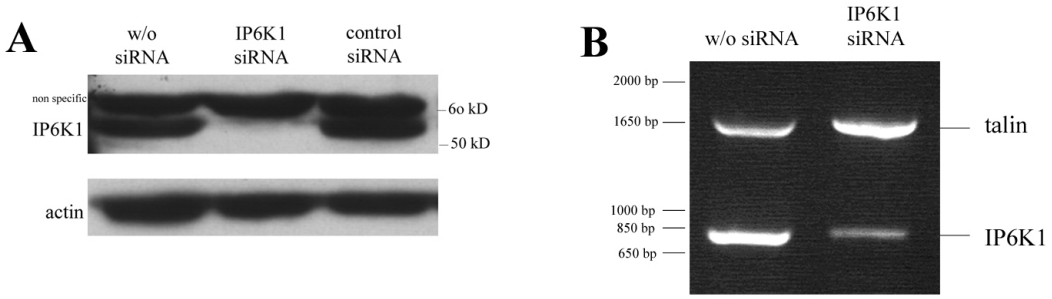

Figure 27: IP_6K1 is depleted in HEK293T cells transfected with IP_6K1 siRNA. A: HEK293T cells were transfected with IP_6K1 siRNA, control siRNA and without siRNA. 10 µg of the lysates were analyzed by SDS-PAGE and immunoblot. The blot was stained with anti IP_6K1 pAb and anti actin mAb as loading control. B: HEK293T cells were transfected with IP_6K1 siRNA and without siRNA. The mRNA was analyzed by RT-PCR using IP_6K1 specific primers and talin primers as control, resulting in a 700 bp and 1500 bp fragment, respectively.

The cell biology data described in chapter 3.4.1-3 led to the conclusion that IP_6K1 might be involved in cell cycle events, specifically in mitosis. Thus, knocking out endogenous IP_6K1 levels might result in a change in the cell cycle profile. To test this hypothesis IP_6K1 wildtype and knock out HEK293T cells were analyzed by flow cytometry using propidium iodide to stain DNA. As a control a siRNA with no homologous region in the human genome (see chapter 2.1.7.2), was used. As shown in figure 28, IP_6K1 knock out cells were arrested in G2/M-phase. 70 % of the cells were in G2/M-phase and only 5 % were in G1-phase, compared to 9.4 % in G2/M and 46.6 % in G1 in untransfected cells (table 10). The control siRNA did not have an effect on the cells (figure 28, upper panel, table 10), supporting the fact that the phenotype resulted from the knock out of IP_6K1 and not from siRNA in general.
To further analyze the IP_6K1 knock out cells arrested in G2/M-phase, the cells were stained with anti phospho-Histone 3 (ser10) antibody and analyzed by flow cytometry. Histone 3 phosphorylation is believed to be involved in chromosome compaction during cell division. Chromosome condensation in different organisms is accompanied by Histone 3 phosphorylation at serine 10 (Hendzel *et al.*, 1997; Van Hooser *et al.*, 1998; Wei *et al.*, 1999). This mitosis specific phosphorylation has been used to distinguish between cells in G2 and M-phase of the cell cycle. IP_6K1 knock out cells stained with phospho-Histone 3 (ser10) specific antibodies and analyzed by flow cytometry did not show a difference in the G2/M ratio compared to wildtype cells. About one third of the G2/M population were progressing through mitosis in both, knock out and wildtype cells (figure 29, lower panel, table 10).

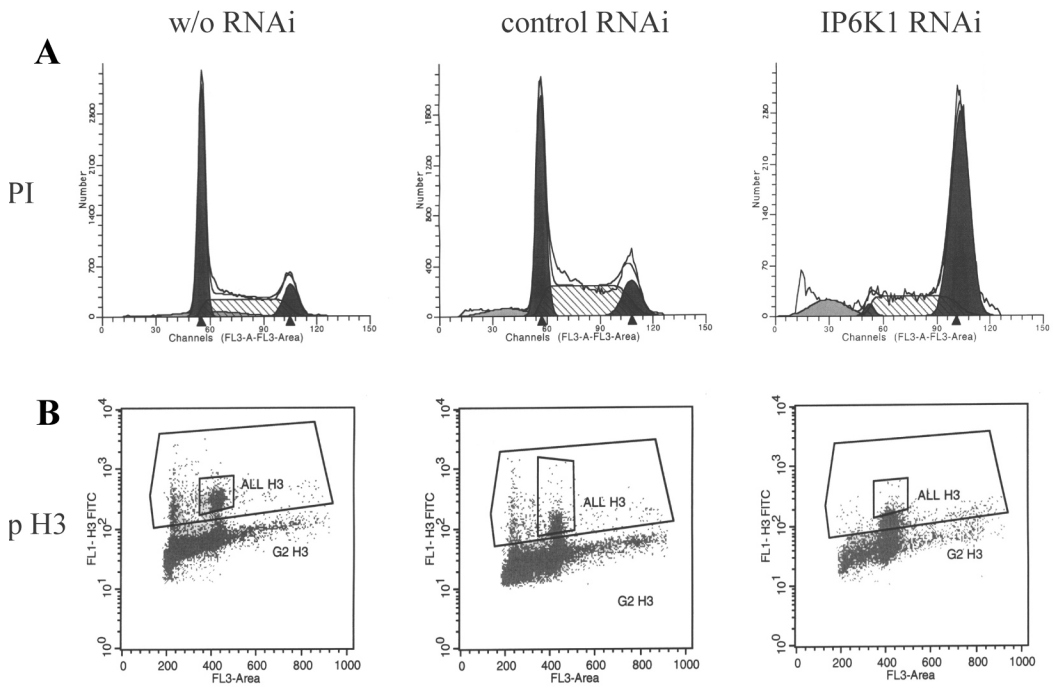

Figure 28: HEK293T IP_6K1 knock out cells are arrested in G2/M-phase of the cell cycle. HEK293T cells were transfected with IP_6K1siRNA, control siRNA and without RNA. 72 hours after transfection the cells were fixed and the DNA was stained with propidium iodide (A). Additionally the cells were stained with anti phospho-Histone 3 (serine 10) (pH3) polyclonal antibody and a FITC conjugated anti rabbit IgG secondary antibody (B) to separate the cells in G2-phase from cells in mitosis. The cells were analyzed by flow cytometry. Cells transfected with IP_6K1 siRNA showed a dramatic increase in cells in G2/M phase of the cell cycle. A: Left black peak: G1-phase, striped area: S-phase, right black peak: G2/M-phase

Table 10: Quantification of flow cytometry data (Figure 13)

siRNA	G1	S	G2/M	pH3 pos
IP_6K1	4.9	45.3	69.9	24
control	38.9	47.8	13.3	3.9
without	46.6	50.8	9.4	3.9

As shown in figure 29 IP_6K1 levels were almost completely depleted in IP_6K1 siRNA transfected cells. HEK293T knock out and wildtype cells were stained for IP_6K1, β-tubulin and DNA. The pictures were taken with the same exposure time to avoid different intensities due to different exposure times. The majority of the IP_6K1 knock out cells contained an intact nucleus and the DNA did not seem to be condensed, but the cells were round up compared to wildtype cells. An obvious phenotype of a smaller amount of IP_6K1 knock out cells was the abnormal mitotic spindle formation in cells arrested in mitosis. These cells showed abnormal morphology of the mitotic spindles (figure 29) and in some cells there were multiple spindle poles were visible (data not shown). Besides the abnormal spindle phenotype in IP_6K1 knock out cells, the DNA in these cells was condensed but was not organized in the metaphase plate, instead the entire cell was filled with DNA. Without organizing the DNA in the metaphase plate and the kinetochore facing the spindle poles, the spindles cannot attach to the chromosome. This results in cells that undergo a mitotic catastrophe and at the end apoptosis.

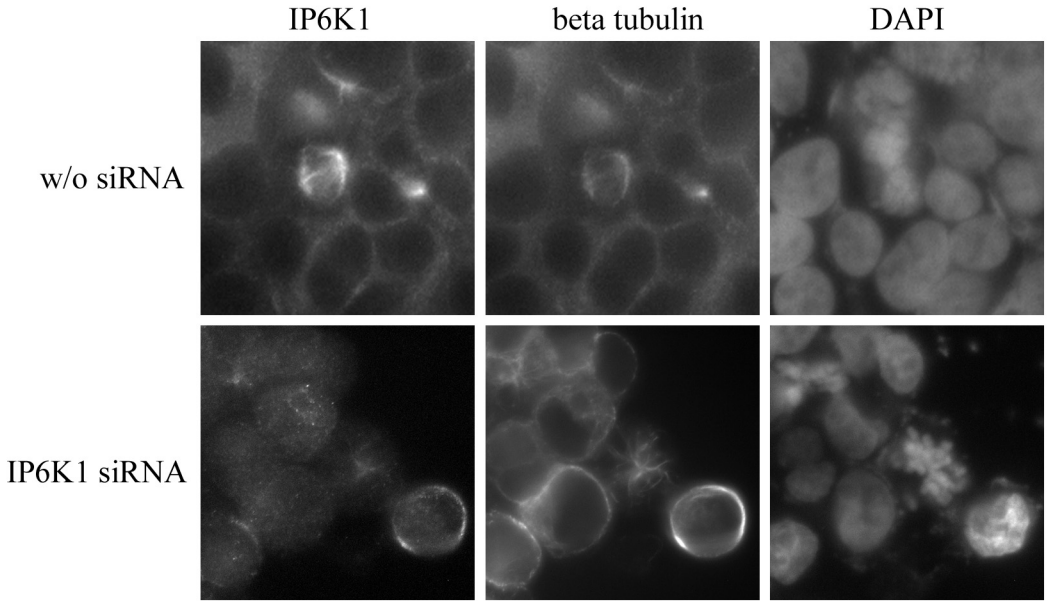

Figure 29: Analysis of HEK293T IP_6K1 knock out cells by immunofluorescence. HEK293T cells were transfected with IP_6K1 siRNA (lower panel) and without siRNA (top panel). The cells were stained for IP_6K1, β-tubulin and DNA. In cells transfected with IP_6K1 siRNA, IP_6K1 levels were almost completely abolished, the cells were round and the mitotic spindles showed an abnormal morphology.

3.6.2 The IP_6K1 knock out phenotype can be rescued by overexpressing hIP_6K1

To confirm that the G2/M arrest is caused by the depletion of IP_6K1 and not by an unspecific knock out, hIP_6K1 with three silent mutations in the siRNA targeting region (hIP_6K1rescue, see material and methods, chapter 2.6.2) was coexpressed with the hIP_6K1 siRNA oligo. As shown in figure 30, hIP_6K1rescue is able to rescue the G2/M arrest. Cells expressing hIP_6K1rescue showed a normal cell cycle profile compared with untransfected knock out cells. Surprisingly, the putative kinase dead hIP_6K1 mutant (hIP_6K1rescueDLK-AAA) was also able to rescue the G2/M arrest (figure 30). Overexpression of both proteins did not have an dramatic effect on the cell cycle profile in wildtype cells. Cells in S-phase were decreased

after overexpression of both IP_6K1 constructs. Since the kinase activity of the enzymes could not be determined (see appendix), it remains unanswered if this mutant still has kinase activity. Overexpression of IP_6K2 was only able to partially rescue the IP_6K1 knock out cells (data not shown), suggesting that at least IP_6K1 protein but possibly also kinase activity might be important for the cells progressing through mitosis. Another possibility is that overexpression of hIP_6K1 causes a different phenotype in HEK293T cells independent of the G2/M arrest resulting from the IP_6K1 knock out. This experiment is described in chapter 3.6.3

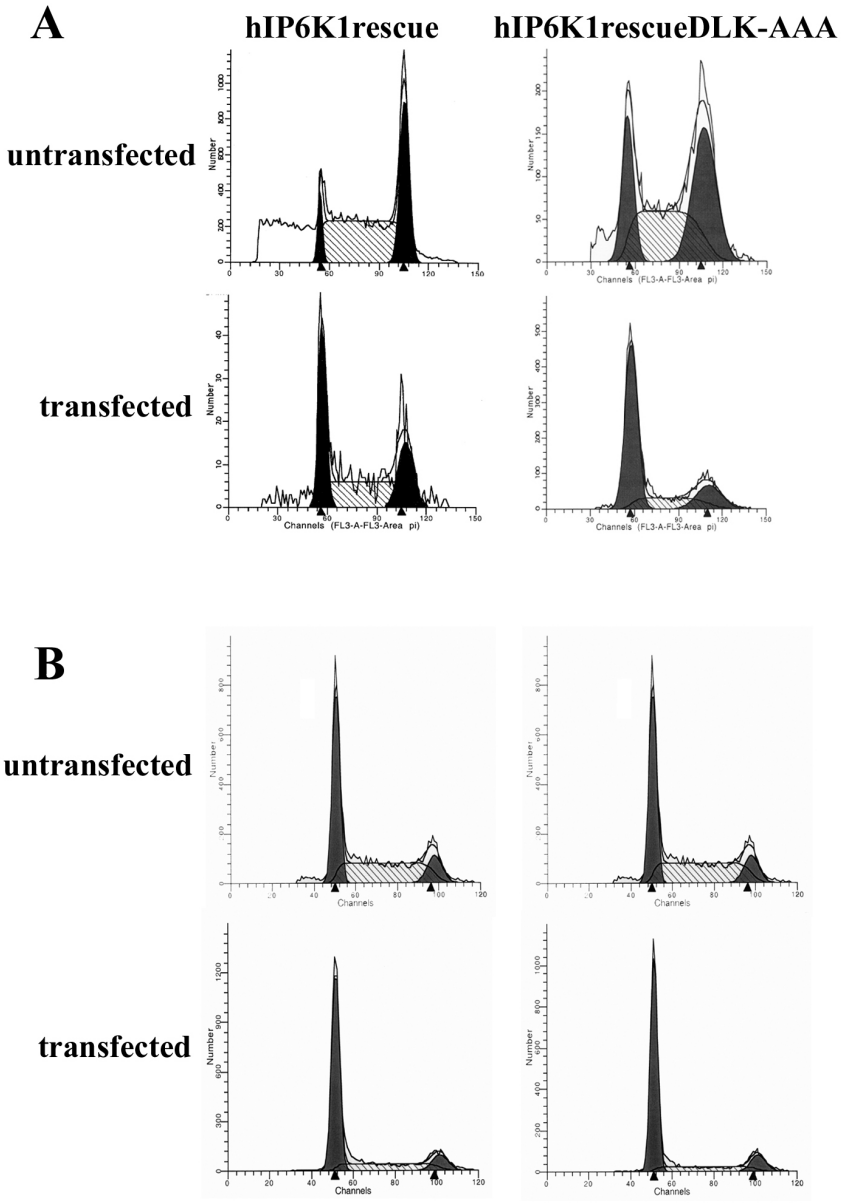

Figure 30: Overexpression of hIP$_6$K1 rescues the knock out phenotype. A: HEK293T cells were cotransfected with IP$_6$K1 siRNA and hIP$_6$K1rescue or hIP$_6$K1rescueDLK-AAA. After 72 hours the cells were stained with anti myc mAb and propidium iodide. The transfection efficiency of both constructs was about 50 %. The hIP$_6$K1rescue and rescueDLK-AAA transfected and untransfected cells from one tissue culture dish were analyzed by flow cytometry. The transfected (IP$_6$K1rescue and IP$_6$K1rescueDLK-AAA) cells did not arrest in G2/M, though they were also transfected with IP$_6$K1 siRNA. B: HEK293T cells were only transfected with the IP$_6$K1 constructs as control.

Table 11: Quantification of figure 30

siRNA		% G1	% S	% G2/M
IP_6K1	IP_6K1rescue neg	15.4	35.1	49.6
	IP_6K1rescue pos	55.2	25.7	19.1
	IP_6K1rescueDLK-AAA neg	28.8	35.7	35.6
	IP_6K1rescueDLK-AAA pos	60.4	21.9	17.7
	vector	23.5	38.4	38.1
	untransfected	4.9	45.3	69.9
without	IP_6K1rescue neg	38	52.8	9.2
	IP_6K1rescue pos	62.9	28.4	8.7
	IP_6K1rescueDLK-AAA neg	40	54.5	5.5
	IP_6K1rescueDLK-AAA pos	64	27.7	8.3
	vector	44.3	50.7	6
	untransfected	46.6	50.8	9.4

3.6.3 Depletion of IP_6K1 in U2OS cells increased amount of cells in G2M and apoptotic cells

To determine whether the G2/M arrest in IP_6K1 knock out cells occurs not only in HEK293T cells, U2OS cells were also transfected with the IP_6K1 specific siRNA oligo and incubated for 54 and 72 hours. 54 hours after transfection, U2OS cells depleted of IP_6K1 also showed an increase of cells in G2/M, but the increase was not as dramatic as in HEK293T cells. U2OS IP_6K1 ko cells contained 30 % cells in G2/M-phase compared to 70 % in HEK293T IP_6K1 ko cells (table 10 and 12). Instead, 15 % of the cells underwent apoptosis 72 hours after transfection (figure 31, table 12). Since the control cells were not apoptotic, apoptosis was not an unspecific effect of siRNAs in U2OS cells.

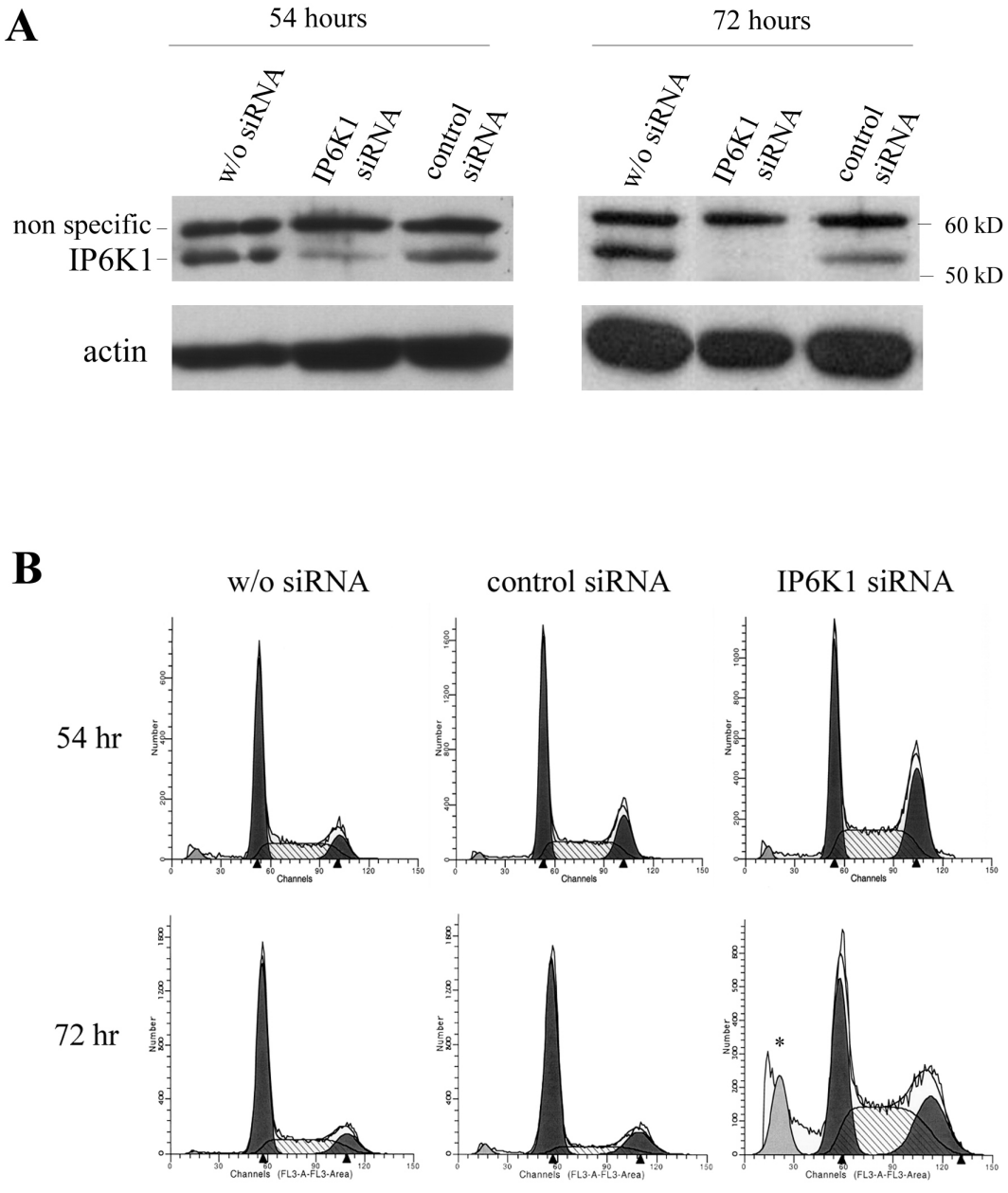

Figure 31: IP_6K1 knock out caused apoptosis in U2OS cells. HEK293T cells transfected with IP_6K1 siRNA, control siRNA or without siRNA were analyzed by immunoblot with staining for IP_6K1 and actin as loading control (A) and flow cytometry with staining for DNA (B). 72 hours post transfection IP_6K1 was depleted from HEK293T cells and the number of cells in apoptosis (*) increased.

Table 12: Quantification of flow cytometry data from figure 31

hours after transfection	siRNA	% G1	% S	% G2/M	% apoptosis
54	IP_6K1	35.1	35.6	28.8	1.8
	control	48.6	32.2	18.6	1.6
	without	53.2	33.3	12.5	3
72	IP_6K1	32.2	33.5	22.4	14.7
	control	61.9	22.6	13.8	3.1
	without	57.3	30.9	11.3	0.6

3.6.4 Analysis of different mitotic regulating proteins in HEK239T IP_6K1 ko cells

Mitosis in vertebrate cells is thought to be triggered by cyclin dependent kinase 1 (Cdk1). Cdk1 activation is performed in multiple steps. In G2 phase of the cell cycle levels of the regulatory subunit of Cdk1, cyclin B, begin to rise and peak in mitosis. Before mitosis the Cdk1-cyclin B complex is held in an active state by phosphorylation of Cdk1 at position threonine 14 (Thr14) and tyrosine 15 (Tyr15) by two different kinases, Wee1 and Myt1. At the onset of mitosis the phosphatase Cdc25C dephosphorylates Cdk1 at Thr14 and Tyr15 and thereby activates it (Lew *et al.*, 1996; Morgan, 1997; Ohi *et al.*, 1999). Specific antibodies against Cdk1 phosphorylated at residue tyrosine 15 (pTyr15Cdk1) can be used to determine if Cdk1 is activated and cell enter mitosis. Cell lysates of IP_6K1 knock out and wildtype cells were analyzed using anti pTyr15Cdk1 antibodies. As control, HEK29T cells were blocked in mitosis with nocodazol. IP_6K1 knock out cells contained dephosphorylated Cdk1, as did nocodazol treated cells (figure 32), suggesting that Cdk1 was active in IP_6K1 knock out cells and the cells entered mitosis. Since Histone 3 phosphorylation was not completed as shown before in figure 28, it seems more logical that the cells are arrested at the G2/M border, after Cdk1 dephosphorylation but before Histone 3 phosphorylation is completed.

Key steps in the progression through and exit out of mitosis are controlled by degradation of mitotic proteins. Ubiquitination and degradation of cyclin B is required for the cells to exit

from mitosis (Morgan, 1999). In HEK293T IP_6K1 knock out cells cyclin B was not degraded. Compared to wildtype and nocodazol treated cells, IP_6K1 ko cells contained the same amount of cyclin B1 (figure 32). This data suggests that the Cdk1-cyclinB1 complex is active in IP_6K1 knock out cells.

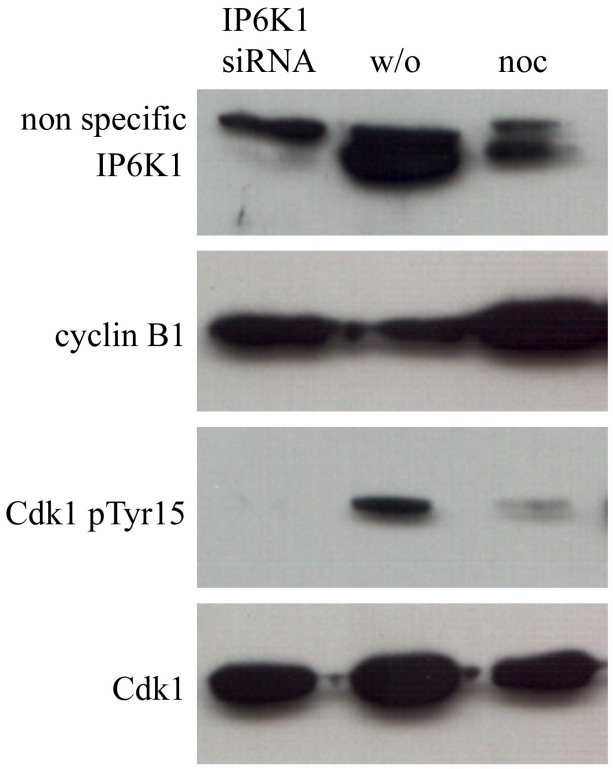

Figure 32: Analysis of key mitotic proteins in HEK293T IP_6K1 knock out cells. HEK293T cells were transfected with IP_6K1 siRNA, untransfected or treated with nocodazol (noc) as control for mitotic cells. 10 µg of the cell lysates were analyzed by immuno blotting using anti IP_6K1 pAb, anti cyclin B1 mAb, anti phospho Tyr15 Cdk1 mAb and anti Cdk1 mAb

3.7 Overexpression of hIP$_6$K1 in HEK293T cells arrests the cells in G1

As discussed in chapter hIP$_6$K1 seems to be able to rescue the IP$_6$K1 knock out induced G2/M arrest. There is the possibility that IP$_6$K1 overexpression has an additional effect on cell cycle progression. To test this possibility, HEK293T cells were transfected with different IP$_6$K1 and IP$_6$K2 constructs. The cells were then blocked in mitosis with nocodazol. Analysis by flow cytometry showed, that IP$_6$K1 transfected cells were not blocked in mitosis after nocodazol treatment, instead the cells were accumulated in G1 phase of the cell cycle (figure 33, table 13). Thus, IP$_6$K1 transfected cells have never progressed through the cell cycle and nocodazol did not have an effect on them.

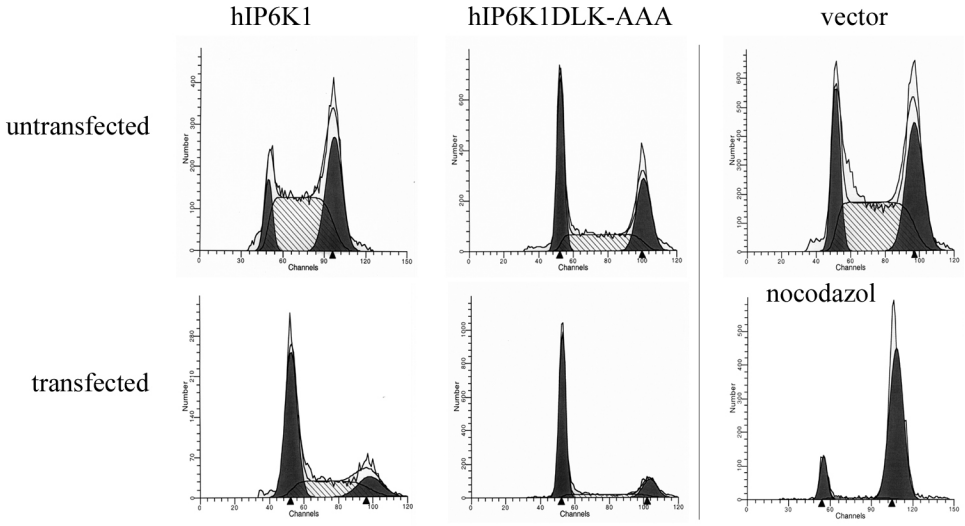

Figure 33: IP$_6$K1 induced arrest in G1 phase of the cell cycle in HEK293T cells. Left panel: HEK293T cells were transiently transfected with hIP$_6$K1 or hIP$_6$K1DLK-AAA. After 32 hours expression the cells were treated with 100 ng/ml nocodazol over night, stained with anti myc mAb and propidium iodide and analyzed by flow cytometry. IP$_6$K1 and IP$_6$K1DLK-AAA transfected cells seemed to be resistant against nocodazol treatment. Right panel: HEK293T cells were mock transfected (vector) and treated with nocodazol or treated with nocodazol without transfection reagent as controls

Table 13: Quantification of figure 33

treatment		% G1	% S	% G2/M
DMSO	IP_6K1 neg	42.3	45.9	11.8
	IP_6K1 pos	65.7	24.1	10.2
	IP_6K1DLK-AAA neg	49	40.3	10.7
	IP_6K1DLK-AAA pos	71.3	17.7	11
	vector	49.3	43.1	7.6
nocodazol	IP_6K1 neg	19.2	44.7	36.1
	IP_6K1 pos	57.1	25.7	17.2
	IP_6K1rescueDLK-AAA neg	37.1	32.7	30.1
	IP_6K1rescueDLK-AAA pos	70	14.5	15.5
	vector	30	39.1	30.1
	untransfected	12.3	3.4	84.3

3.8 Inositol pyrophosphate levels don't change during cell cycle

To examine if the production of inositol pyrophosphates is upregulated during mitosis, HEK293T cells were labeled with ^{3}H-inositol for at least four days and then treated with cell cycle blocking agents over night. The cell lysates were analyzed by HPLC with ^{3}H-IP_6 as standard. There was only one peak of inositol pyrophosphates visible in the HPLC profile. Due to the age of the column, it is possible that the detector was not able to distinguish between the IP_7 and IP_8 peak. No significant difference of IP_7 and IP_8 levels between untreated and aphidicolin treated cells could be observed (figure 34). Nocodazol treated cells seemed to contain more IP_7 and IP_8, but this number varied in untreated cells. In a different experiment the amount of IP_7 and IP_8 was almost as high as in nocodazol treated cells (see appendix). Thus, this result needs to be confirmed and investigated further. Inositol pyrophosphates are in very low concentration in the cell and are turned over very fast (Menniti *et al.*, 1993). To increase the intracellular concentration of inositol pyrophosphates cells were treated as described above and then incubated for 30 min in 50 mM NaF to

prevent the turn over of the inositol pyrophosphates. NaF inhibits phosphatases and was specifically used to inhibit diphosphoinositolphosphate phosphatase (DIPP) to increase inositolpyrophosphate concentration (Menniti *et al.*, 1993). Treatment with NaF increased the intracellular IP_7, IP_8 and $PPIP_4$ concentration as expected. Interestingly, there was no $PPIP_4$ detectable in aphidicolin treated cells compared to untreated and nocodazol treated cells (figure 35). Since there are no ^3H-IP_7 and -IP_8 standards commercially available, the retentiontime $PPIP_4$ and IP_7 peak need to be confirmed by IP_6K kinase assays

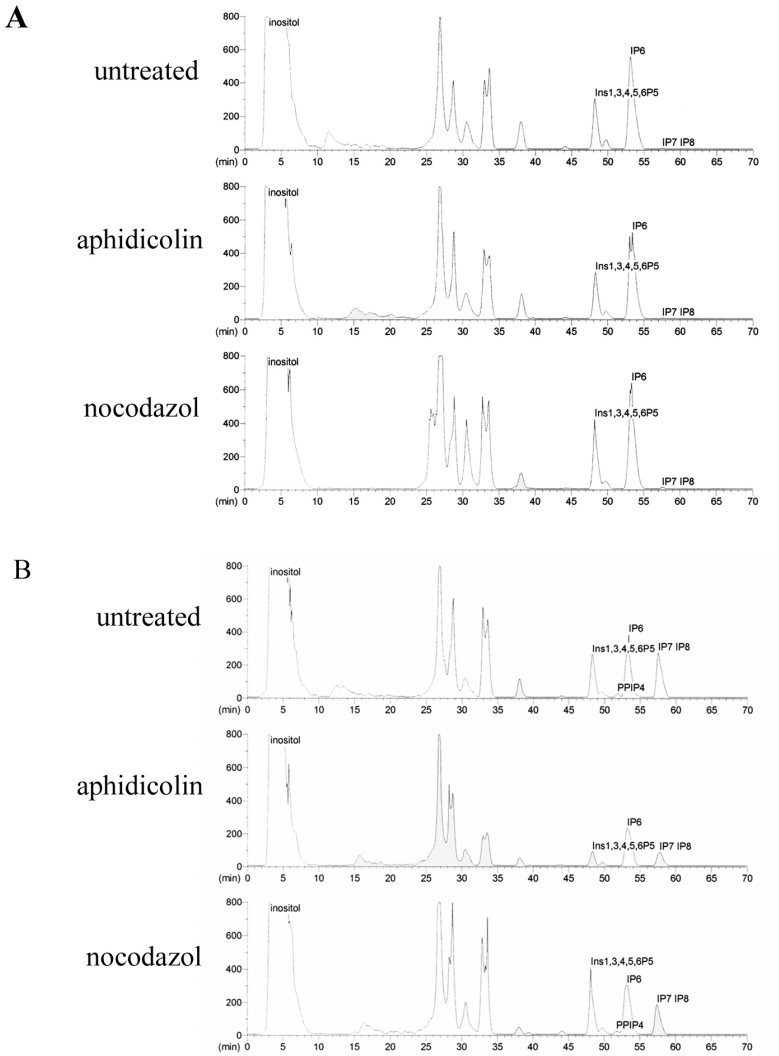

Figure 34: Metabolic labeling of cell cycle arrested HEK293T cells with ^3H-inositol. HEK293T cells were labeled with 25 µCi/ml ^3H-inositol for 4.5 days. The cells were treated with aphidicolin, nocodazol or DMSO over night. The cells were analyzed by HPLC without (A) or with 1 hour treatment of 40 mM NaF (B). (The y-axis represents counts per minute.)

Table 14: Quantification of inositol phosphate levels in HEK293T cells

treatment	Inositol phosphate	Peak area (CPM)	$IP_6/IP_{7/8}$
untreated w/o NaF	ins 1,3,4,5,6P_5	1982	
	$PPIP_4$	nd	
	IP_6	5117	
	IP_7/IP_8	12	426
aphidicolin w/o NaF	ins 1,3,4,5,6P_5	1908	
	$PPIP_4$	nd	
	IP_6	5559	
	IP_7/IP_8	15	370
nocodazol w/o NaF	ins 1,3,4,5,6P_5	2610	
	$PPIP_4$	nd	
	IP_6	6127	
	IP_7/IP_8	56	109
untreated with NaF	ins 1,3,4,5,6P_5	1910	
	$PPIP_4$	95	
	IP_6	2779	
	IP_7/IP_8	2475	1.1
aphidicolin with NaF	ins 1,3,4,5,6P_5	627	
	$PPIP_4$	nd	
	IP_6	2579	
	IP_7/IP_8	847	3.0
nocodazol with NaF	ins 1,3,4,5,6P_5	2429	
	$PPIP_4$	141	
	IP_6	3485	
	IP_7/IP_8	1664	2.1

nd: non detectable

4 Discussion

The existence of inositol pyrophosphates is known for 10 years, but the biological function of these putative high energy second messengers still remains unknown. The main goal of this thesis was to characterize one isoform of the inositol hexakisphosphate kinases, which produces inositol pyrophosphates. This should help to elucidate the biological function of inositol pyrophosphates as second messengers. The obtained data suggests that inositol hexakisphosphate kinase type 1 might be involved in cell cycle regulating events

4.1 Subcellular localization of IP_6K1

4.1.1 IP_6K1 is localized in the nucleus

Characterization of subcellular localization of IP_6K1 in different cell lines showed that myc-IP_6K1 localized in the cytoplasm and the nucleus in NIH3T3, MG63, COS-7 and U2OS cell. IP_6K1 has a molecular size of 50 kDa. Molecules this size might be able to diffuse through the nuclear membrane when overexpressed. Saiardi *et al*. showed that the GFP IP_6K1 fusion protein is localized in the nucleus and cytoplasm of HEK293 cells (Saiardi *et al.*, 2001). GFP has a molecular size of 25 kDa. The fusion protein is too large to diffuse through the nuclear membrane, implicating that IP_6K1 may be imported into the nucleus and may be involved in nuclear signaling events. In this study GFP-fusion proteins were not used, to avoid a possible toxic effect of GFP. In order to confirm the subcellular localization of IP_6K1 stable NIH3T3 and U2OS cells with the integrated IP_6K1 gene under a cytomegalovirus (CMV) promotor would have been desirable. Unfortunately, the attempt failed to produce such cells. The cells did not express IP_6K1 after several selection steps.

4.1.2 IP_6K1 is able to shuttle in and out of the nucleus

Overexpression of a protein is helpful to understand a possible localization of a protein in the cell, but often it does not show the actual localization. The concentration of an overexpressed protein is dramatically higher than endogenous levels of the protein. Therefore it is important to confirm the localization by staining for endogenous protein. For this study rabbit polyclonal anti mIP_6K1 antibodies were made and characterized. It was shown that the antibody did not cross react with IP_6K2 *in vitro* and *in vivo*. Unfortunately, the antibody showed a second protein of larger molecular size than IP_6K1 by immunoblotting. This protein does not relate to IP_6K1, because reverse transcriptase PCR, using amino- and carboxyl-terminal primers of IP_6K1 resulted in a single band in every cell line tested, implicating that this protein of larger molecular size than IP_6K1 is not a splice variant. It is not likely that the band is a posttranslational modified form of IP_6K1, since the protein corresponding to that band could not be depleted in the RNAi experiment. The unknown protein could not be immunoprecipitated using anti IP_6K1 antibody, implicating that this protein is not recognized under native conditions. This control confirmed that the protein stained in cell lines with anti IP_6K1 antibody by immunofluorescence, is IP_6K1.

NIH3T3 cells stained with this IP_6K1 antibody resulted in cells with bright nuclear staining but also in cells with cytoplasmic staining, in which IP_6K1 was excluded from the nucleus. This suggests, that IP_6K1 might be shuttling in and out of the nucleus. There are two possibilities why protein are shuttling between compartments. First, it is possible that a protein has different functions in different compartments of the cells. For example, β-catenin interacts with E-cadherin in the cytosol and is involved in cell adhesion (Ozawa *et al.*, 1989; Ozawa *et al.*, 1990). After activation of the Wnt signaling pathway β-catenin translocates to the nucleus, where it interacts with proteins of the T cell factor and lymphoide enhancer factor family of transcription factors to induce transcription of specific target genes, such as c-myc and cyclin D1 (He *et al.*, 1998; Eastman *et al.*, 1999; Mann *et al.*, 1999). A second possibility why proteins are localized at different compartments in the cells, is that they are only active in one compartment. For example, nuclear protein kinase C δ (PKCδ) is transported into the nucleus during apoptosis, where it is involved in regulating apoptotic signaling events (DeVries *et al.*, 2002). Different transcription factors, for example NFκB are

being activated in the cytoplasm after certain stimuli and then transported into the nucleus (Baldwin, 1996; de Martin *et al.*, 1999; Mercurio *et al.*, 1999; Carlotti *et al.*, 2000). Another group of proteins shuttling in and out of the nucleus are cell cycle protein such as cyclins and cyclin dependent kinases (Cdks), which are transported into the nucleus in specific phases of the cell cycle.

To determine where IP_6K1 has activity and why it is shuttling between the nucleus and the cytosol, the following experiment needs to be done. Nuclear and cytosolic fractions of NIH3T3 cells can be used for immunoprecipitation of IP_6K1, followed by IP_6K1 kinase assays with ^3H-IP_6. This experiment should give information about whether the kinase is regulated dependent on its localization.

4.2 A role for inositol pyrophosphates in cell cycle regulation

4.2.1 Nuclear localization of IP_6K1 is cell cycle dependent

A variety of proteins shuttle between the nucleus and the cytosol in a cell cycle dependent manner. It was shown in chapter 3.4.1 that nuclear localization of IP_6K1 is also cell cycle dependent. Etoposide (VP16) blocked the cells in G2-phase of the cell cycle as confirmed by flow cytometry analysis. IP_6K1 was localized in the nucleus in cells treated with VP16. VP16 is an topoisomerase II inhibitor, which causes DNA double strand breaks. To exclude that DNA damage led to nuclear localization of IP_6K1, other DNA damage inducing agents were tested. Irradiation, which also causes DNA double strand breaks did not have an effect on IP_6K1 localization. Thus, DNA damage is not the cause of IP_6K1's nuclear translocation. Because of its DNA damaging effect cells are also treated with VP16 to induce apoptosis. To induce apoptosis a concentration of 50 μM VP16 is commonly used, whereas in this study to arrest the cells in G2 phase of the cell cycle the cells were treated with only 0.5 μM VP16. Flow cytometry analysis did not show any cells in apoptosis, implicating that the import of IP_6K1 into the nucleus after VP16 treatment might be due to the G2 arrest and not due to

DNA damage and apoptosis. This result has to be confirmed by staining of synchronized cells with anti IP_6K1 pAb. Therefore, NIH3T3 cells can be blocked at the G1/S border by double treatment with thymidin. After release in thymidine free media the cells will be analyzed by flow cytometry and immunofluorescence every hour till the cells went through mitosis.

It would be interesting to determine whether the kinase activity of IP_6K1 is regulated during the cell cycle. Therefore, IP_6K1 can be immunoprecipitated from synchronized cells and its kinase activity can be determined in different phases of the cell cycle in a kinase assay with ^3H-IP_6

4.2.2 IP_6K1 translocates from the kinetochore to the mitotic spindle in mitosis

It was shown that IP_6K1 is able to translocate from the kinetochore in prophase to the mitotic spindle during mitosis, which is characteristic for mitotic checkpoint proteins. The mitotic checkpoint is important to assure that the chromatides are separated correctly, resulting in two identical daughter cells. For example Bub1, Bub3, Mad1, Mad2 and BubR1 are proteins localized at the kinetochore during prophase and monitor the attachment of mitotic spindles to the kinetochore (figure 35) (Chen *et al.*, 1996; Taylor *et al.*, 1997; Chen *et al.*, 1998; Sharp-Baker *et al.*, 2001; Taylor *et al.*, 2001). Different spindle checkpoint proteins, such as Mad2, are also transported from the kinetochore to the spindle pole along the spindle microtubles (Howell *et al.*, 2000). Mad2 is a key protein in the spindle checkpoint. Yeast Mad2 deletion mutants showed an increase in frequency of spontaneous chromosome loss. In mammalian cells, microinjection of anti Mad2 antibodies resulted in an incomplete alignment of the chromosomes in anaphase. Furthermore, Mad2-null mice did not arrest in response to spindle damage and showed chromosome missegregation. Mad2 is localized at unattached kinetochores and binds Cdc20, the APC/C activator. After microtuble attachment at the kinetochore Mad2 is transported to the spindle pole, where it is not bound to Cdc20 anymore. Cdc20 can activate APC/C and the cells can progress into anaphase (figure 13 and 35). IP_6K1 localized to the kinetochore and mitotic spindles similar to Mad2 suggesting that IP_6K1

might be involved in signaling events at the metaphase to anaphase transition. To examine the exact time points of the different localizations of IP_6K1, cells have to be monitored through mitosis.

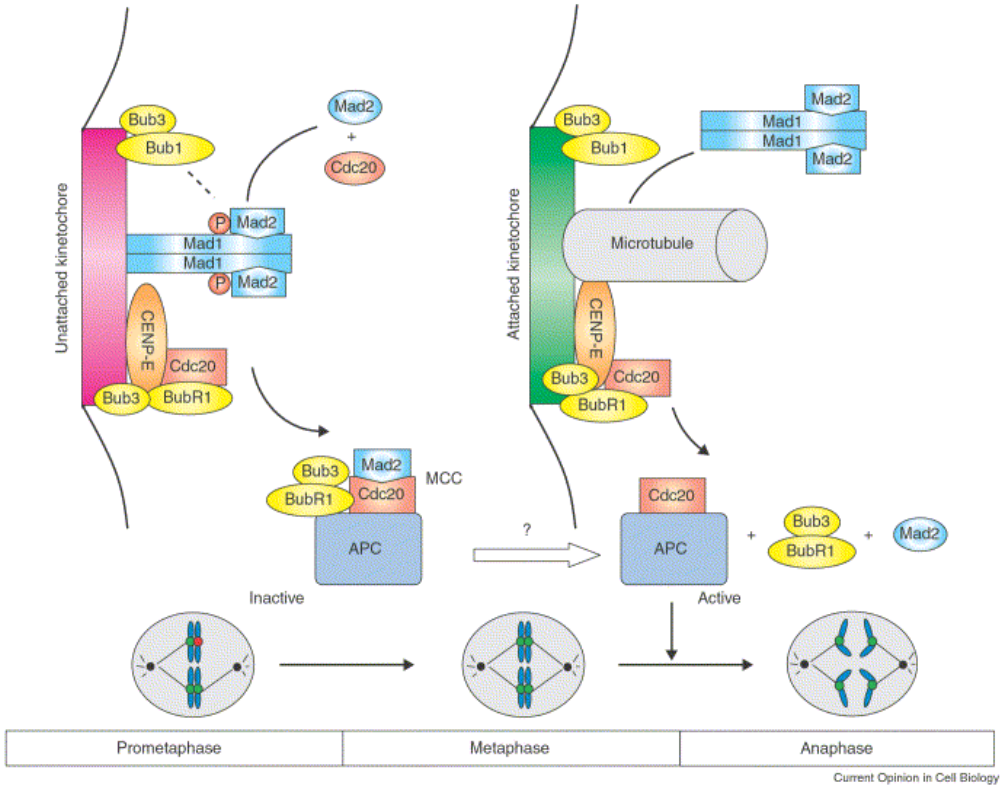

Figure 35: Model for spindle checkpoint (Yu, 2002). Nearly all checkpoint proteins are enriched at unattached kinetochores. In this model, Mad2 is recruited to the kinetochore by Mad1. Mad2 dissociates from Mad1, that makes it more suitable for Cdc20. Mad2 bound to Cdc20 inhibits the APC/C complex. When the kinetochores are attached to the mitotic spindle, Mad1 and Mad2 no longer localize to the kinetochore and Mad2 does not bind Cdc20 anymore, which leads to an activation of the APC/C complex and the transition to anaphase.

4.2.3 IP_6K1 is postranslational modified in mitosis

Treatment of cells with agents that block cells in mitosis such as nocodazol and taxol resulted in a posttranslational modification of IP_6K1 as shown in apparent mobility shift in SDS-PAGE. It was shown, that IP_6K1 was phosphorylated in cells arrested in mitosis. Treatment of mitotic lysates with calf alkaline phosphatase abolished the mobility shift. It was difficult to separate the putative phosphorylated and unphosphorylated form of IP_6K1 in a 10 and 7.5 % SDS-PAGE. To confirm that IP_6K1 is phosphorylated in mitosis, mitotic cell extracts will have to be incubated with or without recombinant IP_6K1 in a kinase assay with ^{32}P-γATP. A variety of proteins are phosphorylated in mitosis by specific kinases to strictly regulate this part of the cell cycle. One example of a kinase with high activity in mitotic cells is protein kinase B (PKB). PKB is a key downstream effector of phosphatidylinositol 3-kinase (PI3K) and is best known for its antiapoptotic effects and its role in initiation of S-phase (Franke *et al.*, 1997; Vanhaesebroeck *et al.*, 2000). Recent studies showed that PKB activity increased in transition from G2 to early mitosis in epithelial cells. Inhibition of PI3K by Ly294002 resulted in a G2/M arrest in Hela and MDCK cells which could be rescued by overexpression of a constitutively active form of PKB, suggesting that PKB plays in important role in G2/M progression . The conserved PKB phosphorylation site is RXRXXS (Obata *et al.*, 2000). Interestingly, IP_6K1 contains a PKB phosphorylation site (figure 36). It might be possible that IP_6K1 is phosphorylated in mitosis by PKB in epithelial cells since fibroblast did not show a mobility shift of IP_6K1 after nocodazol treatment. The direct phosphorylation of IP_6K1 by PKB now has to be examined by *in vitro* kinase assays.

IP_6K1 contains four potential recognition motifs of the monoclonal antibody MPM2 (figure36). MPM2 recognize a pS/pT-P motif which is present in more than forty phosphoproteins involved in regulation of mitosis (Westendorf *et al.*, 1994). It remains to be determined whether MDM2 interacts with one of theses putative phosphorylation sites in IP_6K1 after nocodazol treatment. When probing cells in mitosis phospho specific antibodies recognize their antigen only in kinetochores, which are not attached to the mitotic spindle, but not in kinetochores, which are attached, suggesting that phosphorylation at the kinetochore is required for checkpoint activation (Gorbsky *et al.*, 1993). Since nocodazol

leads to G2/M-phase arrest, one would expect that MDM2 will detect phosphorylated IP_6K1, which would implicate a role for IP_6K1 in the regulation of this checkpoint. Two examples of proteins, specifically phosphorylated in mitosis are the spindle checkpoint proteins Bub1 and BubR1, which are protein kinases that are localized at the kinetochore during mitosis and monitor together with other checkpoint proteins the attachment of the kinetochores to the spindle (Taylor *et al.*, 1997; Chan *et al.*, 1998; Jablonski *et al.*, 1998; Chan *et al.*, 1999; Sharp-Baker *et al.*, 2001). Bub1 and BubR1 are phosphorylated after nocodazol and taxol treatment. Bub1 seems to be phosphorylated in normal mitosis, whereas BubR1 is only phosphorylated in response to spindle damage, for example after nocodazol treatment (Taylor *et al.*, 2001) A similar observation was made for IP_6K1. IP_6K1 migrated slower in a SDS PAGE after nocodazol and taxol treatment, but there was no mobility shift visible in untreated cells. This might be due to the low amount of mitotic cells in cell lysates, so that the slower migrating band was not visible by immunoblotting. But even very long exposure times did not show a second band. To examine the time point when IP_6K1 might be phoshorylated, cells have to be synchronized and analyzed by flow cytometry and immunoblot. If IP_6K1 is phosphorylated independent of spindle damage, a mobility shift should be visible in cells progressing through mitosis.

```
  1 MCVCQTMEVG QYGKNASRAG DRGVLLEPFI HQVGGHSSMM RYDDHTVCKP LISREQRFYE
 61 SLPPEMKEFT PEYKGVVSVC FEGDSDGYIN LVAYPYVESE TVEQDDTTER EQPRRKHSRR
121 SLHRSGSGSD HKEEKASLSL ETSESSQEAK SPKVELHSHS EVPFQMLDGN SGLSSEKISH
                    * *  *
181 NPWSLRCHKQ QLSRMRSESK DRKLYKFLLL ENVVHHFKYP CVLDLKMGTR QHGDDASAEK
241 AARQMRKCEQ STSATLGVRV CGMQVYQLDT GHYLCRNKYY GRGLSIEGFR NALYQYLHNG
301 LDLRRDLFEP ILSKLRGLKA VLERQASYRF YSSSLLVIYD GKECRAESCL DRRSEMRLKH
361 LDMVLPEVAS SCGPSTSPSN TSPEAGPSSQ PKVDVRMIDF AHSTFKGFRD DPTVHDGPDR
421 GYVFGLENLI SIMEQMRDEN Q
```

Figure 36: Putative phosphorylation sites in hIP_6K1. Putative phosphorylation motifs are underlined. There are four putative MDM2 recognition motifs pS/pT-P. The amino acid (S or T), which might be phosphorylated is shown in blue. The protein kinase B phosphorylation consensus sequence is labled with asterisks and the serine, which is phosphorylated is shown in red**.**

4.2.4 Characterization of G2/M arrest induced by depletion of IP_6K1

It was shown that IP_6K1 siRNA depleted IP_6K1 levels in HEK293T cells. A second IP_6K1 siRNA oligo was also used, but though it knocked down IP_6K1 levels it did not result in the G2/M arrest. While it is difficult to quantitate the actual amount of IP_6K1 in a single cell after siRNA transfection. RT-PCR experiments showed a 10 fold decrease of mRNA levels in average for a given sample, but never a complete knock out. It is possible that with the second siRNA oligo the IP_6K1 concentration in the cell was above a certain level and thus, did not result in a phenotype. Both IP_6K1 siRNA oligos knocked out IP_6K1 levels in U2OS cells, resulting in an increase in mitotic and later in apoptotic cells with both oligos. It might be possible that the second siRNA oligo did not work as well as the other in HEK293T cells.
Depletion of IP_6K1 in HEK293T cells resulted in a dramatic increase in cells in G2/M-phase (70 %). Phosphorylation of Histone 3 at serine 10 (ser10) is another marker for cells in mitosis (Hendzel *et al.*, 1997; Van Hooser *et al.*, 1998; Wei *et al.*, 1998). Staining for Histone 3 phosphorylation showed that Histone 3 was not phosphorylated at ser10 in the majority of IP_6K1 knock out cells. Only one third of the cells arrested in G2/M contained phosphorylated Histone 3 and the majority of these cells showed less intense staining for phospho Histone 3 than wildtype cells. Phosphorylation of Histone 3 at ser10 is involved in initiation of chromosome condensation (Van Hooser *et al.*, 1998), which begins in early G2 phase of the cell cycle (Hendzel *et al.*, 1997). There are two mitotic kinases, Aurora A and Aurora B, which have been postulated to phosphorylate Histone 3 at position ser10 (Crosio *et al.*, 2002). In IP_6K1 knock out cells the majority of cells contained non condensed DNA, which is consistent with the observation that Histone 3 is not phosphorylated in these cells. This data suggests that chromosome condensation by Histone 3 is inhibited or at least slowed down in the majority of IP_6K1 knock out cells. It is possible that IP_6K1 acts upstream of Aurora kinases and its necessary for their activation (figure 37). This hypothesis needs to be tested with Aurora specific kinase assays in IP_6K1 knock out cells.

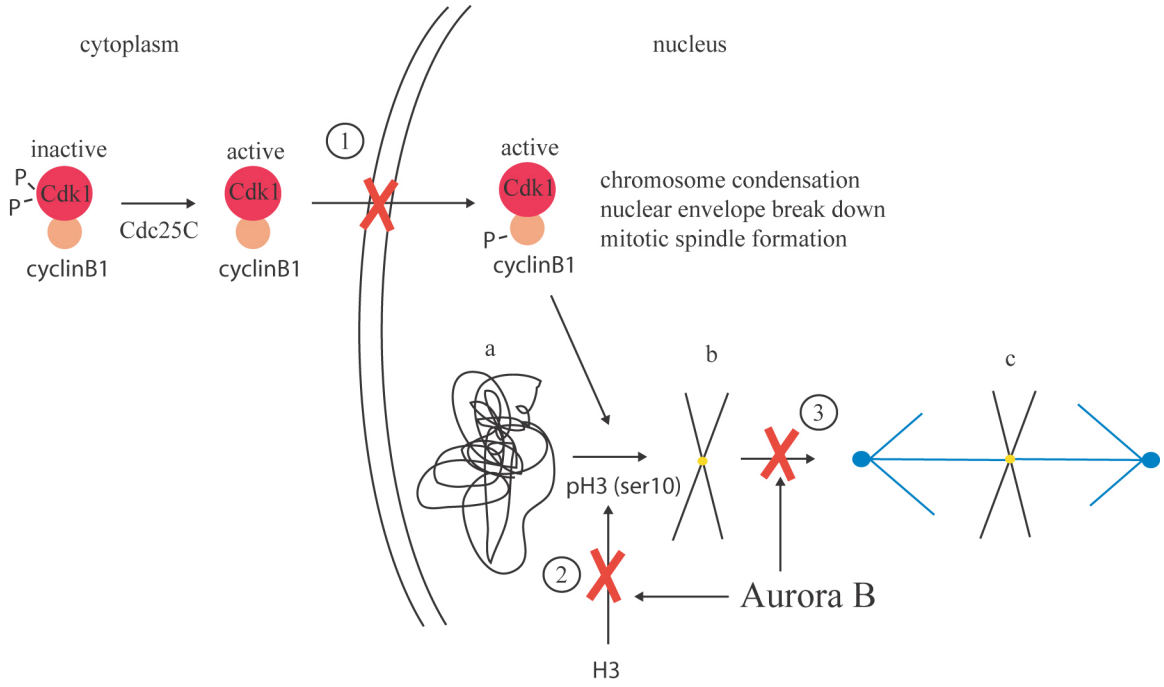

Figure 37: Model of pathways IP_6K1 might be involved in. First, dephosphorylation of Cdk1-cyclinB1 was not effected in IP_6K1 knock out cells, but the nuclear import of the active complex might have been impaired. Second, Histone 3 (H3) phosphorylation at serine 10 (pH3 (ser10)) was inhibited and third, the correct alignment of chromosomes in metaphase was inhibited. Aurora B kinase is involved in the second and third pathway. The red X demonstrates the pathway, that are impaired in IP_6K1 knock out cells. a: interphase chromosomes, b: condensed prophase chromosomes, c: spindle (blue) are attached to the kinetochore (yellow) in metaphase.

It was shown that cyclin dependent kinase 1 (Cdk1) is dephosphorylated in IP_6K1 knock out cells. Cdk1 and its regulatory subunit cyclinB1 are the key factors for entry into mitosis (Lew *et al.*, 1996; Morgan, 1997; Ohi *et al.*, 1999). During interphase Cdk1 is kept inactive through phosphorylation at position Tyr15 and is localized in the cytoplasm (Gould *et al.*, 1989; Pines *et al.*, 1991; Parker *et al.*, 1992; Parker *et al.*, 1992; Atherton-Fessler *et al.*, 1994; Mueller *et al.*, 1995). Dephosphorylation at position Tyr15 by the phosphatase Cdc25C activates the Cdk1-cyclinB1 complex, which then abruptly translocates to the nucleus, where it is involved in processes such as nuclear envelope break down, chromosome condensation

and spindle pole formation (Russell *et al.*, 1986; Gautier *et al.*, 1991; Lee *et al.*, 1992; Borgne *et al.*, 1996). Though Cdk1 was completely dephosphorylated at position Tyr15 in IP_6K1 knock out cells, the majority of the cells did not enter mitosis, as shown by phospho Histone 3 staining. As shown by immunofluorescence staining of IP_6K1 knock out cells, the majority of the cells contained an intact nucleus and the DNA was not condensed, which leads to the hypothesis that the cells are in transition from G2-phase to mitosis, because translocation of the active Cdk1-cyclinB1 complex may have been inhibited. Nuclear translocation of Cdk1-cyclinB1 is triggered and activated by phosphorylation of cyclinB1 at its nuclear export sequence (NES). It has been reported that nuclear translocation occurs after Histone 3 phosphorylation and that the active Cdk1-cyclinB1 complex appears first at the centrosome, before it enters the nucleus (Jackman *et al.*, 2003). Since two pathways, that are thought to be independent, might be effected by a single knock out, perhaps chromosome condensation is coupled to nuclear import of Cdk1-cyclinB1. Thus, by inhibition of Histone 3 phosphorylation in IP_6K1 knock out cells, the active Cdk1-cyclinB1 complex remains at the centrosome. This hypothesis can be tested using cyclinB1 specific antibodies to stain IP_6K1 knock out cells to confirm its localization. This experiment was done with a Cdk1 specific antibody, which did not work for immunofluorescence in HEK293T cells.

Another phenotype observed in IP_6K1 knock out cells, was a mitotic phenotype. These cells showed abnormal spindle morphology and the microtubles were not attached to the kinetochore, resulting in a mitotic catastrophe. In wildtype cells IP_6K1 is localized at the kinetochore in prophase and translocates to the spindle poles during mitosis. A similar localization was observed for proteins involved in the spindle checkpoint, such as Mad2. It is possible that IP_6K1 is involved in attachment of the microtubles to the kinetochore either directly or indirectly by recruiting kinetochore proteins to their localization. The second possibility can be tested by staining the knock out cells with antibodies for specific kinetochore proteins. It is also possible to stain the cells with antibodies against a mitotic specific phosphorylation site, to determine whether the kinetochore is phosphorylated or not. The kinetochore is phosphorylated, when the spindles are not attached to it (Gorbsky *et al.*, 1993). Thus, with this method it can be determined, if the spindles are attached to the kinetochore in IP_6K1 knock out cells or not. Interestingly, AuroraB kinase has also been reported to play a role in chromosome alignment in metaphase (Ditchfield *et al.*, 2003). It

might be possible that in IP_6K1 knock out cells Aurora B activation was inhibited, because this kinase is involved in Histone 3 phosphorylation and chromosome alignment (figure 37).
The different IP_6K1 knock out induced phenotypes were not only rescued by overexpressing the IP_6K1 rescue construct, the putative IP_6K1 kinase dead mutant was also able to rescue the G2/M arrest. Since it could not be shown that the kinase dead mutant is indeed dead it remains unanswered whether the protein or inositol pyrophosphates are responsible for the rescue. The concentration of IP_6Ks is not very high in cells (Menniti *et al.*, 1993). Even 1% remaining kinase activity of the kinase dead mutant could be efficient to produce enough inositol pyrophosphates to reach the intracellular concentration of IP_7 and IP_8. IP_6K2 could only partially rescue the IP_6K1 knock out phenotype suggesting that not only the intracellular concentration of inositol pyrophosphates in general but also the localization is important.
A suprising result was that overexpression of IP_6K1 and the putative IP_6K1 kinase dead construct increased the number of cells in G1, even after nocodazol treatment. This means, that the cells were blocked in G1 phase of the cell cycle or cell cycle progression was slowed down dramatically, so that treatment with nocodazol could not block the cells in mitosis, since the cells never left G1-phase. Unfortunately, this result makes the rescue experiment described above useless, because the cells were transfected at the same time with IP_6K1rescue and siRNA. Since overexpression of IP_6K1 arrests the cells in G1-phase, the siRNA could not have an effect on the cells in G1-phase. To determine, if IP_6K1 is able to rescue the knock out phenotype, IP_6K1rescue stably expressing HEK293T cells will have to be used to transfected with IP_6K1siRNA. These cells will have to be selected for low IP_6K1rescue expressing cells, to avoid phenotypes, resulting from overexpression
Nevertheless, overexpression of IP_6K1 caused the cells to arrest in G1-phase. It might be possible that overproduction of inositol pyrophosphates has an effect on cell cycle progression. Studies showed that IP_6 can act as anti cancer agent (see chapter 1.1.3). It has been reported that adding exogenous IP_6 to different cell lines resulted in a arrest in G1-phase (El-Sherbiny *et al.*, 2001; Singh *et al.*, 2003). The molecular basis of this effect are still unknown. Studies showed that the G1 arrest forced by exogenous IP_6 is caused by inhibiting protein kinase B/NFκB pathway (Ferry *et al.*, 2002) and/or by increasing the expression of cyclin dependent kinase inhibitors (CDKI) (Singh *et al.*, 2003). It has been suggested that lower phosphorylated inositol phosphates are the actual second messengers of the effect of

IP_6. There is no report about a role of inositol pyrophosphates in the IP_6 induced G1 arrest. It is possible that IP_6 is not only dephosphorylated, but also phosphorylated and that the inositol pyrophosphates are the physiological significant molecules in IP_6 induced arrest in G1-phase. To further define a possible role for inositol pyrophosphates cell cycle inhibition, expression levels of different CDKIs in IP_6K1 overexpressing cells can be determined. Additionally, it would be important to determine proteinkinase activities of cyclin dependent kinases, involved in G1, and protein kinase B in cells overexpressing IP_6K1.

4.2.5 Inositol pyrophosphate levels do not change during mitosis

Inositol pyrophosphates are in very low concentration in the cell, that makes it difficult to detect these molecules in cell systems. Metabolic labeling of HEK293T cells with ^{3}H-inositol did not show a significant change in inositol pyrophosphate levels after blocking the cells in G1-phase. This is not suprising, because there are three mammalian inositol hexakisphosphate kinase. The three isoforms may have different function in the cell, so that it is difficult to detect intracellular changes of inositol pyrophosphates. Cells treated with nocodazol showed an increase in IP_7/IP_8 levels, but IP_7/IP_8 levels differed in untreated cells. In a different experiment the IP_7/IP_8 levels were almost as high as in nocodazol treated cells (see Appendix).this experiment needs to be repeated a few times to determine whether this increase is significant. Furthermore, the spatial production of inositol pyrophosphates might be more important than the total cellular concentration. It might be interesting to analyze the inositol pyrophosphate levels in isolated the nuclei after VP16 induced G2 arrest.

It was shown in this study that inositol pyrophosphate exist in HEK293T cells and that their turnover is very high in this cell line. After treatment with 40 mM NaF, the concentration of IP_7 and/or IP_8 increased dramatically. Interestingly, it seemed that $PPIP_4$ was not produced at all in cells arrested at the G1/S border with aphidicolin. $PPIP_4$ is also produced by inositolphosphate multikinase (IPMK, see chapter 1.1.2). The data in this study suggest, that neither IPMK nor one of the IP_6K isoforms produces $PPIP_4$ in aphidicolin treated cells. Since there are no radioactive standard for the inositolpyrophosphates available, it is not certain

that the shown peaks in the HPLC profile are $PPIP_4$, IP_7 and IP_8, but in comparison with the literature it seems most likely to be the case. The $PPIP_4$ and IP_7 peaks will be confirmed with IP_6K kinase assays with ^3H-IP_5 and ^3H-IP_6 as substrates.

5 References

Abel, K., Anderson, R. A. and Shears, S. B. (2001). Phosphatidylinositol and inositol phosphate metabolism. *J Cell Sci* **114**, 2207-8.

Albert, C., Safrany, S. T., Bembenek, M. E., Reddy, K. M., Reddy, K., Falck, J., Brocker, M., Shears, S. B. and Mayr, G. W. (1997). Biological variability in the structures of diphosphoinositol polyphosphates in Dictyostelium discoideum and mammalian cells. *Biochem J* **327 (Pt 2)**, 553-60.

Aoki, M., Sobek, V., Maslyar, D. J., Hecht, A. and Vogt, P. K. (2002). Oncogenic transformation by beta-catenin: deletion analysis and characterization of selected target genes. *Oncogene* **21**, 6983-91.

Arnone, A. and Perutz, M. F. (1974). Structure of inositol hexaphosphate--human deoxyhaemoglobin complex. *Nature* **249**, 34-6.

Ashar, H. R., James, L., Gray, K., Carr, D., Black, S., Armstrong, L., Bishop, W. R. and Kirschmeier, P. (2000). Farnesyl transferase inhibitors block the farnesylation of CENP-E and CENP-F and alter the association of CENP-E with the microtubules. *J Biol Chem* **275**, 30451-7.

Atherton-Fessler, S., Liu, F., Gabrielli, B., Lee, M. S., Peng, C. Y. and Piwnica-Worms, H. (1994). Cell cycle regulation of the p34cdc2 inhibitory kinases. *Mol Biol Cell* **5**, 989-1001.

Baldwin, A. S., Jr. (1996). The NF-kappa B and I kappa B proteins: new discoveries and insights. *Annu Rev Immunol* **14**, 649-83.

Bechet, J., Greenson, M. and Wiame, J. M. (1970). Mutations affecting the repressibility of arginine biosynthetic enzymes in Saccharomyces cerevisiae. *Eur J Biochem* **12**, 31-9.

Beck, K. A. and Keen, J. H. (1991). Self-association of the plasma membrane-associated clathrin assembly protein AP-2. *J Biol Chem* **266**, 4437-41.

Bernstein, E., Caudy, A. A., Hammond, S. M. and Hannon, G. J. (2001). Role for a bidentate ribonuclease in the initiation step of RNA interference. *Nature* **409**, 363-6.

Bessman, M. J., Frick, D. N. and O'Handley, S. F. (1996). The MutT proteins or "Nudix" hydrolases, a family of versatile, widely distributed, "housecleaning" enzymes. *J Biol Chem* **271**, 25059-62.

Borgne, A. and Meijer, L. (1996). Sequential dephosphorylation of p34(cdc2) on Thr-14 and Tyr-15 at the prophase/metaphase transition. *J Biol Chem* **271**, 27847-54.

Caffrey, J. J., Safrany, S. T., Yang, X. and Shears, S. B. (2000). Discovery of molecular and catalytic diversity among human diphosphoinositol-polyphosphate phosphohydrolases. An expanding Nudt family. *J Biol Chem* **275**, 12730-6.

Carlotti, F., Dower, S. K. and Qwarnstrom, E. E. (2000). Dynamic shuttling of nuclear factor kappa B between the nucleus and cytoplasm as a consequence of inhibitor dissociation. *J Biol Chem* **275**, 41028-34.

Chadwick, C. C., Timerman, A. P., Saito, A., Mayrleitner, M., Schindler, H. and Fleischer, S. (1992). Structural and functional characterization of an inositol polyphosphate receptor from cerebellum. *J Biol Chem* **267**, 3473-81.

Chan, G. K., Jablonski, S. A., Sudakin, V., Hittle, J. C. and Yen, T. J. (1999). Human BUBR1 is a mitotic checkpoint kinase that monitors CENP-E functions at kinetochores and binds the cyclosome/APC. *J Cell Biol* **146**, 941-54.

Chan, G. K., Schaar, B. T. and Yen, T. J. (1998). Characterization of the kinetochore binding domain of CENP-E reveals interactions with the kinetochore proteins CENP-F and hBUBR1. *J Cell Biol* **143**, 49-63.

Chang, M. P., Mallet, W. G., Mostov, K. E. and Brodsky, F. M. (1993). Adaptor self-aggregation, adaptor-receptor recognition and binding of alpha-adaptin subunits to the plasma membrane contribute to recruitment of adaptor (AP2) components of clathrin-coated pits. *Embo J* **12**, 2169-80.

Chang, S. C., Miller, A. L., Feng, Y., Wente, S. R. and Majerus, P. W. (2002). The human homolog of the rat inositol phosphate multikinase is an inositol 1,3,4,6-tetrakisphosphate 5-kinase. *J Biol Chem* **277**, 43836-43.

Chen, R. H., Shevchenko, A., Mann, M. and Murray, A. W. (1998). Spindle checkpoint protein Xmad1 recruits Xmad2 to unattached kinetochores. *J Cell Biol* **143**, 283-95.

Chen, R. H., Waters, J. C., Salmon, E. D. and Murray, A. W. (1996). Association of spindle assembly checkpoint component XMAD2 with unattached kinetochores. *Science* **274**, 242-6.

Choi, K. Y., Kim, H. K., Lee, S. Y., Moon, K. H., Sim, S. S., Kim, J. W., Chung, H. K. and Rhee, S. G. (1990). Molecular cloning and expression of a complementary DNA for inositol 1,4,5-trisphosphate 3-kinase. *Science* **248**, 64-6.

Choo, K. H. (2000). Centromerization. *Trends Cell Biol* **10**, 182-8.

Cohen-Fix, O., Peters, J. M., Kirschner, M. W. and Koshland, D. (1996). Anaphase initiation in Saccharomyces cerevisiae is controlled by the APC-dependent degradation of the anaphase inhibitor Pds1p. *Genes Dev* **10**, 3081-93.

Communi, D., Dewaste, V. and Erneux, C. (1999). Calcium-Calmodulin-dependent Protein Kinase II and Protein Kinase C-mediated Phosphorylation and Activation of D-myo-

Inositol 1,4,5-Trisphosphate 3-Kinase B in Astrocytes. *J. Biol. Chem.* **274**, 14734-14742.

Communi, D., Vanweyenberg, V. and Erneux, C. (1997). D-myo-inositol 1,4,5-trisphosphate 3-kinase A is activated by receptor activation through a calcium:calmodulin-dependent protein kinase II phosphorylation mechanism. *Embo J* **16**, 1943-52.

Crosio, C., Fimia, G. M., Loury, R., Kimura, M., Okano, Y., Zhou, H., Sen, S., Allis, C. D. and Sassone-Corsi, P. (2002). Mitotic phosphorylation of histone H3: spatio-temporal regulation by mammalian Aurora kinases. *Mol Cell Biol* **22**, 874-85.

Cullen, P. J., Hsuan, J. J., Truong, O., Letcher, A. J., Jackson, T. R., Dawson, A. P. and Irvine, R. F. (1995). Identification of a specific Ins(1,3,4,5)P4-binding protein as a member of the GAP1 family. *Nature* **376**, 527-30.

Cullen, P. J., Irvine, R. F. and Dawson, A. P. (1990). Synergistic control of Ca2+ mobilization in permeabilized mouse L1210 lymphoma cells by inositol 2,4,5-trisphosphate and inositol 1,3,4,5-tetrakisphosphate. *Biochem J* **271**, 549-53.

de Martin, R., Schmid, J. A. and Hofer-Warbinek, R. (1999). The NF-kappaB/Rel family of transcription factors in oncogenic transformation and apoptosis. *Mutat Res* **437**, 231-43.

DeVries, T. A., Neville, M. C. and Reyland, M. E. (2002). Nuclear import of PKCdelta is required for apoptosis: identification of a novel nuclear import sequence. *Embo J* **21**, 6050-60.

Dewaste, V., Moreau, C., De Smedt, F., Bex, F., De Smedt, H., Wuytack, F., Missiaen, L. and Erneux, C. (2003). The three isoenzymes of human inositol 1,4,5-trisphosphate 3-kinase show specific intracellular localization but comparable Ca 2+ responses upon transfection in COS-7 cells. *Biochem J* **Pt**.

Dewaste, V., Pouillon, V., Moreau, C., Shears, S., Takazawa, K. and Erneux, C. (2000). Cloning and expression of a cDNA encoding human inositol 1,4,5-trisphosphate 3-kinase C. *Biochem J* **352 Pt 2**, 343-51.

Ditchfield, C., Johnson, V. L., Tighe, A., Ellston, R., Haworth, C., Johnson, T., Mortlock, A., Keen, N. and Taylor, S. S. (2003). Aurora B couples chromosome alignment with anaphase by targeting BubR1, Mad2, and Cenp-E to kinetochores. *J Cell Biol* **161**, 267-80.

Dubois, E., Scherens, B., Vierendeels, F., Ho, M. M., Messenguy, F. and Shears, S. B. (2002). In Saccharomyces cerevisiae, the inositol polyphosphate kinase activity of Kcs1p is required for resistance to salt stress, cell wall integrity, and vacuolar morphogenesis. *J Biol Chem* **277**, 23755-63.

Dunckley, T. and Parker, R. (1999). The DCP2 protein is required for mRNA decapping in Saccharomyces cerevisiae and contains a functional MutT motif. *Embo J* **18**, 5411-22.

Eastman, Q. and Grosschedl, R. (1999). Regulation of LEF-1/TCF transcription factors by Wnt and other signals. *Curr Opin Cell Biol* **11**, 233-40.

Elbashir, S. M., Harborth, J., Lendeckel, W., Yalcin, A., Weber, K. and Tuschl, T. (2001). Duplexes of 21-nucleotide RNAs mediate RNA interference in cultured mammalian cells. *Nature* **411**, 494-8.

El-Sherbiny, Y. M., Cox, M. C., Ismail, Z. A., Shamsuddin, A. M. and Vucenik, I. (2001). G0/G1 arrest and S phase inhibition of human cancer cell lines by inositol hexaphosphate (IP6). *Anticancer Res* **21**, 2393-403.

Fang, G., Yu, H. and Kirschner, M. W. (1998). The checkpoint protein MAD2 and the mitotic regulator CDC20 form a ternary complex with the anaphase-promoting complex to control anaphase initiation. *Genes Dev* **12**, 1871-83.

Feng, Y., Wente, S. R. and Majerus, P. W. (2001). Overexpression of the inositol phosphatase SopB in human 293 cells stimulates cellular chloride influx and inhibits nuclear mRNA export. *PNAS* **98**, 875-879.

Ferry, S., Matsuda, M., Yoshida, H. and Hirata, M. (2002). Inositol hexakisphosphate blocks tumor cell growth by activating apoptotic machinery as well as by inhibiting the Akt/NF{kappa}B-mediated cell survival pathway. *Carcinogenesis* **23**, 2031-2041.

Fire, A., Xu, S., Montgomery, M. K., Kostas, S. A., Driver, S. E. and Mello, C. C. (1998). Potent and specific genetic interference by double-stranded RNA in Caenorhabditis elegans. *Nature* **391**, 806-11.

Franke, T. F., Kaplan, D. R. and Cantley, L. C. (1997). PI3K: downstream AKTion blocks apoptosis. *Cell* **88**, 435-7.

Gaudon, C., Chambon, P. and Losson, R. (1999). Role of the essential yeast protein PSU1 in p6anscriptional enhancement by the ligand-dependent activation function AF-2 of nuclear receptors. *Embo J* **18**, 2229-40.

Gautier, J., Solomon, M. J., Booher, R. N., Bazan, J. F. and Kirschner, M. W. (1991). cdc25 is a specific tyrosine phosphatase that directly activates p34cdc2. *Cell* **67**, 197-211.

Glennon, M. C. and Shears, S. B. (1993). Turnover of inositol pentakisphosphates, inositol hexakisphosphate and diphosphoinositol polyphosphates in primary cultured hepatocytes. *Biochem J* **293 (Pt 2)**, 583-90.

Gorbsky, G. J. and Ricketts, W. A. (1993). Differential expression of a phosphoepitope at the kinetochores of moving chromosomes. *J Cell Biol* **122**, 1311-21.

Gould, K. L. and Nurse, P. (1989). Tyrosine phosphorylation of the fission yeast cdc2+ protein kinase regulates entry into mitosis. *Nature* **342**, 39-45.

Grana, X. and Reddy, E. P. (1995). Cell cycle control in mammalian cells: role of cyclins, cyclin dependent kinases (CDKs), growth suppressor genes and cyclin-dependent kinase inhibitors (CKIs). *Oncogene* **11**, 211-9.

Guse, A. H., Greiner, E., Emmrich, F. and Brand, K. (1993). Mass changes of inositol 1,3,4,5,6-pentakisphosphate and inositol hexakisphosphate during cell cycle progression in rat thymocytes. *J Biol Chem* **268**, 7129-33.

Hagting, A., Den Elzen, N., Vodermaier, H. C., Waizenegger, I. C., Peters, J. M. and Pines, J. (2002). Human securin proteolysis is controlled by the spindle checkpoint and reveals when the APC/C switches from activation by Cdc20 to Cdh1. *J Cell Biol* **157**, 1125-37.

Hanakahi, L. A., Bartlet-Jones, M., Chappell, C., Pappin, D. and West, S. C. (2000). Binding of inositol phosphate to DNA-PK and stimulation of double- strand break repair. *Cell* **102**, 721-9.

Hanakahi, L. A. and West, S. C. (2002). Specific interaction of IP6 with human Ku70/80, the DNA-binding subunit of DNA-PK. *Embo J* **21**, 2038-44.

He, T. C., Sparks, A. B., Rago, C., Hermeking, H., Zawel, L., da Costa, L. T., Morin, P. J., Vogelstein, B. and Kinzler, K. W. (1998). Identification of c-MYC as a target of the APC pathway. *Science* **281**, 1509-12.

Hendzel, M. J., Wei, Y., Mancini, M. A., Van Hooser, A., Ranalli, T., Brinkley, B. R., Bazett-Jones, D. P. and Allis, C. D. (1997). Mitosis-specific phosphorylation of histone H3 initiates primarily within pericentromeric heterochromatin during G2 and spreads in an ordered fashion coincident with mitotic chromosome condensation. *Chromosoma* **106**, 348-60.

Hidaka, K., Caffrey, J. J., Hua, L., Zhang, T., Falck, J. R., Nickel, G. C., Carrel, L., Barnes, L. D. and Shears, S. B. (2002). An adjacent pair of human NUDT genes on chromosome X are preferentially expressed in testis and encode two new isoforms of diphosphoinositol polyphosphate phosphohydrolase. *J Biol Chem* **277**, 32730-8.

Hilton, J. M., Plomann, M., Ritter, B., Modregger, J., Freeman, H. N., Falck, J. R., Krishna, U. M. and Tobin, A. B. (2001). Phosphorylation of a Synaptic Vesicle-associated Protein by an Inositol Hexakisphosphate-regulated Protein Kinase. *J. Biol. Chem.* **276**, 16341-16347.

Holloway, S. L., Glotzer, M., King, R. W. and Murray, A. W. (1993). Anaphase is initiated by proteolysis rather than by the inactivation of maturation-promoting factor. *Cell* **73**, 1393-402.

Howell, B. J., Hoffman, D. B., Fang, G., Murray, A. W. and Salmon, E. D. (2000). Visualization of Mad2 dynamics at kinetochores, along spindle fibers, and at spindle poles in living cells. *J Cell Biol* **150**, 1233-50.

Huang, C. F., Voglmaier, S. M., Bembenek, M. E., Saiardi, A. and Snyder, S. H. (1998). Identification and purification of diphosphoinositol pentakisphosphate kinase, which synthesizes the inositol pyrophosphate bis(diphospho)inositol tetrakisphosphate. *Biochemistry* **37**, 14998-5004.

Huang, K. N. and Symington, L. S. (1995). Suppressors of a Saccharomyces cerevisiae pkc1 mutation identify alleles of the phosphatase gene PTC1 and of a novel gene encoding a putative basic leucine zipper protein. *Genetics* **141**, 1275-85.

Irniger, S., Piatti, S., Michaelis, C. and Nasmyth, K. (1995). Genes involved in sister chromatid separation are needed for B-type cyclin proteolysis in budding yeast. *Cell* **81**, 269-78.

Irvine, R. F. (1991). Inositol tetrakisphosphate as a second messenger: confusions, contradictions, and a potential resolution. *Bioessays* **13**, 419-27.

Irvine, R. F., Moor, R. M., Pollock, W. K., Smith, P. M. and Wreggett, K. A. (1988). Inositol phosphates: proliferation, metabolism and function. *Philos Trans R Soc Lond B Biol Sci* **320**, 281-98.

Ives, E. B., Nichols, J., Wente, S. R. and York, J. D. (2000). Biochemical and Functional Characterization of Inositol 1,3,4,5,6-Pentakisphosphate 2-Kinases. *J. Biol. Chem.* **275**, 36575-36583.

Jablonski, S. A., Chan, G. K., Cooke, C. A., Earnshaw, W. C. and Yen, T. J. (1998). The hBUB1 and hBUBR1 kinases sequentially assemble onto kinetochores during prophase with hBUBR1 concentrating at the kinetochore plates in mitosis. *Chromosoma* **107**, 386-96.

Jackman, M., Lindon, C., Nigg, E. A. and Pines, J. (2003). Active cyclin B1-Cdk1 first appears on centrosomes in prophase. *Nat Cell Biol* **5**, 143-8.

Kennerdell, J. R. and Carthew, R. W. (1998). Use of dsRNA-mediated genetic interference to demonstrate that frizzled and frizzled 2 act in the wingless pathway. *Cell* **95**, 1017-26.

King, R. W., Peters, J. M., Tugendreich, S., Rolfe, M., Hieter, P. and Kirschner, M. W. (1995). A 20S complex containing CDC27 and CDC16 catalyzes the mitosis-specific conjugation of ubiquitin to cyclin B. *Cell* **81**, 279-88.

Kohtz, D. S. and Puszkin, S. (1988). A neuronal protein (NP185) associated with clathrin-coated vesicles. Characterization of NP185 with monoclonal antibodies. *J Biol Chem* **263**, 7418-25.

Laussmann, T., Pikzack, C., Thiel, U., Mayr, G. W. and Vogel, G. u. n. (2000). Diphospho-myo-inositol phosphates during the life cycle of Dictyostelium and Polysphondylium. *Eur J Biochem* **267**, 2447-2451.

Lee, M. S., Ogg, S., Xu, M., Parker, L. L., Donoghue, D. J., Maller, J. L. and Piwnica-Worms, H. (1992). cdc25+ encodes a protein phosphatase that dephosphorylates p34cdc2. *Mol Biol Cell* **3**, 73-84.

Lee, S. Y., Sim, S. S., Kim, J. W., Moon, K. H., Kim, J. H. and Rhee, S. G. (1990). Purification and properties of D-myo-inositol 1,4,5-trisphosphate 3-kinase from rat brain. Susceptibility to calpain. *J Biol Chem* **265**, 9434-40.

Lew, D. J. and Kornbluth, S. (1996). Regulatory roles of cyclin dependent kinase phosphorylation in cell cycle control. *Curr Opin Cell Biol* **8**, 795-804.

Liao, H., Winkfein, R. J., Mack, G., Rattner, J. B. and Yen, T. J. (1995). CENP-F is a protein of the nuclear matrix that assembles onto kinetochores at late G2 and is rapidly degraded after mitosis. *J Cell Biol* **130**, 507-18.

Loomis-Husselbee, J. W., Cullen, P. J., Dreikausen, U. E., Irvine, R. F. and Dawson, A. P. (1996). Synergistic effects of inositol 1,3,4,5-tetrakisphosphate on inositol 2,4,5-triphosphate-stimulated Ca2+ release do not involve direct interaction of inositol 1,3,4,5-tetrakisphosphate with inositol triphosphate-binding sites. *Biochem J* **314 (Pt 3)**, 811-6.

Luo, H. R., Saiardi, A., Nagata, E., Ye, K., Yu, H., Jung, T. S., Luo, X., Jain, S., Sawa, A. and Snyder, S. H. (2001). GRAB: a physiologic guanine nucleotide exchange factor for Rab3A, which interacts with inositol hexakisphosphate kinase. *Neuron* **31**, 439-51.

Luo, H. R., Saiardi, A., Yu, H., Nagata, E., Ye, K. and Snyder, S. H. (2002). Inositol pyrophosphates are required for DNA hyperrecombination in protein kinase c1 mutant yeast. *Biochemistry* **41**, 2509-15.

Ma, Y. and Lieber, M. R. (2002). Binding of inositol hexakisphosphate (IP6) to Ku but not to DNA-PKcs. *J Biol Chem* **277**, 10756-9.

Mann, B., Gelos, M., Siedow, A., Hanski, M. L., Gratchev, A., Ilyas, M., Bodmer, W. F., Moyer, M. P., Riecken, E. O., Buhr, H. J. and Hanski, C. (1999). Target genes of beta-catenin-T cell-factor/lymphoid-enhancer-factor signaling in human colorectal carcinomas. *Proc Natl Acad Sci U S A* **96**, 1603-8.

Martin, J. B., Foray, M. F., Klein, G. and Satre, M. (1987). Identification of inositol hexaphosphate in 31P-NMR spectra of Dictyostelium discoideum amoebae. Relevance to intracellular pH determination. *Biochim Biophys Acta* **931**, 16-25.

Menniti, F. S., Miller, R. N., Putney, J. W., Jr. and Shears, S. B. (1993). Turnover of inositol polyphosphate pyrophosphates in pancreatoma cells. *J Biol Chem* **268**, 3850-6.

Mercurio, F. and Manning, A. M. (1999). Multiple signals converging on NF-kappaB. *Curr Opin Cell Biol* **11**, 226-32.

Messenguy, F. and Dubois, E. (1993). Genetic evidence for a role for MCM1 in the regulation of arginine metabolism in Saccharomyces cerevisiae. *Mol Cell Biol* **13**, 2586-92.

Morgan, D. O. (1997). Cyclin-dependent kinases: engines, clocks, and microprocessors. *Annu Rev Cell Dev Biol* **13**, 261-91.

Morgan, D. O. (1999). Regulation of the APC and the exit from mitosis. *Nat Cell Biol* **1**, E47-53.

Morris, S. A., Schroder, S., Plessmann, U., Weber, K. and Ungewickell, E. (1993). Clathrin assembly protein AP180: primary structure, domain organization and identification of a clathrin binding site. *Embo J* **12**, 667-75.

Morrison, B. H., Bauer, J. A., Kalvakolanu, D. V. and Lindner, D. J. (2001). Inositol Hexakisphosphate Kinase 2 Mediates Growth Suppressive and Apoptotic Effects of Interferon-beta in Ovarian Carcinoma Cells. *J. Biol. Chem.* **276**, 24965-24970.

Mueller, P. R., Coleman, T. R., Kumagai, A. and Dunphy, W. G. (1995). Myt1: a membrane-associated inhibitory kinase that phosphorylates Cdc2 on both threonine-14 and tyrosine-15. *Science* **270**, 86-90.

Nalaskowski, M. M., Bertsch, U., Fanick, W., Stockebrand, M. C., Schmale, H. and Mayr, G. W. (2003). Rat inositol 1,4,5-trisphosphate 3-kinase C is enzymatically specialised for basal cellular inositol trisphosphate phosphorylation and shuttles actively between nucleus and cytoplasm. *J. Biol. Chem.*, M211059200.

Nasmyth, K. (2002). Segregating sister genomes: the molecular biology of chromosome separation. *Science* **297**, 559-65.

Norbis, F., Boll M., Stange G., Markovich, D., Verry,F., Biber, J., and Murer, H. (1997). Identification of a cDNA/Protein Leading to an Increase Pi-uptake in *Xenopus laevis* Oocytes. *J. Membrane Biol.* **156**, 19-24.

Norris, F. A., Ungewickell, E. and Majerus, P. W. (1995). Inositol hexakisphosphate binds to clathrin assembly protein 3 (AP-3/AP180) and inhibits clathrin cage assembly in vitro. *J Biol Chem* **270**, 214-7.

Obata, T., Yaffe, M. B., Leparc, G. G., Piro, E. T., Maegawa, H., Kashiwagi, A., Kikkawa, R. and Cantley, L. C. (2000). Peptide and protein library screening defines optimal substrate motifs for AKT/PKB. *J Biol Chem* **275**, 36108-15.

Odom, A. R., Stahlberg, A., Wente, S. R. and York, J. D. (2000). A role for nuclear inositol 1,4,5-trisphosphate kinase in transcriptional control. *Science* **287**, 2026-9.

Ohi, R. and Gould, K. L. (1999). Regulating the onset of mitosis. *Current Opinion in Cell Biology* **11**, 267-273.

Ozawa, M., Baribault, H. and Kemler, R. (1989). The cytoplasmic domain of the cell adhesion molecule uvomorulin associates with three independent proteins structurally related in different species. *Embo J* **8**, 1711-7.

Ozawa, M., Ringwald, M. and Kemler, R. (1990). Uvomorulin-catenin complex formation is regulated by a specific domain in the cytoplasmic region of the cell adhesion molecule. *Proc Natl Acad Sci U S A* **87**, 4246-50.

Ozes, O. N., Mayo, L. D., Gustin, J. A., Pfeffer, S. R., Pfeffer, L. M. and Donner, D. B. (1999). NF-kappaB activation by tumour necrosis factor requires the Akt serine-threonine kinase. *Nature* **401**, 82-5.

Parker, L. L., Atherton-Fessler, S. and Piwnica-Worms, H. (1992). p107wee1 is a dual-specificity kinase that phosphorylates p34cdc2 on tyrosine 15. *Proc Natl Acad Sci U S A* **89**, 2917-21.

Parker, L. L. and Piwnica-Worms, H. (1992). Inactivation of the p34cdc2-cyclin B complex by the human WEE1 tyrosine kinase. *Science* **257**, 1955-7.

Pines, J. and Hunter, T. (1991). Human cyclins A and B1 are differentially located in the cell and undergo cell cycle-dependent nuclear transport. *J Cell Biol* **115**, 1-17.

Pittet, D., Schlegel, W., Lew, D. P., Monod, A. and Mayr, G. W. (1989). Mass changes in inositol tetrakis- and pentakisphosphate isomers induced by chemotactic peptide stimulation in HL-60 cells. *J Biol Chem* **264**, 18489-93.

Posternak, S. (1919). Sur la synthese de l'ether hexaphosphorique de l'inosite avec le principe phosphoorganique de reserve des plantes vertes. *Compt. Rend. Acad. Sci.* **169**, 138-140.

Poyner, D. R., Cooke, F., Hanley, M. R., Reynolds, D. J. and Hawkins, P. T. (1993). Characterization of metal ion-induced [3H]inositol hexakisphosphate binding to rat cerebellar membranes. *J Biol Chem* **268**, 1032-8.

Qian, Y. W., Erikson, E., Li, C. and Maller, J. L. (1998). Activated polo-like kinase Plx1 is required at multiple points during mitosis in Xenopus laevis. *Mol Cell Biol* **18**, 4262-71.

Rieder, C. L., Cole, R. W., Khodjakov, A. and Sluder, G. (1995). The checkpoint delaying anaphase in response to chromosome monoorientation is mediated by an inhibitory signal produced by unattached kinetochores. *J Cell Biol* **130**, 941-8.

Rieder, C. L. and Salmon, E. D. (1998). The vertebrate cell kinetochore and its roles during mitosis. *Trends Cell Biol* **8**, 310-8.

Russell, P. and Nurse, P. (1986). cdc25+ functions as an inducer in the mitotic control of fission yeast. *Cell* **45**, 145-53.

Safrany, S. T., Caffrey, J. J., Yang, X., Bembenek, M. E., Moyer, M. B., Burkhart, W. A. and Shears, S. B. (1998). A novel context for the 'MutT' module, a guardian of cell integrity, in a diphosphoinositol polyphosphate phosphohydrolase. *Embo J* **17**, 6599-607.

Saiardi, A., Caffrey, J. J., Snyder, S. H. and Shears, S. B. (2000). The Inositol Hexakisphosphate Kinase Family. CATALYTIC FLEXIBILITY AND FUNCTION IN YEAST VACUOLE BIOGENESIS. *J. Biol. Chem.* **275**, 24686-24692.

Saiardi, A., Caffrey, J. J., Snyder, S. H. and Shears, S. B. (2000). Inositol polyphosphate multikinase (ArgRIII) determines nuclear mRNA export in Saccharomyces cerevisiae. *FEBS Lett* **468**, 28-32.

Saiardi, A., Erdjument-Bromage, H., Snowman, A. M., Tempst, P. and Snyder, S. H. (1999). Synthesis of diphosphoinositol pentakisphosphate by a newly identified family of higher inositol polyphosphate kinases. *Curr Biol* **9**, 1323-6.

Saiardi, A., Nagata, E., Luo, H. R., Sawa, A., Luo, X., Snowman, A. M. and Snyder, S. H. (2001). Mammalian inositol polyphosphate multikinase synthesizes inositol 1,4,5-trisphosphate and an inositol pyrophosphate. *PNAS* **98**, 2306-2311.

Saiardi, A., Nagata, E., Luo, H. R., Snowman, A. M. and Snyder, S. H. (2001). Identification and Characterization of a Novel Inositol Hexakisphosphate Kinase. *J. Biol. Chem.* **276**, 39179-39185.

Saiardi, A., Sciambi, C., McCaffery, J. M., Wendland, B. and Snyder, S. H. (2002). Inositol pyrophosphates regulate endocytic trafficking. *Proc Natl Acad Sci U S A* **99**, 14206-11.

Saiki, R. K., Gelfand, D. H., Stoffel, S., Scharf, S. J., Higuchi, R., Horn, G. T., Mullis, K. B. and Erlich, H. A. (1988). Primer-directed enzymatic amplification of DNA with a thermostable DNA polymerase. *Science* **239**, 487-91.

Sambrook, J., Fritsch, E. F. and Maniatis, T. (1989). Molecular cloning: a laboratory manual (1-3). *Cold Spring Harbor Laboratory Press, Cold Spring Harbor, New York*.

Schell, M. J., Erneux, C. and Irvine, R. F. (2001). Inositol 1,4,5-trisphosphate 3-kinase A associates with F-actin and dendritic spines via its N terminus. *J Biol Chem* **276**, 37537-46.

Schell, M. J., Letcher, A. J., Brearley, C. A., Biber, J., Murer, H. and Irvine, R. F. (1999). PiUS (Pi uptake stimulator) is an inositol hexakisphosphate kinase. *FEBS Letters* **461**, 169-172.

Sharp-Baker, H. and Chen, R. H. (2001). Spindle checkpoint protein Bub1 is required for kinetochore localization of Mad1, Mad2, Bub3, and CENP-E, independently of its kinase activity. *J Cell Biol* **153**, 1239-50.

Shears, S. B. (1997). Signalling by Inositides: A Practical Approach. *Oxford University Press, Oxford, UK*, 33-52.

Shen, X., Xiao, H., Ranallo, R., Wu, W.-H. and Wu, C. (2003). Modulation of ATP-Dependent Chromatin-Remodeling Complexes by Inositol Polyphosphates. *Science* **299**, 112-114.

Singh, R. P., Agarwal, C. and Agarwal, R. (2003). Inositol hexaphosphate inhibits growth, and induces G1 arrest and apoptotic death of prostate carcinoma DU145 cells: modulation of CDKI-CDK-cyclin and pRb-related protein-E2F complexes. *Carcinogenesis* **24**, 555-563.

Soriano, S., Thomas, S., High, S., Griffiths, G., D'Santos, C., Cullen, P. and Banting, G. (1997). Membrane association, localization and topology of rat inositol 1,4,5-trisphosphate 3-kinase B: implications for membrane traffic and Ca2+ homoeostasis. *Biochem J* **324 (Pt 2)**, 579-89.

Sousa, R., Tannery, N. H., Zhou, S. and Lafer, E. M. (1992). Characterization of a novel synapse-specific protein. I. Developmental expression and cellular localization of the F1-20 protein and mRNA. *J Neurosci* **12**, 2130-43.

Steger, D. J., Haswell, E. S., Miller, A. L., Wente, S. R. and O'Shea, E. K. (2003). Regulation of Chromatin Remodeling by Inositol Polyphosphates. *Science* **299**, 114-116.

Stephens, L., Radenberg, T., Thiel, U., Vogel, G., Khoo, K., Dell, A., Jackson, T., Hawkins, P. and Mayr, G. (1993). The detection, purification, structural characterization, and metabolism of diphosphoinositol pentakisphosphate(s) and bisdiphosphoinositol tetrakisphosphate(s). *J. Biol. Chem.* **268**, 4009-4015.

Streb, H., Irvine, R. F., Berridge, M. J. and Schulz, I. (1983). Release of Ca2+ from a nonmitochondrial intracellular store in pancreatic acinar cells by inositol-1,4,5-trisphosphate. *Nature* **306**, 67-9.

Sudakin, V., Chan, G. K. and Yen, T. J. (2001). Checkpoint inhibition of the APC/C in HeLa cells is mediated by a complex of BUBR1, BUB3, CDC20, and MAD2. *J Cell Biol* **154**, 925-36.

Sudakin, V., Ganoth, D., Dahan, A., Heller, H., Hershko, J., Luca, F. C., Ruderman, J. V. and Hershko, A. (1995). The cyclosome, a large complex containing cyclin-selective ubiquitin ligase activity, targets cyclins for destruction at the end of mitosis. *Mol Biol Cell* **6**, 185-97.

Szwergold, B. S., Graham, R. A. and Brown, T. R. (1987). Observation of inositol pentakis- and hexakis-phosphates in mammalian tissues by 31P NMR. *Biochem Biophys Res Commun* **149**, 874-81.

Takazawa, K., Lemos, M., Delvaux, A., Lejeune, C., Dumont, J. E. and Erneux, C. (1990). Rat brain inositol 1,4,5-trisphosphate 3-kinase. Ca2(+)-sensitivity, purification and antibody production. *Biochem J* **268**, 213-7.

Takazawa, K., Passareiro, H., Dumont, J. E. and Erneux, C. (1988). Ca2+/calmodulin-sensitive inositol 1,4,5-trisphosphate 3-kinase in rat and bovine brain tissues. *Biochem Biophys Res Commun* **153**, 632-41.

Takazawa, K., Vandekerckhove, J., Dumont, J. E. and Erneux, C. (1990). Cloning and expression in Escherichia coli of a rat brain cDNA encoding a Ca2+/calmodulin-sensitive inositol 1,4,5-trisphosphate 3-kinase. *Biochem J* **272**, 107-12.

Taylor, S. S., Hussein, D., Wang, Y., Elderkin, S. and Morrow, C. J. (2001). Kinetochore localisation and phosphorylation of the mitotic checkpoint components Bub1 and BubR1 are differentially regulated by spindle events in human cells. *J Cell Sci* **114**, 4385-95.

Taylor, S. S. and McKeon, F. (1997). Kinetochore localization of murine Bub1 is required for normal mitotic timing and checkpoint response to spindle damage. *Cell* **89**, 727-35.

Theibert, A. B., Estevez, V. A., Ferris, C. D., Danoff, S. K., Barrow, R. K., Prestwich, G. D. and Snyder, S. H. (1991). Inositol 1,3,4,5-tetrakisphosphate and inositol hexakisphosphate receptor proteins: isolation and characterization from rat brain. *Proc Natl Acad Sci U S A* **88**, 3165-9.

Thomas, S., Brake, B., Luzio, J. P., Stanley, K. and Banting, G. (1994). Isolation and sequence of a full length cDNA encoding a novel rat inositol 1,4,5-trisphosphate 3-kinase. *Biochim Biophys Acta* **1220**, 219-22.

Tijsterman, M., Ketting, R. F., Okihara, K. L., Sijen, T. and Plasterk, R. H. (2002). RNA helicase MUT-14-dependent gene silencing triggered in C. elegans by short antisense RNAs. *Science* **295**, 694-7.

Timerman, A. P., Mayrleitner, M. M., Lukas, T. J., Chadwick, C. C., Saito, A., Watterson, D. M., Schindler, H. and Fleischer, S. (1992). Inositol polyphosphate receptor and clathrin assembly protein AP-2 are related proteins that form potassium-selective ion channels in planar lipid bilayers. *Proc Natl Acad Sci U S A* **89**, 8976-80.

Togashi, S., Takazawa, K., Endo, T., Erneux, C. and Onaya, T. (1997). Structural identification of the myo-inositol 1,4,5-trisphosphate-binding domain in rat brain inositol 1,4,5-trisphosphate 3-kinase. *Biochem J* **326 (Pt 1)**, 221-5.

Uhlmann, F., Lottspeich, F. and Nasmyth, K. (1999). Sister-chromatid separation at anaphase onset is promoted by cleavage of the cohesin subunit Scc1. *Nature* **400**, 37-42.

Uhlmann, F., Wernic, D., Poupart, M. A., Koonin, E. V. and Nasmyth, K. (2000). Cleavage of cohesin by the CD clan protease separin triggers anaphase in yeast. *Cell* **103**, 375-86.

Van Hooser, A., Goodrich, D. W., Allis, C. D., Brinkley, B. R. and Mancini, M. A. (1998). Histone H3 phosphorylation is required for the initiation, but not maintenance, of mammalian chromosome condensation. *J Cell Sci* **111 (Pt 23)**, 3497-506.

Vanhaesebroeck, B. and Alessi, D. R. (2000). The PI3K-PDK1 connection: more than just a road to PKB. *Biochem J* **346 Pt 3**, 561-76.

Verbsky, J. W., Wilson, M. P., Kisseleva, M. V., Majerus, P. W. and Wente, S. R. (2002). The Synthesis of Inositol Hexakisphosphate. CHARACTERIZATION OF HUMAN INOSITOL 1,3,4,5,6-PENTAKISPHOSPHATE 2-KINASE. *J. Biol. Chem.* **277**, 31857-31862.

Voglmaier, S. M., Bembenek, M. E., Kaplin, A. I., Dorman, G., Olszewski, J. D., Prestwich, G. D. and Snyder, S. H. (1996). Purified inositol hexakisphosphate kinase is an ATP synthase: Diphosphoinositol pentakisphosphate as a high-energy phosphate donor. *PNAS* **93**, 4305-4310.

Voglmaier, S. M., Keen, J. H., Murphy, J. E., Ferris, C. D., Prestwich, G. D., Snyder, S. H. and Theibert, A. B. (1992). Inositol hexakisphosphate receptor identified as the clathrin assembly protein AP-2. *Biochem Biophys Res Commun* **187**, 158-63.

Waizenegger, I. C., Hauf, S., Meinke, A. and Peters, J. M. (2000). Two distinct pathways remove mammalian cohesin from chromosome arms in prophase and from centromeres in anaphase. *Cell* **103**, 399-410.

Walker, S. A., Kupzig, S., Lockyer, P. J., Bilu, S., Zharhary, D. and Cullen, P. J. (2002). Analyzing the Role of the Putative Inositol 1,3,4,5-Tetrakisphosphate Receptor GAP1IP4BP in Intracellular Ca2+ Homeostasis. *J. Biol. Chem.* **277**, 48779-48785.

Wei, Y., Mizzen, C. A., Cook, R. G., Gorovsky, M. A. and Allis, C. D. (1998). Phosphorylation of histone H3 at serine 10 is correlated with chromosome condensation during mitosis and meiosis in Tetrahymena. *Proc Natl Acad Sci U S A* **95**, 7480-4.

Wei, Y., Yu, L., Bowen, J., Gorovsky, M. A. and Allis, C. D. (1999). Phosphorylation of histone H3 is required for proper chromosome condensation and segregation. *Cell* **97**, 99-109.

Westendorf, J. M., Rao, P. N. and Gerace, L. (1994). Cloning of cDNAs for M-phase phosphoproteins recognized by the MPM2 monoclonal antibody and determination of the phosphorylated epitope. *Proc Natl Acad Sci U S A* **91**, 714-8.

Woodring, P. J. and Garrison, J. C. (1997). Expression, Purification, and Regulation of Two Isoforms of the Inositol 1,4,5-Trisphosphate 3-Kinase. *J. Biol. Chem.* **272**, 30447-30454.

Wu-Scharf, D., Jeong, B., Zhang, C. and Cerutti, H. (2000). Transgene and transposon silencing in Chlamydomonas reinhardtii by a DEAH-box RNA helicase. *Science* **290**, 1159-62.

Xu, W., Shen, J., Dunn, C. A., Desai, S. and Bessman, M. J. (2001). The Nudix hydrolases of Deinococcus radiodurans. *Mol Microbiol* **39**, 286-90.

Ye, W., Ali, N., Bembenek, M. E., Shears, S. B. and Lafer, E. M. (1995). Inhibition of clathrin assembly by high affinity binding of specific inositol polyphosphates to the synapse-specific clathrin assembly protein AP-3. *J Biol Chem* **270**, 1564-8.

York, J. D., Odom, A. R., Murphy, R., Ives, E. B. and Wente, S. R. (1999). A phospholipase C-dependent inositol polyphosphate kinase pathway required for efficient messenger RNA export. *Science* **285**, 96-100.

Yu, H. (2002). Regulation of APC-Cdc20 by the spindle checkpoint. *Current Opinion in Cell Biology* **14**, 706-714.

Zamore, P. D., Tuschl, T., Sharp, P. A. and Bartel, D. P. (2000). RNAi: double-stranded RNA directs the ATP-dependent cleavage of mRNA at 21 to 23 nucleotide intervals. *Cell* **101**, 25-33.

Zhang, T., Caffrey, J. J. and Shears, S. B. (2001). The transcriptional regulator, Arg82, is a hybrid kinase with both monophosphoinositol and diphosphoinositol polyphosphate synthase activity. *FEBS Lett* **494**, 208-12.

Zhou, S., Tannery, N. H., Yang, J., Puszkin, S. and Lafer, E. M. (1993). The synapse-specific phosphoprotein F1-20 is identical to the clathrin assembly protein AP-3. *J Biol Chem* **268**, 12655-62.

Zhu, X., Mancini, M. A., Chang, K. H., Liu, C. Y., Chen, C. F., Shan, B., Jones, D., Yang-Feng, T. L. and Lee, W. H. (1995). Characterization of a novel 350-kilodalton nuclear phosphoprotein that is specifically involved in mitotic-phase progression. *Mol Cell Biol* **15**, 5017-29.

Zou, H., McGarry, T. J., Bernal, T. and Kirschner, M. W. (1999). Identification of a vertebrate sister-chromatid separation inhibitor involved in transformation and tumorigenesis. *Science* **285**, 418-22.

Abbreviation

APH	aphidicolin
APS	ammonium persulfate
A. thaliana	*Arabidopsis thaliana*
ATP	adenosine trisphosphates
BSA	bovine serum albumin
bp	base pair
C. elegans	*Caenorhabditis elegans*
Cdk1	cyclin dependent kinase 1
CENP-F	centrosome protein F
CIP	calf alkalin phosphatase
Cpm	counts per minute
DAPI	4', 6'-diamidino-2-phenylindole
D. discoideum	*Dictyostelium discoideum*
DIPP	diphosphoinositolphosphate phosphatase
DNA	desoxyribonucleic acid
DMSO	dimethylsulfoxide
DTT	dithiothreitol
E. coli	*Escherichia coli*
EDTA	ethylenediamine tertaacidic acid
FITC	flourescein isothiocyanate
GAP	GTPase activating protein
GEF	guanine nucleotide exchange factor
GFP	green fluorescence protein
GTP	guanosine triphosphate
IP_3	inositol 1,4,5-trisphosphate
IP_4	inositol 1,3,4,5-tetrakisphosphate
IP_5	inositol 1,3,4,5,6-pentakisphoshate
IP_6	inositol hexakisphosphate

IP_7	diphosphoinositol pentakisphosphate
IP_8	bis-diphosphoinositol tetrakisphosphate
IPTG	isopropyl-β-D-thiogalactoside
IP3K	inositol 1,4,5-tetrakisphoshate 3-kinase
IP_6K	inositol hexakisphosphate kinase
IPMK	inositol phosphate multikinase
kD	kilo dalton
ko	knock out
mAb	monoclonal antibody
min	minutes
nd	not detectable
noc	nocodazol
pAb	polyclonal antibody
PCR	polymerase chain reaction
$PPIP_4$	diphosphoinositol tetrakisphosphate
RNA	ribonucleic acid
RNAi	RNA interference
RNase	ribonuclease
RT-PCR	reverse transcriptase PCR
rpm	rounds per minute
S. cerivisiae	*Saccharomyces cerivisiae*
Sec	seconds
SDS	sodium dodecylsulfate
SiRNA	small interfering RNA
S. pombe	*Schizosaccharomyces pombe*
TEMED	N,N,N',N'-teramethylaminomethane
Tris	Trishydroxymethylaminomethane
V	Volt
Wt	wildtype
W/o	without

Appendix

A1 Inositol hexakisphosphate kinase assays

Inositol hexakisphosphate kinase assays were carried out as described in Material and Methods, chapter 2.3.6. A ^{3}H-IP_6 standard was used to determine the retentiontime of IP_6. As shown in figure 38A no higher phosphorylated inositol phosphate than IP_6 was produced after 30, 60 and 120 min. In this assay 10 mM ATP was used. To test if this amount of ATP is too high, different ATP concentrations were used in a second assay. But no IP_6 kinase activity was detectable with 10 mM. 5 mM and 1 mM ATP (figure 38B). The amount of ^{3}H-IP_6 decreased with decreasing ATP concentration, but there was no inositol pyrophosphate detectable. There is no report about how stable inositol pyrophosphates are. Thus, it is possible that IP_6K1 was active with lower ATP concentration, but the inositol pyrophosphates were degraded. The faster retentiontime of IP_6 in figure B is due to the age of the column. The experiment in panel B was performed later than in panel A. Finally, IP_6K1 was transiently transfected into ^{3}H-inositol labeled HEK293T cells and the lysates were analyzed as described before. There might be an increase in IP_7 and IP_8 in IP_6K1 transfected cells compared to vector transfected cells. Transfection of IP_6K1DLK-AAA, the putative kinase dead mutant, resulted also in an increase in IP_7/IP_8 levels (figure 39). The numbers for IP_7 and IP_8 levels varied in ^{3}H-inositol labeled cells. Thus, since this experiment was only carried out once, it is impossible to say if the increase in IP_7 and IP_8 is due to overexpression of IP_6K1. If this experiment can be repeated with the same result, then the putative kinase dead mutant is not kinase dead.

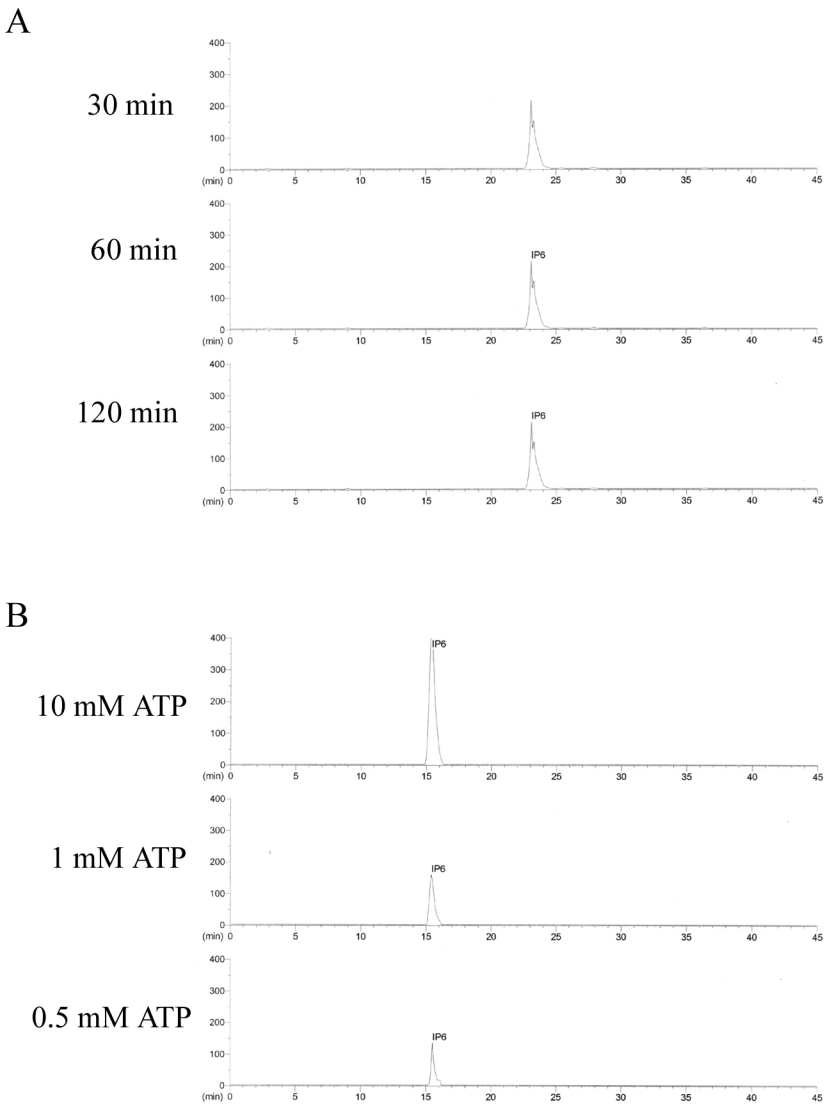

Figure 38: IP$_6$K1 kinase assays. A: 1 µCi ^{3}H-IP$_6$ was incubated with 100 ng recombinant IP$_6$K1 for 30, 60 and 120 min. and analyzed by HPLC. ^{3}H-IP$_6$ was used as a standard to determine the retention time. B: 1 µCi 3H-IP6 was incubated with 100 ng recombinant IP6 for 1 hour with various ATP concentrations

Table 15: Quantification of figure 38

condition	IP_6 area peak (cpm)
0 min	1200
30 min	1100
60 min	1145
120 min	1233
10 mM ATP	2280
5 mM ATP	710
1 mM ATP	315

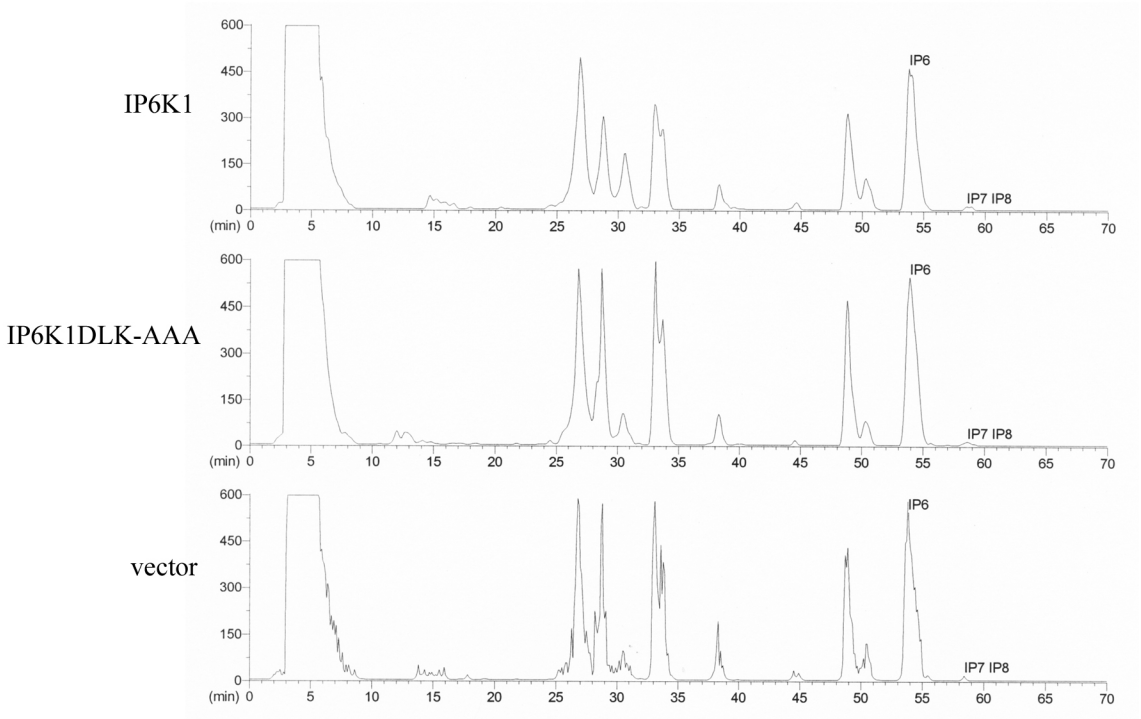

Figure 39: Analysis of HEK293T cells overexpressing IP_6K1 and IP_6K1DLK-AAA. HEK293T cells were labeled with ^{3}H-inositol for four days and then transfected with IP_6K1 constructs. After 36 hours expression the lysates were analyzed by HPLC.

Table 16: Quantification of figure 39

Transfected with	Area peak (cpm) IP_6	Area peak (cpm) IP_7 IP_8
hIP6K1	4563	88
hIP6K1DLK-AAA	5278	95
vector	4999	34

A2 Characterization of type 2 inositol hexakisphosphate kinase

A2.1 Characterization of IP_6K1 antibodies

As described in chapter polyclonal antibodies were made against recombinant IP_6K2. As shown in figure 18 (results, chapter 3.3.1), IP_6K2 does not cross react with IP_6K1 *in vivo*. Unfortunately, this antibody did not work well in immunoblot experiments. A shown in figure 40the antibody did not cross react with recombinant IP_6K1 and in U2OS cells overexpressed IP_6K1. But it was not able to recognize a single band by immuno blotting. There was a high background and multiple bands visible.

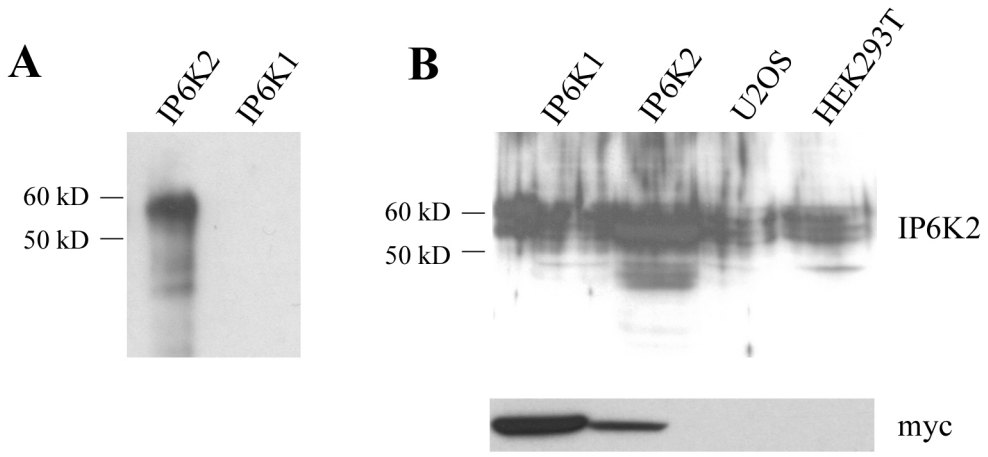

Figure 40: Characterization of anti IP_6K2 polyclonal antibody. A: 3 ng of recombinant IP_6K1 and IP_6K1 were analyzed by immunoblot using anti IP_6K2 pAb. B: 8 µg U2OS cells overexpressing myc-IP_6K1 and myc-IP_6K2 and 12 µg U2OS and HEK293T cell lysates were separated on a SDS-PAGE and analyzed by immunoblot using anti IP_6K2 pAB (upper panel) and anti myc mAb (lower panel) as control to confirm overexpression of the myc-IP_6K1 and myc-IP_6K2.

A2.2IP_6K2 may localize to nuclear speckles

Since this antibody could not be used in immunoprecipitation experiments, it was not clear, if the antibody recognizes the right protein by immunofluorescence. Nevertheless, the antibody was used to determine the putative localization of IP_6K1 in NIH3T3 cells. As shown in figure 41 IP_6K2 may be nuclear and seems to be localized in distinct nuclear foci. After costaining with an antibody against a family of splice factors (anti sm antibody), it turned out that IP_6K2 colocalizes with these splice factors in nuclear speckles. This colocalization was increased after treatment with the transcription inhibitor5,6–dichlorobenzimidazole1-β-D-ribofuranoside (DRB). Inhibiting transcription results in a larger size of nuclear speckles.
Treatment with DNA damaging reagent, such as VP16, irradiation and hydroxyurea did not have an effect on IP_6K2 localization

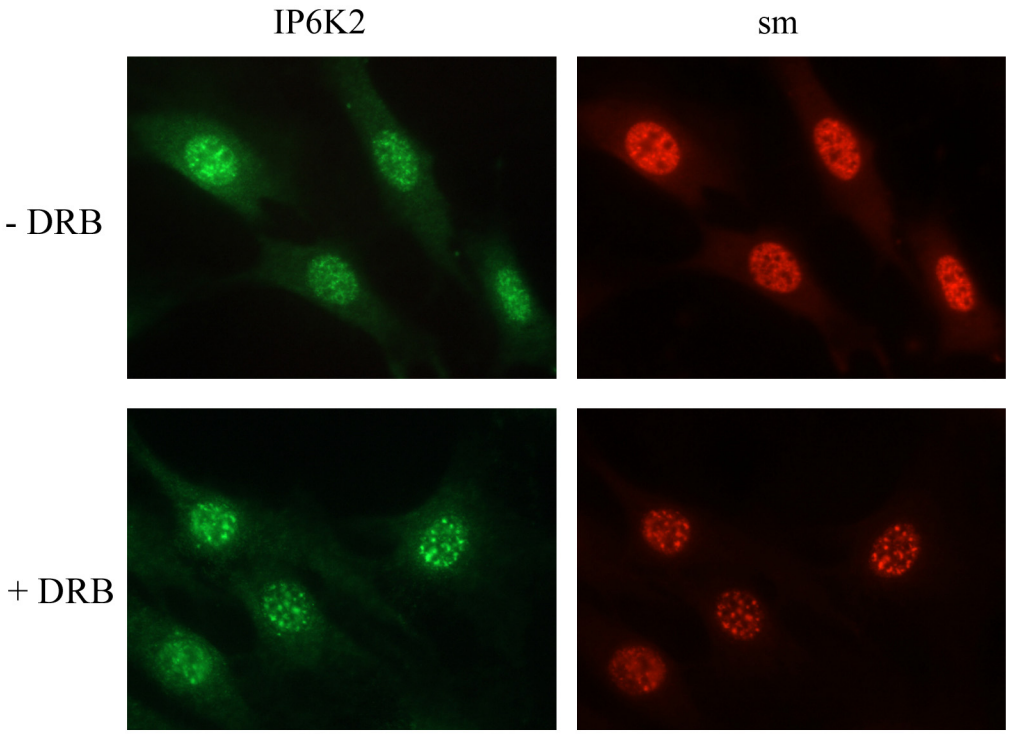

Figure 41: IP_6K2 colocalizes with sm proteins at nuclear speckles. NIH3T3 cells were grown over night on coverslips and stained for IP_6K2 (green) and sm-proteins (red) after 0 and 4 hours treatment with DRB. IP_6K2 colocalizes with sm-proteins in nuclear speckles.

Erklärung

Ich versichere, dass ich meine Dissertation

Functional Studies of Type I Inositol Hexakisphosphate Kinase and its Role in Cell Signaling

selbstständig und ohne fremde Hilfe angefertigt und mich dabei keiner anderen als der von mir ausdrücklich bezeichneten Quellen und Hilfen bedient habe.

Die Dissertation wurde in der jetzigen oder einer ähnlichen Form noch in keiner anderen Hochschule eingereicht und hat noch keinen sonstigen Prüfungszweck gedient.

Ort, Datum	Unterschrift

Lebenslauf

Zur Person	Karen Abel Geboren am 2.4.1974 in Oldenburg, Deutschland Ledig

Schulbildung

1983-1987	Herrmann-Ehlers Grundschule in Oldenburg
1987-1989	Orientierungsstufe Marschweg in Oldenburg
1987-1993	Altes Gymnasium in Oldenburg
1993-1996	Carl von Ossietzky Universität in Oldenburg, Vordiplom (Sommersemester 1996)
1996-1999	Philipps Universität in Marburg
Nov 1999	Diplom Titel der Diplomarbeit: *In vitro* Characterisierung der Don3 Proteinkinase aus *Ustilago maydis*
Seit Mai 2000	Promotion an der University of Wisconsin-Madison, in Madison, USA

Konferenzen

2001	Molecular and Cellular Pharmacolgy Program Symposia, Madison, Wisconsin, USA Poster: A role for inositol hexakisphoshate in the nucleus
2002	Keystone Symposia: Regulation of Cellular Responses by Lipid Mediators; Taos, New Mexico, USA Poster: A role for inositol hexakisphosphate kinases in the nucleus
2002	Molecular and Cellular Pharmacolgy Program Symposia, Madison, Wisconsin, USA Poster: A role for inositol hexakisphoshate in the nucleus

Publikationen

Abel, K., Anderson, R. A. and Shears, S. B. (2001). Phosphatidylinositol and inositol phosphate metabolism. *J Cell Sci* **114**, 2207-8.